Dynamic Transverse Force Regulation of Axially-Moving Flexible Media with Advanced Guiding and Actuation

A thesis presented in partial fulfilment of the

requirements for the degree of

Master of Engineering

in

Mechatronics

by

Riichi NAGAO

School of Engineering and Advanced Technology,

Massey University, Albany

New Zealand

2011

Abstract

The rapid growth of computing and information technology has enabled pervasive access to the World Wide Web. Over 280EB of digital data has been generated from around the world and flowing in the digital universe; as a result, the need for data storage has grown rapidly. A variety of information storage solutions such as hard disk drive (HDD) products that are common information storages for personal computing are available in the market. Modern magnetic tape data storage in terms of its capacity and reliability has been employed as an ideal solution for enterprise-level storage of archival data with applications that include financial records, satellite images, and consumer databases.

In magnetic tape technology, the thin, flexible media is transported between the supply and take up packs at a prescribed speed and tension, and over guides and the read/write head. As the tape is transported, in-plane vibration of axially moving tape, known as lateral tape motion (LTM), arises from excitation sources such as the run out of tape pack and impacts between the tape and the flanges on guides or packs. LTM has been identified as a major factor that degrades recording accuracy. Limiting the LTM is the one of the keys that enables the multi-terabytes data storage, and flanged roller guides are commonly implemented in modern tape drives. However, for higher recording density, thinner media is desirable. Reducing the thickness of media can significantly decrease its stiffness and increase the likelihood of damage to media edges by adjacent mechanical components on the guiding path. To avoid this, alternative tape guiding and actuation are required, and many advanced guiding mechanisms without the use of flanged guides have been developed to reduce lateral tape motion in industry and academia. The transverse force (tension) applied to the travelling tape is another key element of LTM dynamics and is controlled using the dynamics of tape pack driving sources in the modern tape drive products in using an open loop control logic. However, the developing advanced guiding and actuation technologies influence the tension irregularly and the current tension control algorithm is not able to handle the irregular changes of tension. An active tension control is required to feasibly advance LTM actuations.

This thesis is motivated by the need for future engineering advances in guiding and actuation technologies for magnetic tape. Advanced guiding and actuation technologies have been developed to enable the active tension (transverse force) actuation of axially moving tape. An advanced tension actuation technology of axially moving media with dynamic tape path alternation using a novel rotary guider is considered in this thesis, and its effectiveness and technical feasibility is analysed in the context of actuating travelling tape tension. The specific issues addressed in this thesis are listed below.

Development of linear magnetic tape transport system with an advanced active tension actuation.

- A homemade linear magnetic tape transport system is developed.
- The footsteps of development including technical design details of hardware and software are described.
- A tape transport system that enables an actuation of travelling tape tension with dynamic tape path alternation using a novel rotary guider was purposely developed.
- The tension is regulated actuating the amount of surface friction force between the tape and the rotary guider by altering the tape path dynamically rotating the rotary guider based on the feedback from strain gauge based tension sensor.

Experimental studies of travelling tape tension shift phenomena with fixed tape path.

- Parameter studies are carried to investigate the transitions of travelling tape tension during the tape transport process with the fixed angle of rotary guider (fixed tape path) in the travelling speed of tape and the angle of rotary guider.
- Through experimental studies, it is found that the tension gradually increases as the tape is transported and the state of change in tension is heavily relay on the dynamics of tape pack driving source.
- The angle of rotary guider shifts the level of tension. Generally, higher rotation angle of the rotary guider and the travelling speed of tape apply greater tension to the tape.

Transverse force regulation with dynamic tape path alternation.

- The effectiveness of tension regulation with dynamic tape path alternation using the rotary guider is investigated through experimental studies.
- A closed loop control algorism of rotary guider controller is developed in order to control the operations of the rotary guider and implemented to the tape transport system.
- The developed controller has a significant influence to the transition of tension.
- The travelling tape tension is successfully regulated as targeted with the designed controller. It can be concluded that the rotary guider with a closed loop control algorism has an ability to actuate the travelling tape tension without relying on the dynamics of tape pack driving sources to control the tension.

Acknowledgements

I am greatly indebted to a number of people for their help and support during the course of this research, and would like to express my gratitude towards all of them.

First, I would like to thank my thesis advisor Dr. Jen-Yuan (James) Chang for his invaluable guidance, advise and mentoring throughout this research. It has been a pleasure being a member of Dynamics and Precision Mechatronics Laboratory under Dr. Chang's supervision.

I would also like to thank Dr, Johan Potgieter, Mr. Eddie Rogers, and Mr. Paul Thornton for manufacturing mechanical components with top quality, Mr. Joe Wang for electronics and instrumentation supports, Mrs. Lynne Tunna and Mrs. Colleen Vas Es for secretary supports, and other Massey University staff members for their variety of supports during this course of research.

I greatly acknowledge the technical advice of Mr. Jeff McAllister of Hewlett-Packard and Turguy Goker of Quantum, USA.

I thank my colleagues, both past and present, at the Dynamics and Precision Mechatronics Laboratory for useful discussions and assistance during this course of research. I also thank many others for making my stay at Massey pleasant and fruitful.

Finally and most importantly, I would like to express my gratitude to my family, especially to my parents, for their endless support over many years. Without their encouragement and patience, this work would not have been possible.

This research was supported by Information Storage Industry Consortium, United State of America.

Contents

Figures and Tables

Chapter 1

Introduction

1.1 Data Storage Industry Dimensions

Parallel to rapid growing of computing, data storage industry is one of the fastest growing industries since the 1960s; it has become a multibillion-dollar industry and continues to grow every year. During the two decades the World Wide Web has been populated, nearly 800 EB (exabytes, 1 EB = 10^{18} bytes) of data is flowing in the digital universe (EMC Corporation, 2010, para. 6), and the amount of digital data generated grows exponentially every year. Late in the first decade of the 2000s, visual and sound media was evaluated from Standard Definition (SD) to High Definition (HD) and data sizes dramatically increased to enable their superior visual and sound quality. Based on these developments, the importance of data storage devices has increased greatly as without data storage devices with large data storage capacity, the WWW would not be able to maintain its world. Further, in near future, as Cloud Computing is populated, it will accelerate the growth of the data storage industry. Currently, many data storage devices such as hard disk drive (HDD), optical drives, compact disk (CD) storage, and the new solid-state drives (SSD) are available in the market. Most data is stored in such devices and the accumulated amount of data stored in these devices expands annually. Broadly speaking, the ultimate goal for any available data storage is catering to customer demand for higher data storage capacity. Use in business and public sector enterprises as well as consumer computing devices market will increase that demand.

1.2 High Density Magnetic Tape Storage

For decades, magnetic tape media has been commonly used for the archival storage of digital data; many other data storage products such as HDD products are also available and commonly used for storage of data from personal computers (PCs) and servers. However, magnetic tape media is the ideal solution for archival storage since magnetic tape technology enables the lowest unit cost of storage among available data storage solutions. Fig. 1.1 shows a Hewlett-Packard commercial tape drive with a LTO4 high-density magnetic tape cartridge. Before the year 2000, there were no integrated standards for magnetic tape. Major magnetic manufacturing companies such as IBM, Hewlett-Packard, Seagate (Quantum), and Sony were developing their own data recording formats for magnetic tape, and manufacturing tape derived products optimized for the developed standard. In 2000, an integrated open standard for magnetic tape Linear Tape Open (LTO) was developed for the first time through co-operation between IBM, Hewlett-

Packard, and Seagate (Quantum). The designated first generation magnetic tape standard enabled a data capacity of 100 GB with 20 MB/s as its data transfer speed (Hewlett-Packard, IBM and Quantum, 2011). LTO continued to improve significantly in terms of its data capacity and transfer rate as the next generation of LTO standard were released. In 2010, the open standard fifth generation (LTO5) was released. LTO5 has 1.5 TB (terabytes, 1 TB = 10^{12} bytes) native data capacity with a 120 MB data transfer rate which is more than twice as fast as other available HDD products and proves that magnetic tape still has the capability to compete with other storage devices such as HDD and optical devices (Hewlett-Packard, IBM and Quantum, 2011). Tape drive products are economical solutions for archival storage: Fig. 1.2 shows an example of an automated tape library that can hold many cartridges and that accommodates petabytes of total storage capacity. The storing of tape cartridges is managed by a robotic arm that grabs a cartridge and inserts it into the tape drive. Once the tape cartridge has been fully recorded to the limit of its storing capacity, the robotic arm ejects the tape cartridge and stores it at specified location. The major advantage of a tape library is the expandability of its storage capacity. With magnetic tape technology, unlike with HDD products, the drive that the device reads and records the data from is separated from the recording media. Therefore, the data storing capacity of tape literally can be expanded to increase the number of tape cartridges the library can hold. Further, the costs of data storage capacity expansion are relatively small compared to other data storage products since the magnetic tape has the lowest cost per gigabyte ratio. Hence, the further improvements of magnetic tape such as larger storage capacity, higher recording density, and faster data transfer speed are highly demanded. In order to catch up with consumer demand, the tape manufacturers are aiming to double the recording capacity for the next generation of LTO standard tape products.

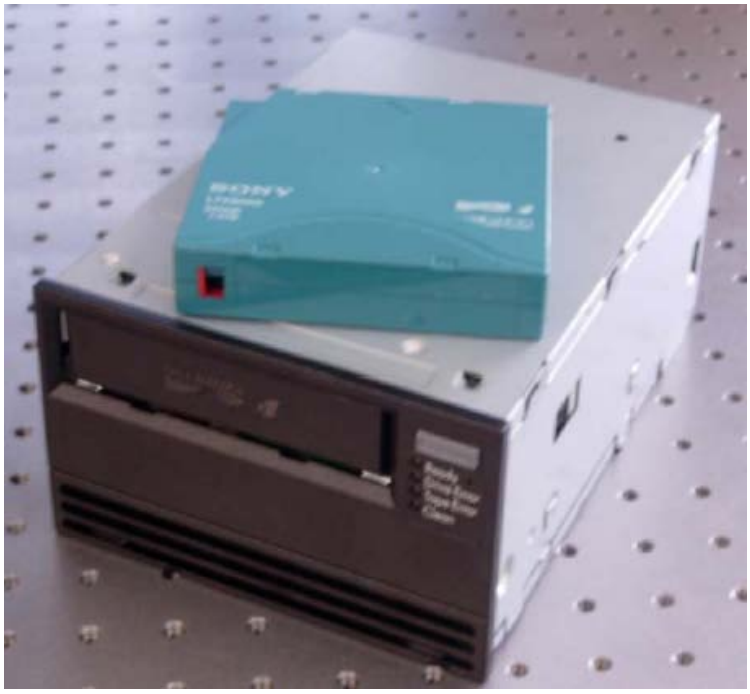

Fig. 1.1: A screenshot of commercial tape drive with a LTO4 standard based magnetic tape cartridge.

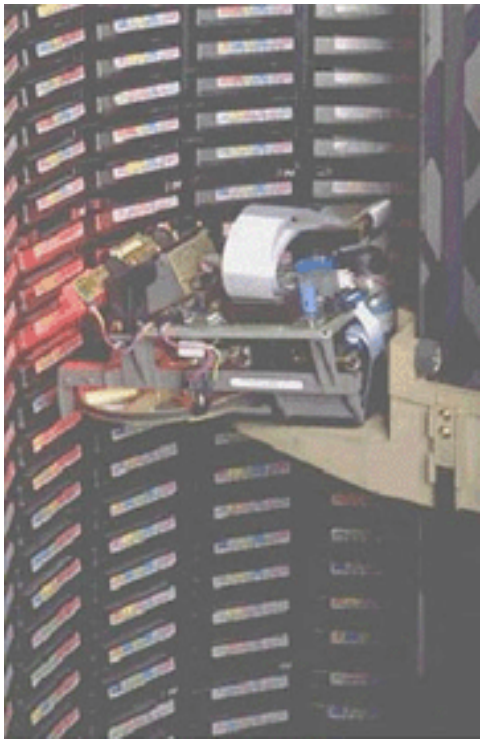

Fig. 1.2: An automated high-density magnetic tape data library.

(Hitachi, Ltd., 2005)

1.3 Guiding and Actuation for Magnetic Tape Storage

1.3.1 Lateral Tape Motion (LTM)

Tape is transported between the supply and take up packs over flanged roller guides and the read/write head at a prescribed speed and tension. Fig. 1.3 shows a photograph of key components in a commercial high-density magnetic tape drive. As tape is transported, in-plane vibration that is known as lateral tape motion (LTM) arises and Fig. 1.4 shows schematic of LTM. This off-track displacement of the tape relative to the read/write head has been identified as a major factor of degrading recording accuracy (Shelton & Reid, 1971; Koseki et al., 1987; Keshavan & Wickert, 1998; Richards & Sharrock, 1998) and a cause of track miss-registration (TMR) (Ono, 1976; Ono, 1997; Wickert & Mote, 1990; Boyle & Bhishan, 2005; Zen & Mu, 2006; Raeymaekers & Talke, 2009). The major excitation sources that trigger LTM are reported as impacts between the tape and the flanges on the packs and the guiders (Taylor & Talke, 2005; Taylor et al., 2006). In order to track the misalignment of tape, the read/write head that is shown in Fig. 1.3 is mounted on the servo tracking mechanism in modern tape drive products; however, its tracking performance is limited, and is particularly problematic when this off-track displacement occurs in higher frequency. Flanged guides are another LTM countermeasure and have proved to be one of the best solutions to limit LTM (Lakshmikumaran & Wickert, 1998). However, the technology trend of magnetic tape migrates towards a thinner media substrate and higher tape travelling speeds in order to improve data storage capacity, density, and access time to catch up with consumer demand. Thinner tape is more likely to be damaged by mechanical components such as flanged guiders during the handing process. Fig. 1.5 shows a summary of technical issues that magnetic tape is facing and magnetic tape development cycle. Therefore, LTM is one of the key obstacles to achieving further improvements; a breakthrough is required to develop a new magnetic tape guiding mechanism without relying on a flanged guider and thus enable further improvements of magnetic tape products. Reducing LTM will lead to a reduction of the aspect ratio of bit cell, and enable a higher recording density as a result.

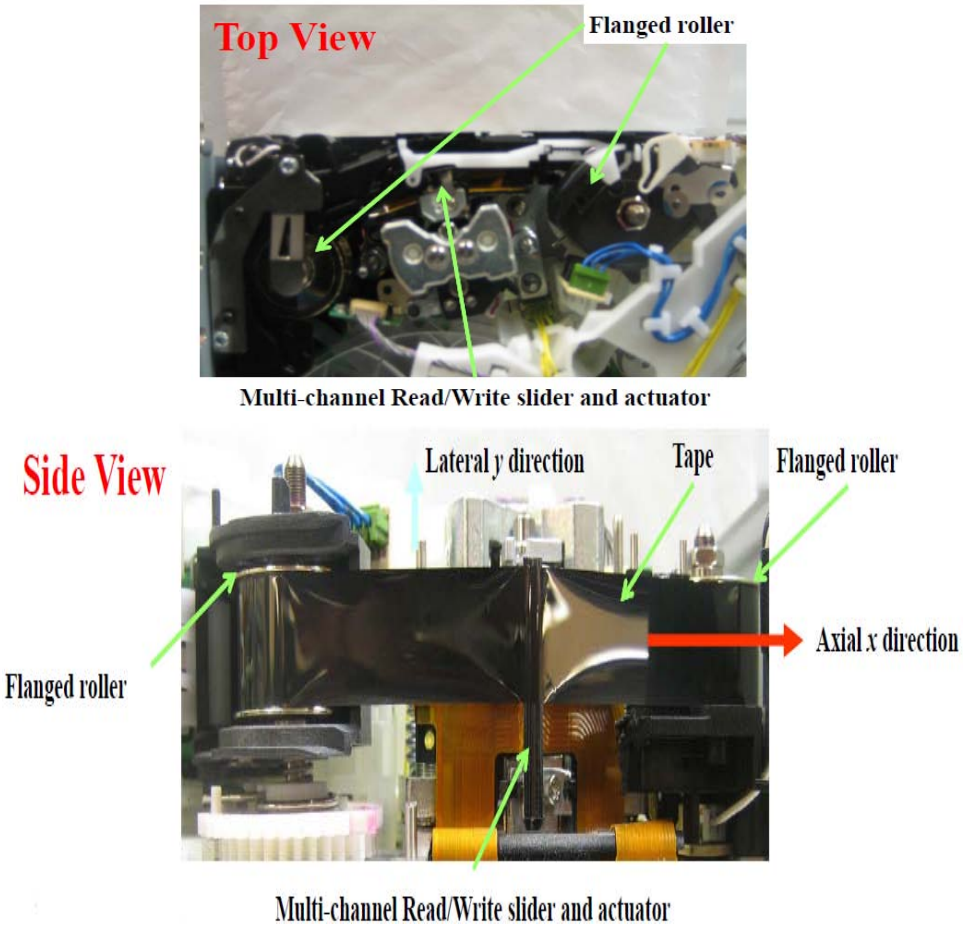

Fig. 1.3: Screenshots of tape handing mechanism of a commercial magnetic tape drive product.

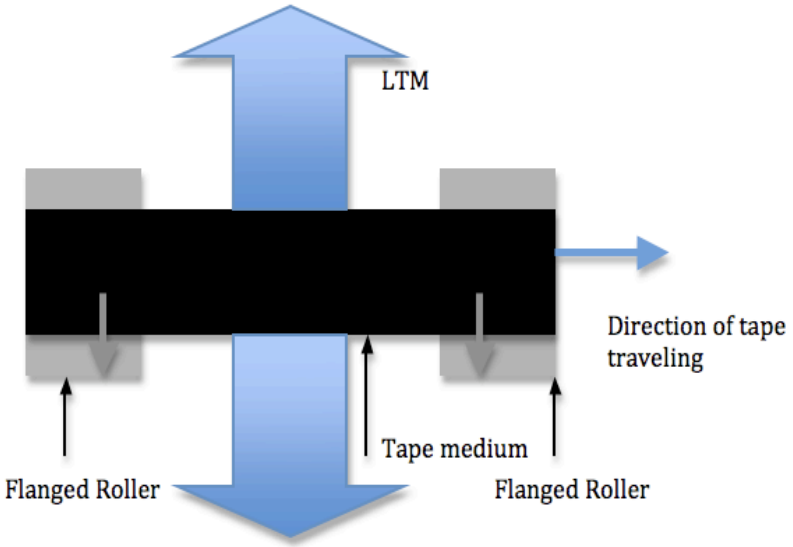

Fig. 1.4: A schematic of lateral tape motion (LTM).

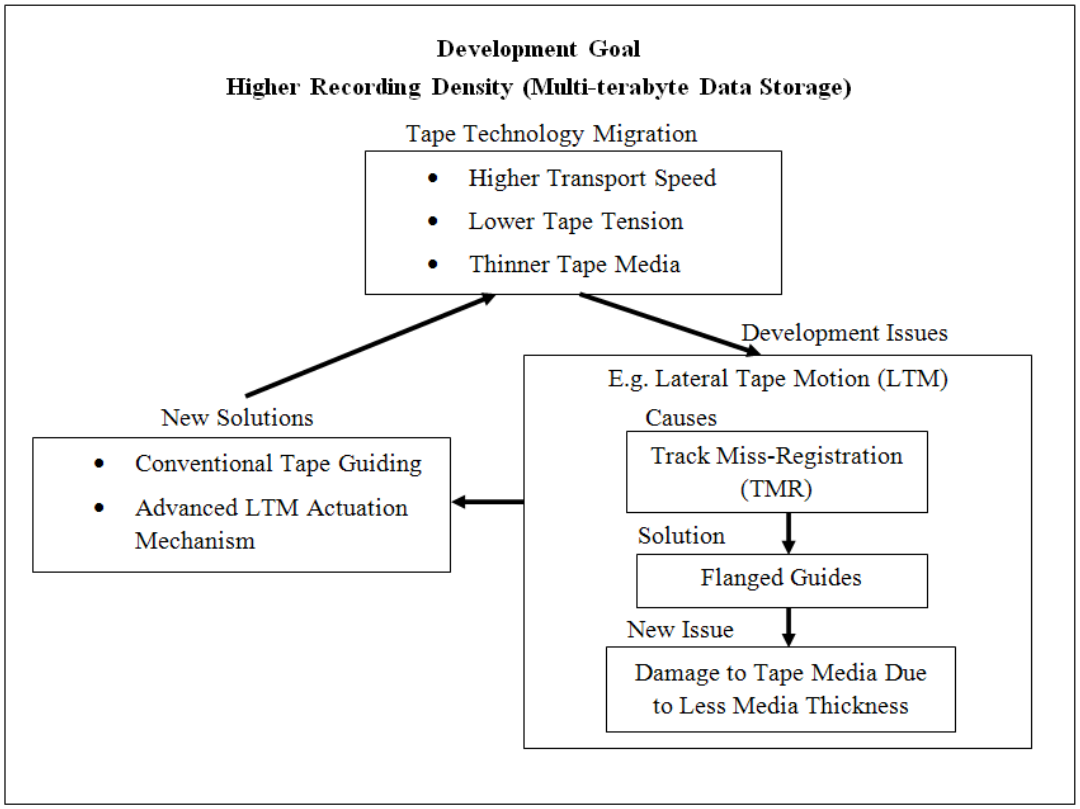

Fig. 1.5: Multi-terabyte magnetic tape data storage development cycle.

1.3.2 Conventional Tape Guiding and Actuation

In order to minimize LTM, many studies have been done and are ongoing in industry and academia. There are two types of approach to improving the LTM tracking ability of read/write head and developing a new conventional tape guiding. On the head tracking ability development side, Kartik, Pantazi, and Lantz have investigated a novel PZT-based read/write head actuator in order to enable a high read/write head response for tracking high frequency LTM (Kartik et al, 2010). In the tape guiding approach, Jordan and Chang proposed and validated a novel tape guiding mechanism that controls LTM using local motion created by a PZT-based actuator and non-flanged guiders (Jordan & Chang, 2008); Pantazi, Lantz, Häberle, Imaino, Jelitto, and Eleftheriou have investigated the effectiveness of the active tape guiding mechanism (Pantazi et al., 2010).

1.4 Transverse Force Actuation for Tape Storage

In tape guiding, Wickert identified that friction contact with the read/write head is an excitation source that contributes to LTM (Wickert, 1993). In other words, a stable contact between travelling tape and the head that provides a constant tape tension is a key element for LTM characteristics. Among the available

tape drive products, tape tension is controlled by the dynamics of a motor that drives the tape pack (Yu & Messner, 2001; Yu & Messner, 2001; Panda & Engelmann, 2003). The designed servo controller is calibrated through laboratory experiments, and in the actual products; it is operated with an open loop control based on the calibrated results. Such a controller does not have the ability to maintain the tape tension at a constant when the cases of aforementioned advanced tape guiding mechanisms are implemented since advanced tape guiding irregularly interferes in tape tension. Therefore, an advanced tape tension control mechanism with closed loop is required to enable state-of-the-art tape guiding. This thesis, motivated by the aforementioned reasons, presents the development of a linear, high track-density, magnetic tape drive system that enables travelling tape tension regulation with dynamic tape path alternation, and friction guiding by integrating a closed loop controlled, novel rotary guider into the tape path. The developed system and tension regulation technology are validated through experimental studies in order to determine their technical feasibility. Fig. 1.6 illustrates the positioning of this thesis based research in the function of data storage capacity of magnetic tape.

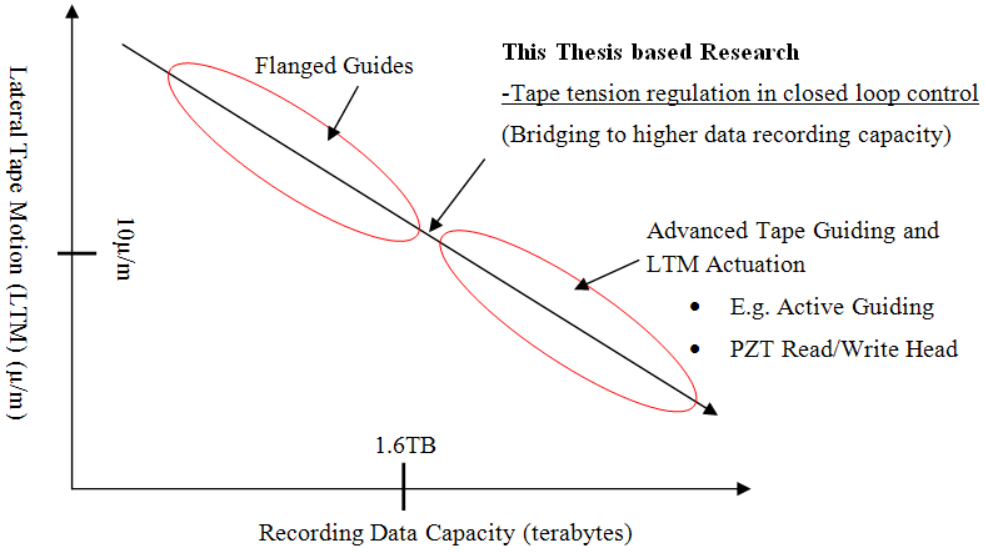

Fig. 1.6: Status of this thesis based research.

1.5 Organization

This thesis develops a technology of transverse force regulation of axially moving flexible media in closed loop control for high-density magnetic tape drives and investigates the effectiveness of the aforementioned technology through experimental studies. This section provides a brief overview of Chapter 2, 3, and 4; the literature is summarized in Chapter 5.

Chapter 2 presents the steps of development of a linear tape transport system that enables the regulation of travelling tape tension. The system is designed by PDSA design cycle with mechatronics integration. The technical details of design from a hardware and software aspect highlight the process of construction including all mechanical components designing, choosing of tape driving source, development of all electronic circuits, control algorithm, and tape system driving software development.

Chapter 3 describes the experimental studies of tape tension transitions with fixed tape path during the transportation process. The parameter studies are carried out on the travelling speed of tape and the angle of the rotary guider.

Chapter 4 investigates the ability to regulate travelling tape tension in the developed tape transport system through experimental studies. Two control algorithms are developed and evaluated their effectiveness; one is for an open loop controller that enables the wrap angle regulation of rotary guider without tension feedback; the other is for a closed loop proportional gain controller that enables real-time tension actuation based on the tension feedback.

Chapter 5 lists the conclusions based on the technical results obtained through the study, briefly highlights limitations, makes recommendations, and suggests possible future work.

Chapter 2

Tape Transport System Mechatronics Integration

2.1 Chapter Overview

Minimizing lateral tape motion and regulating the tension applied to the travelling magnetic tape are key elements for enabling higher recording density and accuracy of high track-density magnetic tape drives. Among the modern tape drive products, flanged guides are commonly implemented in a tape path to limit lateral tape motion; tape tension is prescribed by actuating the dynamics of tape pack driving motors in an open loop control. A variety of advanced tape guiding mechanisms without the use of flanged guides have been developed to reduce lateral tape motion in industry and academia. However, these guiding mechanisms are likely to cause irregular tape tension changes and the aforementioned tape tension control technology does not have the ability to handle irregular tension changes. As a result, the tape tension cannot be maintained at a constant level. To avoid this, a closed loop controlled tape tension actuation is required. This chapter presents the development of a linear high track-density magnetic tape transport system that enables tape tension regulation by applying dynamic tape path alternation and friction guiding mechanisms during the tape transportation process using a closed loop controlled novel rotary guider. The development of this system is carried out based on a PDCA design cycle with mechatronics integration at design. Detailed steps of system development are described from both hardware and software aspects and include mechanical and electrical components design, software development, and computing of the technical issues of the developed system.

2.2 Design Planning

2.2.1 Mechatronics Integration at Design

Mechatronics integration at design is commonly applied to develop a system that involves mechanical, electrical, software, and computer engineering. Fig. 2.1 shows a diagram of mechatronics integration at design. One of the key advantages of this design method is that it introduces engineers to the over-the-wall approach (Xu, 2009, p9). This approach allows different engineering fields such as mechanical engineering and electrical engineering to work concurrently and it enables a synergy between hardware and software integration (Xu, 2009, p9). Therefore, mechatronics design at integration is a highly valuable way to fluidly manage the design and development of mechatronics systems or products.

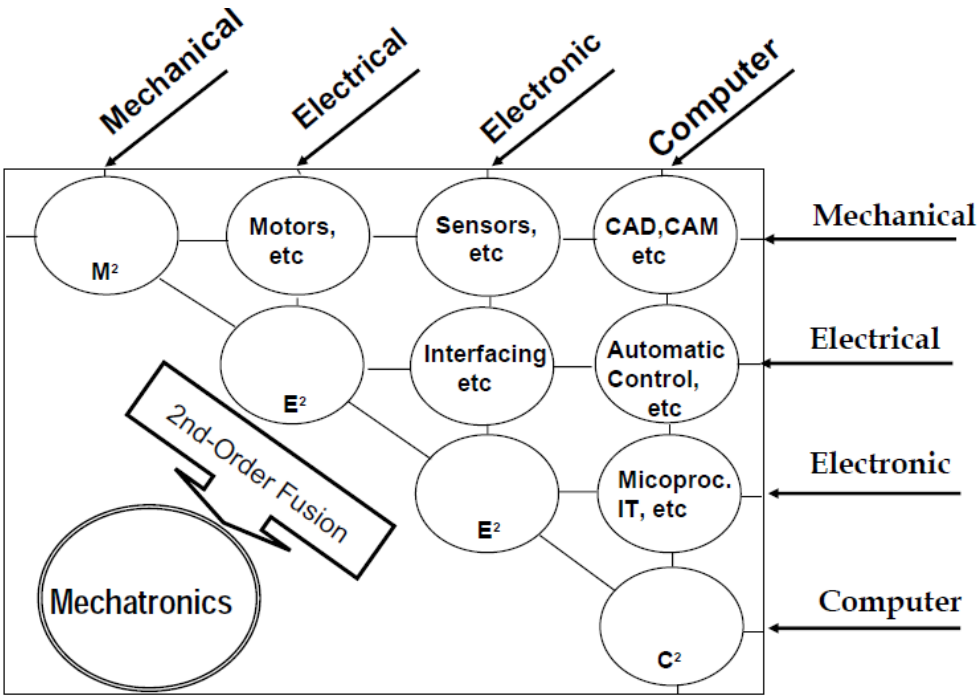

Fig. 2.1: Mechatronics integration at design.

(Retrieved from Xu, 2009, p4)

2.2.2 Design Cycle

The tape transport system developed in this thesis involves both hardware and software. Applying the mechatronics integration to the design enables an efficient development of the system. Fig 2.2 shows how a design cycle of the tape transport system is applied to develop the system. This design cycle is formed by merging the Plan-Development-Study-Analysis (PDSA) design cycle and mechatronics integration. The mechatronics integration is applied during the development phase (D) in the PDSA cycle. The system is developed by cycling the four phases of PDSA. The process begins with the plan phase (P) in which the objectives and foundations of the system such as the key features and the required mechanical and electrical components, required software, time schedule of work, and resource management are decided. During the development phase, the hardware and software are developed in parallel work. Some of the engineering fields such as electrical and software engineering are related to each other. For example, the micro-control unit (electrical) and its operation driver (software) are deeply related each other; therefore, they should be developed concurrently. During the development phase, many works are done concurrently. After all components are developed, hardware and software are integrated and the operation of the system is tested and software is debugged as the Study phase. If any technical errors are detected, their causes are analysed and we return to the plan phase to start a new cycle.

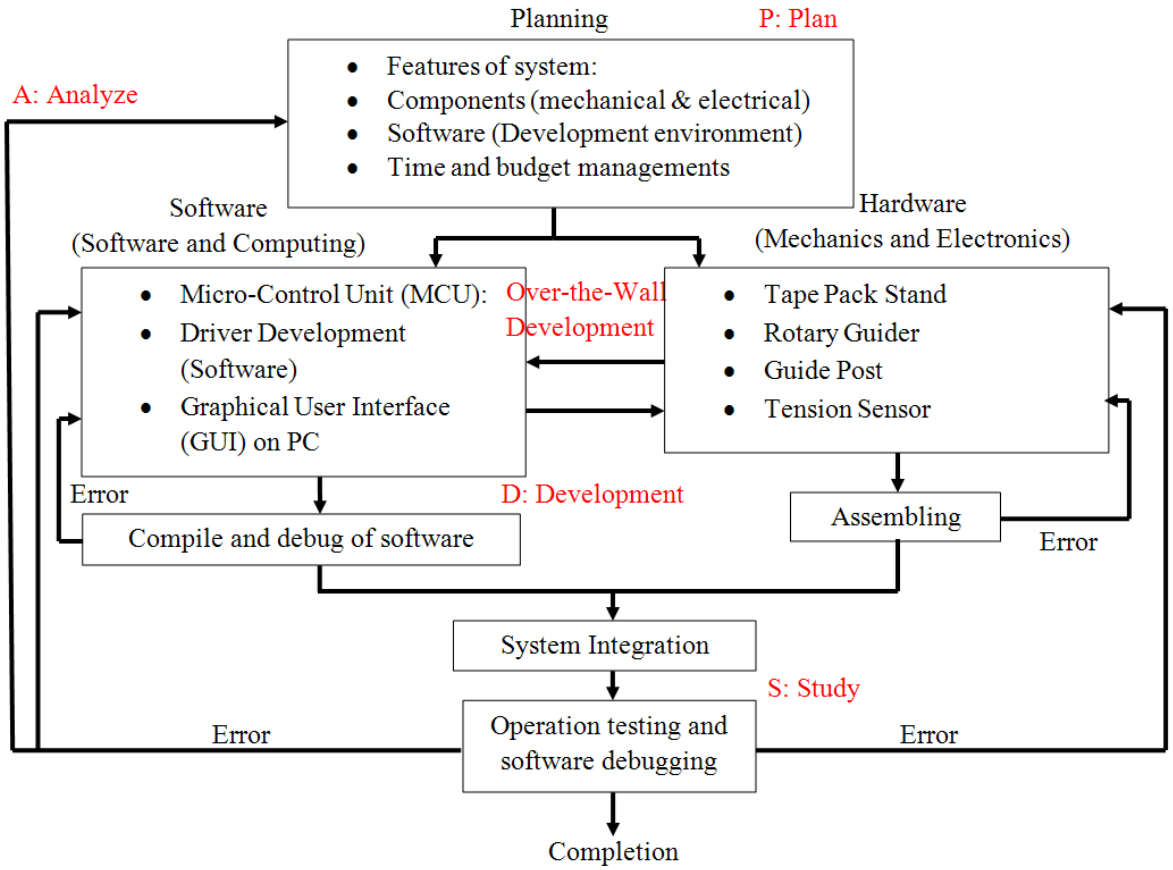

Fig. 2.2: PDCA design cycle of tape transport system.

2.2.3 Development Planning

The objective of this thesis is to develop a tape transport system that enables the travelling tape tension actuation in a closed loop control. Modern tape drive products that are available in the market control the tension by using the dynamics of tape pack driving motors in open loop control based on pre-calibrated laboratory results. However, to enable further improvement of tape performance, the thickness of the tape must be reduced. Thinner media presents a challenge though; it is more likely to have damage to its edges caused by impact on the flanges on guides that are commonly used to limit the LTM in modern tape drive products. A number of conventional tape guiding mechanisms that actuate LTM without relying on flanges on guides have been studied. However, those guiding mechanisms tend to interfere with the tape tension irregularly and current tape tension control technology is not able to handle such irregular tension changes. Therefore, a tape transport system that enables tape tension actuation in closed loop control is required to make feasible the new tape guiding mechanism. Hence, a prototype tape transport system as developed in this thesis needs to satisfy the following requirements.

- Actuate travelling tape tension in a closed loop in order to regulate the tension free from any disturbances.
- Regulate the tape travelling speed.
- Allow easy operation of system in order to carry out the experiment.
- Provide feasible tension actuation with low cost.

In the beginning of the planning phase, the method used by the tension control mechanism and the core components of system such as tape pack driving sources and the sensor that measures the travelling tape tension are decided. The travelling tape tension is actuated applying surface friction guiding (Kartik, 2006). The surface friction guiding is accomplished by using the friction between the tape and the guide. A novel rotary guider that changes the amount of surface friction force between the tape and the guide by changing the wrap angle by rotating the rotary guider is proposed. Rotating the rotary guider also alters the tape path. Therefore, the tape path is dynamically altered during the tape transportation process. Brushed DC motors are employed as the driving source of tape packs due to their ease of actuation. DC motors are selected in order to transport tape over guides at a prescribed speed. A strain gauge is selected as the sensor that measures the tension by implementing it to the guide due to its high resolution, accuracy, and low unit cost. The next step is planning the design of mechanical components that are required to be manufactured. In this thesis, the tape transport system transports tape between two tape packs over the rotary guider and stationary guides. Therefore, the mechanical components that must be manufactured are the tape pack stands, the rotary guider, and stationary flanged guides. However, the mechanical components such as tape packs, ball bearing shafts of the tape pack, and flanged guides are taken from a HP commercial tape drive due to technical difficulty of manufacturing them. Other mechanical components are planned to be designed using a mechanical 3-dimensional computer-aided design (3D CAD) environment (SolidWorks 2009 SP4), and will be manufactured by the Massey University Albany Workshop. The last step of design planning is selection of the system's control unit. The tape transport system requires several control elements such as the tension and motors. Therefore, multiple channels of pulse width modulation (PWM) and analogue-to-digital converters are essential. The processing speed of the control unit is another important factor for this system. For the aforementioned reasons, the Hitachi Renesas H8/3052f 16-bit micro control unit (MCU) based AKI H8/3052f is chosen as the brain of this system. For development of the tape system driver for MCU, the GCC Developer Lite (BestTechnology Co., Ltd., 2010) was selected as the development environment. To monitor and record output signal from the tension sensor, Windows HyperTerminal based GUI was selected and a serial communication line was established between MCU and GUI in order to enable real time communication. The GUI was also planned to be used to command the operations of systems. The system driving software required controls

the operation of DC motors and rotary guider, sensor reading, and display of the measured tension on the GUI. Fig. 2.3 shows a 3D CAD initial mage of the planned tape transport system. This system was developed based on the design plan for this design phase.

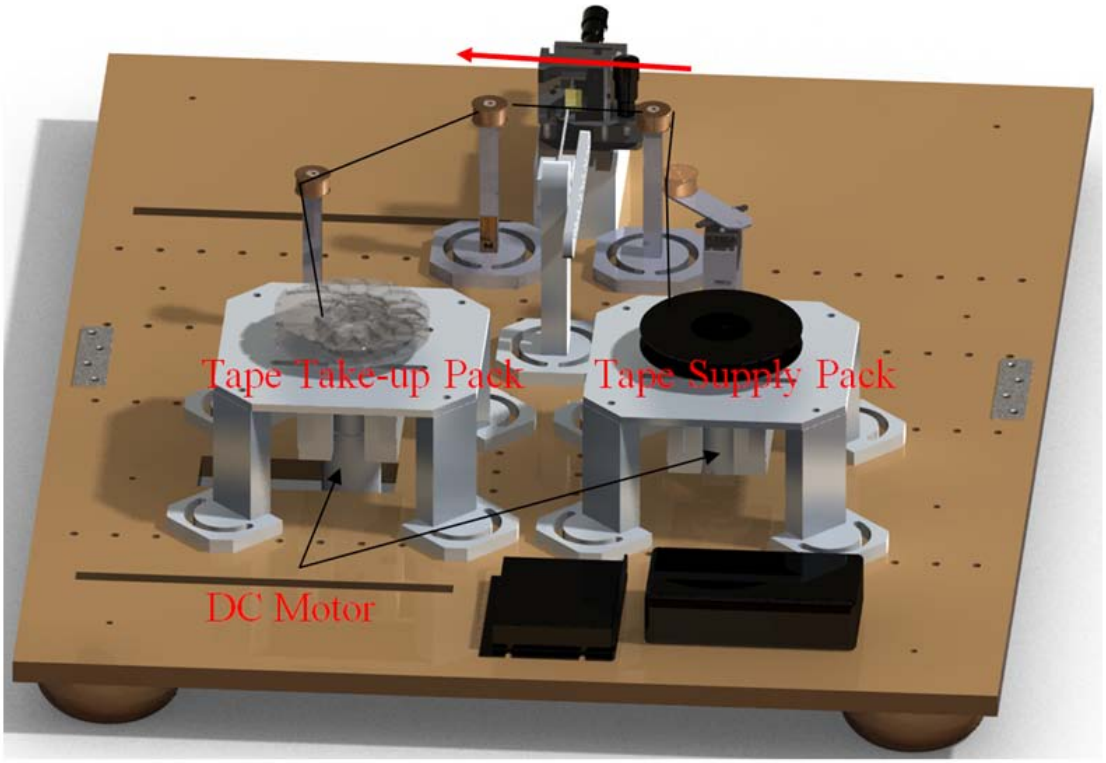

Fig. 2.3: A 3D CAD image of designed tape transport system.

2.3 Tape Transport System Overview

A linear magnetic tape transport system was purposely developed in order to regulate tape tension during the transportation process in a closed loop control under standard laboratory conditions (25°C, 1atm). Fig. 2.4 shows the schematic of a developed tape transport system. The Linear Tape Open 4th generation (LTO4) standard magnetic tape is transported between the supply and take up packs, and over guides. The tension between guide B and C is regulated by a novel rotary guider that forms a part of the tape path in Fig2.4. The rotary guider is structured with a cylindrical flanged slider A, a cylindrical flanged guide B, and a rectangular rigid plate. The slider A and the guide B are mounted diagonally on each edge of a rigid plate.

The rigid plate is mounted on a DC servo motor and is able to rotate setting the guide B as a rotation centre with its workspace between 0º and 180º horizontally. The tension is generated from the surface friction force between the tape and the slider A of the rotary guider. Current tape tension is measured

using the strain gauge based tension sensor that is implemented in the guide C in Fig. 2.4. The rotary guider actuates the amount of surface friction force between the tape and the slider A by rotating the rotary guider based on the feedback from tension sensor. The tape transport operation is driven by the tape pack driving motors. Each tape pack is driven by a single high power brushed DC motor. The system has forward and backward capability with forward pass defined as being when the tape is transported from the supply pack [1] to the take up pack [2] in Fig. 2.4. The angular speed of the tape pack is controlled by a micro-control unit (MCU) based on a homemade DC motor controller A for the supply pack and the motor controller B for the take up pack. Both tape packs have a 44 mm inner diameter and a 98 mm diameter when the tape is fully loaded. The tape path is defined by a novel rotary guider and the flanged posts. The total length of the tape path is 640 mm initially, and it changes corresponding to rotation of the rotary guider. The tape tension is regulated when the tape is transported forward.

The reverse pass is only used to rewind the tape from the take up pack to the supply pack; the tape tension regulation is disabled during this process. The operations of the system, including the tape transportation and the rotary guider, are commanded by the control PC through Graphical User Interface (GUI). Serial Communication (SC) is established to communicate between PC and both motor controllers (MCUs). The measured tape tension by the tension sensor and the trajectory of the rotary guider angle are displayed on GUI and recorded on Data Acquisition (DAQ) PC in .txt file format. Fig. 2.5 and 2.6 show the apparatus of the developed tape transport system and a zoom-in view of the system including the connections of mechanical components, control units, and GUIs respectively. A complete list of components and instrumentation used in the system is summarized in Appendix A. The following sections separately describe the detailed technical designs of the tape transport system’s hardware and software. For the hardware development, the designs of tape pack stands, the rotary guider, the flanged guides, and the tension sensor are described. For the software development, descriptions of the control components of the system include the MCU and the motor controllers, the development of the tape transport system driver, GUI, and the serial communication line setting.

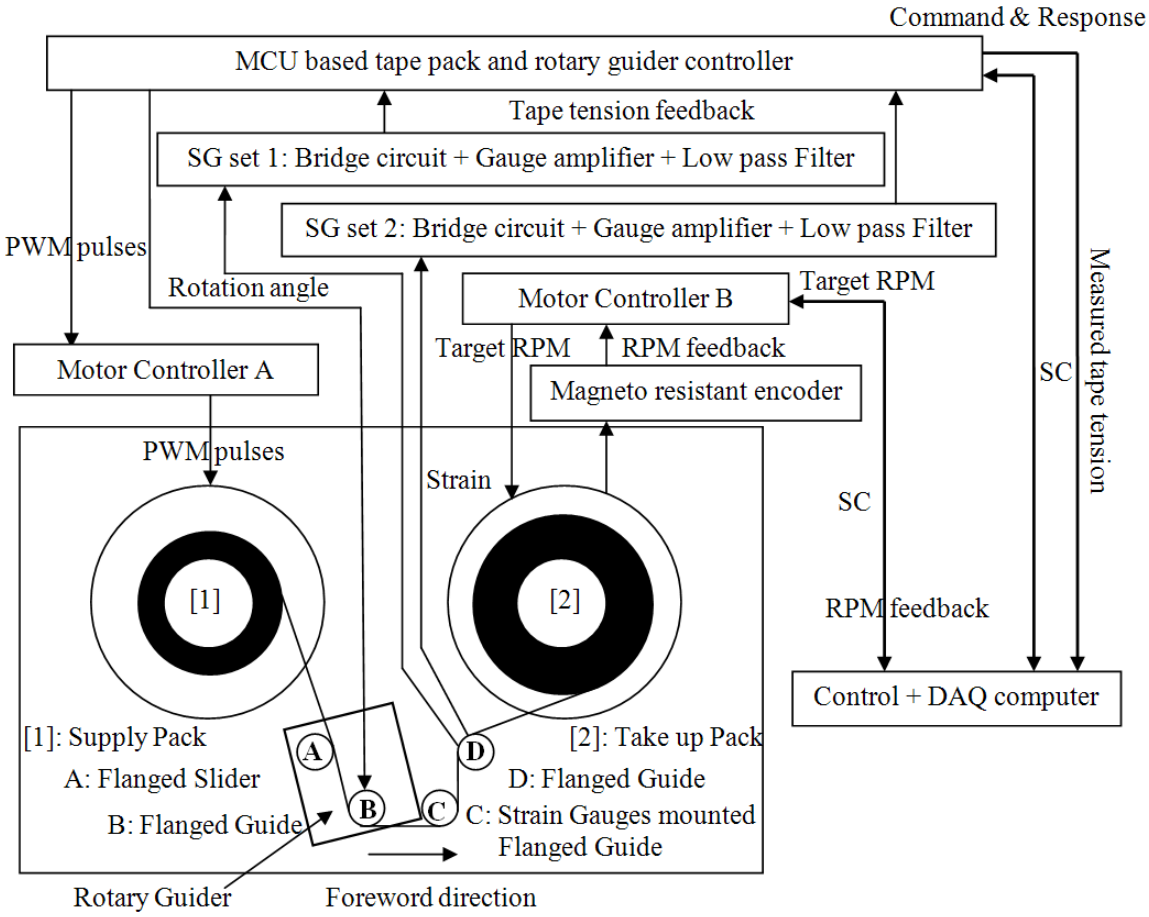

Fig. 2.4: A laboratory test stands of tape transportation system.

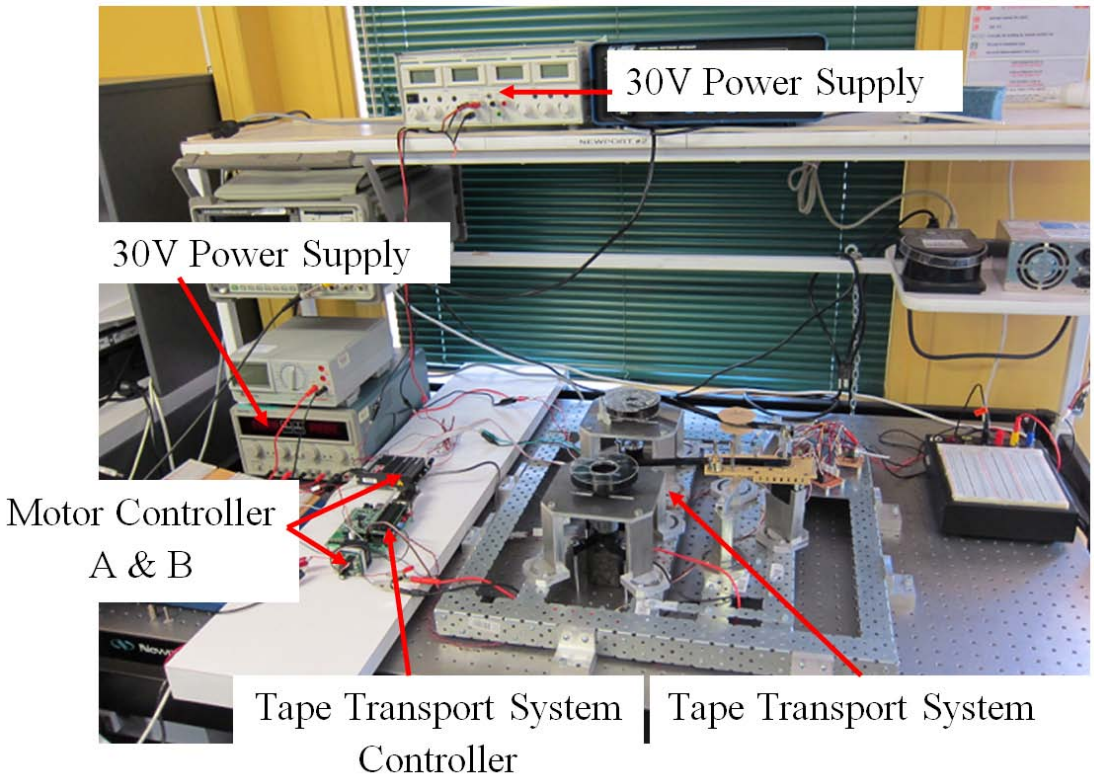

Fig. 2.5: Developed tape transport system apparatus.

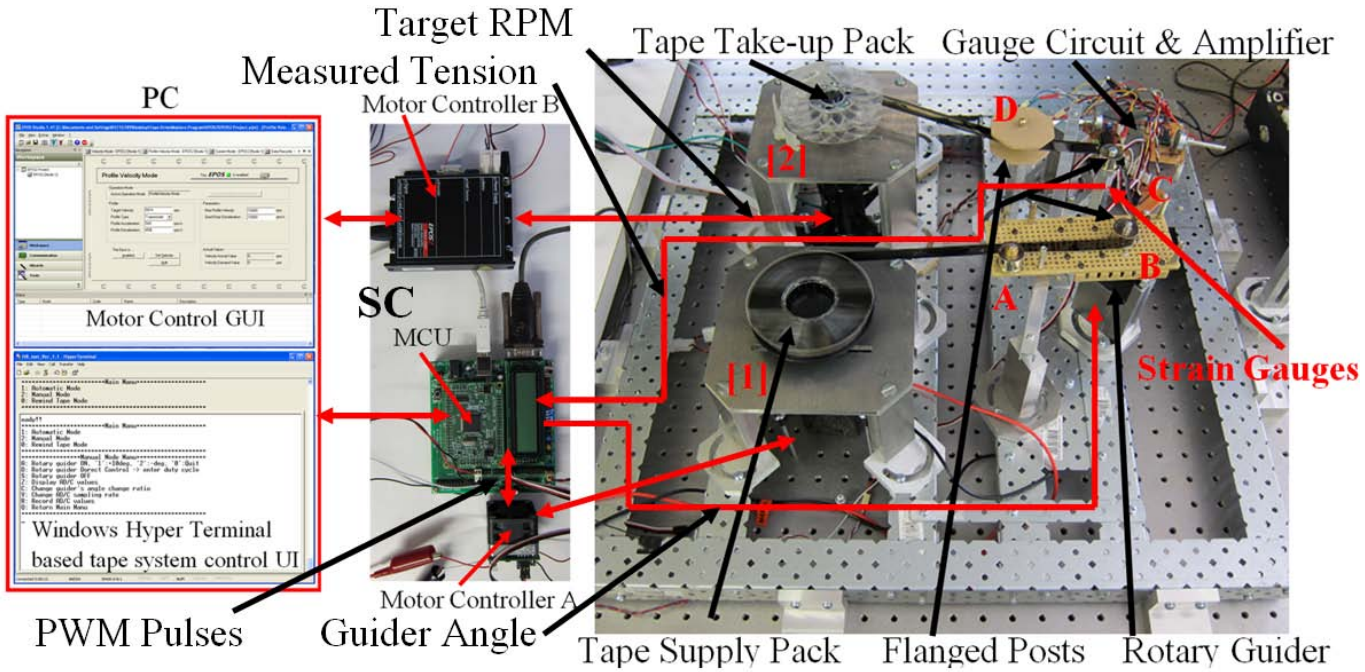

Fig. 2.6: Zoom in view of magnetic tape transport system with connections of components and instrumentations.

2.4 Hardware Development

Hardware of the tape transport system consists of the supply and takes up stands, a rotary guide, and stationary guides. This section describes in detail the technical design of mechanical components and assembly. The majority of mechanical components are designed in a 3D CAD environment and manufactured by Massey University Workshop Albany with top quality. Some of the components such as ball bearing shafts and tape packs are diverted from a commercial tape drive due to the technical difficulty of manufacture. The tension sensor including the bridge circuit, amplifier, filter, and the calibration of the sensor is also described. There are two elements needed to control this tape transport system: the tape travelling speed and the tension. The travelling speed of the tape is controlled by the tape stands; the tension is controlled by the rotary guider by dynamically alternating the tape path.

2.4.1 Tape Pack Stands

The designs of tape pack stands, the supply stand, and the take up stand are described. The tape pack stands are structured using three mechanical components; a body, four legs, and four feet. The tape pack is fixed to the body using a ball bearing shaft that is diverted from the commercial tape drive. The ball bearing shaft is connected to a high power DC motor with a brass coupler. The speed and direction of the DC motor are controlled by a motor controller with micro controller pulse width modulation (PWM). In this system, the average travelling speed of tape is used since the angular speed of the tape pack in rpm is prescribed. The detailed explanations of travelling speed control, selection of DC motor, and the structures of both the supply and the take up stands are discussed in the following sections.

(A) Tape Transport Speed Regulation

The Linear Tape Open 4th generation (LTO4) standard magnetic tape is transported between the supply pack and the take up pack in this system. Both tape packs have a 44 mm inner diameter and a 98 mm diameter when the tape is fully loaded. The length of magnetic tape the supply pack contains is 820m. Fig. 2.7 shows both the supply and take up tape packs.

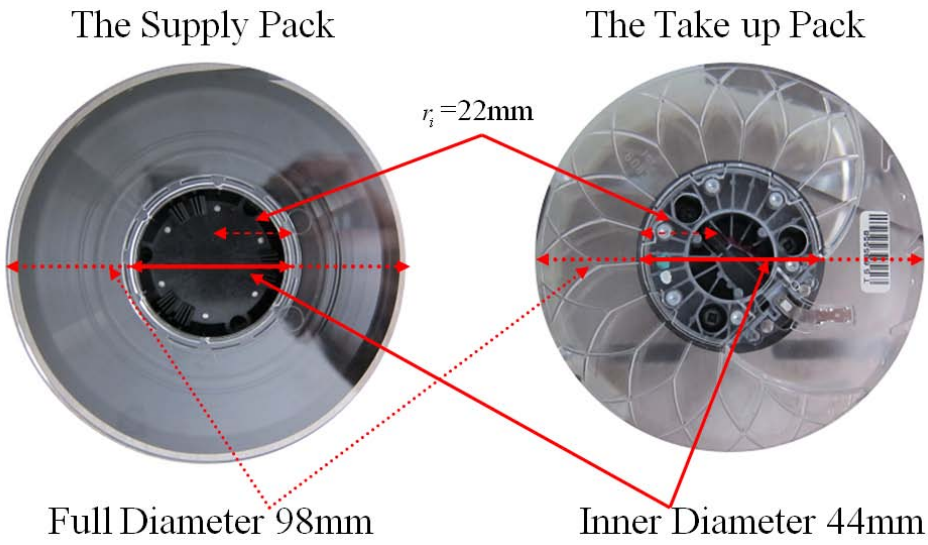

Fig. 2.7: The supply and the take up pack.

The tape pack performs a circular motion and the travelling speed of tape changes in correspondence with the diameter of the tape pack with the fixed angular speed of the tape pack. A control algorithm such as robust servo control logic is essentially required to actuate the tape travelling speed as prescribed. However, in this developed tape transport system, the angular speed of the tape pack in RPMs is actuated, and the average tape travelling is taken as the tape travelling speed. Target angular speed RPMs are calculated based on the corresponding tape travelling speed when the remaining tape on the supply pack is at half-length, 410m. The radius of the empty tape pack "r_i" is 22mm as shown in Fig 2.7. The total radius when the remaining tape length on the supply pack is half-length is calculated as 37.975mm; the number of tape wraps "W" is 2176. Total tape thickness "h" including the gap between adjacent tapes is 7.34µm.

Equation (1) calculates the target angular speed of the tape pack in rpms from the corresponding tape travelling speed v (m/s). Substituting corresponding parameters to equation (1), equation (2) is obtained. Table 2.1 summaries the target tape travelling speed and corresponding target RPM. Fig. 2.8 shows the transition of actual tape travelling speed in the function of length of tape transported.

$$RPM = \frac{30v}{(r_i + hW)\pi} \quad \text{- (1)}$$

Where RPM is target angular speed (rpm), v is target tape average travelling speed (m/s), r_i is inner radius of empty tape pack (m), h is total thickness of the tape (m), and W is number of tape wraps of the supply pack.

$$RPM = 251v \text{ - (2)}$$

Where PRM is target angular speed of tape (rpm), v is target tape average travelling speed (m/s).

target tape transport speed	Target RPM of tape pack (With 3:1 gear head)
1m/s	251 (753)
2m/s	502 (1506)
3m/s	753 (2259)
4m/s	1004 (3012)
5m/s	1255 (3765)
6m/s	1506 (4518)
7m/s	1757 (5271)

Table 2.1: Target angular speeds of tape pack and corresponding travelling tape speeds.

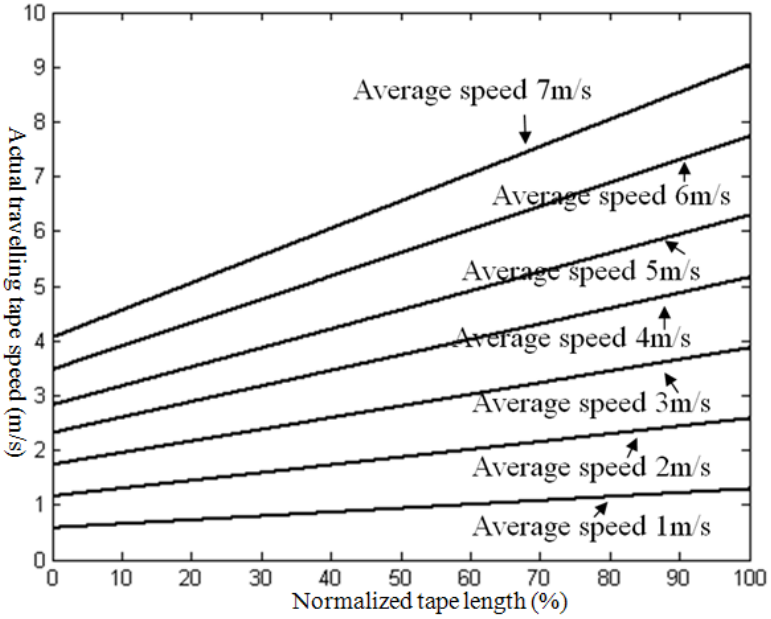

Fig. 2.8: Transition of travelling tape speeds.

The DC motor that drives the tape pack is selected using the calculated results above and the following requirements:

- Minimum RPM requirement of DC motor is 1757rpm (5271rpm).
- Minimum torque requirement of DC motor is 120mNm.
- Encoder is required to actuate rpm of DC motor as prescribed angular speed.
- GUI based operation of DC motor.

The maximum rpm of the DC motor is required to be faster than 1757 rpm that corresponds to the average tape travelling speed 7m/s in Table 2.1. In modern tape drive products, 7m/s is the common transportation

speed of fast-forward. Therefore, the developed tape system requires enabling a faster than 7 m/s of maximum tape travelling speed. From Nagao and Chang, the required minimum DC motor's torque that enables tape travelling speed at 7m/s is approximately 40 mNm (Nagao & Chang, 2009). In this system, tension is regulated using friction guiding with the rotary guider. Therefore, the minimum tongue requirement can be larger than 40 mNm. Taking the safety factor by 3, the minimum torque requirement is set at 120mNm in order to avoid a stall of the DC motor during the transportation. Since the angular speed of the tape pack is actuated in closed loop, an encoder is essentially required to measure the current rpm of motor as feedback. The Maxon RE35 Graphite Brushed DC motor with a 3.1 ratio permanent gear head and a 10-bit magnet resistant encoder was chosen as the driving motor for the tape pack. This motor was chosen as a way to become familiar with the Maxon motor products, and was applied to one side of the tape pack stand, the take up pack, to save the cost of tape transport system development. Therefore, for the other side of the tape pack stand, the supply pack, a direct drive 6V high power DC motor was applied. Hence, in this developed tape transport system, tape tension regulation is enabled during the forward pass when the tape is transported from the supply pack to the take up pack, and disabled when the reverses pass. The reverse pass is used to rewind the tape to the supply pack; the tape speed regulation is also disabled during the reverse pass. Further, during the transportation process, both motors are connected to the tape pack. However, only one of the motors corresponding to the direction of transportation is operated. The maximum torque of Maxon DC motor is 77.7mNm and the 3:1 ratio gear head triples the torque of the motor. Therefore, the actual target RPM is three times larger than the calculated rpm in table 2.1. The maximum rpm of the Maxon motor is 7070rpm. The motor satisfies the minimum rpm and torque requirement for the tape pack driving motor. Parameters such as the prescribed rpm and operations of motor are able to be controlled by the Maxon motor control GUI through a motor controller which is described later in this chapter.

(B) Tape Supply Stand

The tape supply stand is structured with an aluminium rigid plate, four cube legs, and another four feet. The summary of mechanical components of the supply pack stand and a photographic image of the developed supply stand are shown in Table 2.2 and Fig. 2.9 (a) respectively. The tape pack and the ball bearing shaft that links the tape pack and the driving DC motor are diverted by a commercial tape drive due to the technical difficulty of manufacturing. A schematic of the supply stand is shown in Fig. 2.9 (b). The driving source of the supply stand is a 6V high power brushed DC motor; the tape pack and the motor are connected by a ball bearing shaft in Fig. 2.9 (b) in order to reduce the excitation of the DC motor. The ball bearing shaft and the motor are linked by a brass coupler. The motor is driven by angular

speed micro-controller pulse width modulation (PWM) generated by a homemade motor controller formed by the MCU and the motor controller A (Parallax HB-25) that are described later in this chapter.

Tape Pack Stand	DC_Motor_Base: DWG No 1 (Appendix B) × 1 DC_Motor_Leg: DWG No 2 (Appendix B) × 4 DC_Motor_Foot: DWG No 3 (Appendix B) × 4
Ball Bearing Shaft	Diverted from a HP Commercial Tape Drive × 1
Coupler	Brass made 6mm to 6mm Female Coupler × 1
Driving Source	6V High Power DC Motor × 1
Supply Pack	Quantum LTO4 Tape Cartridge × 1

Table 2.2: Mechanical components of the supply stand.

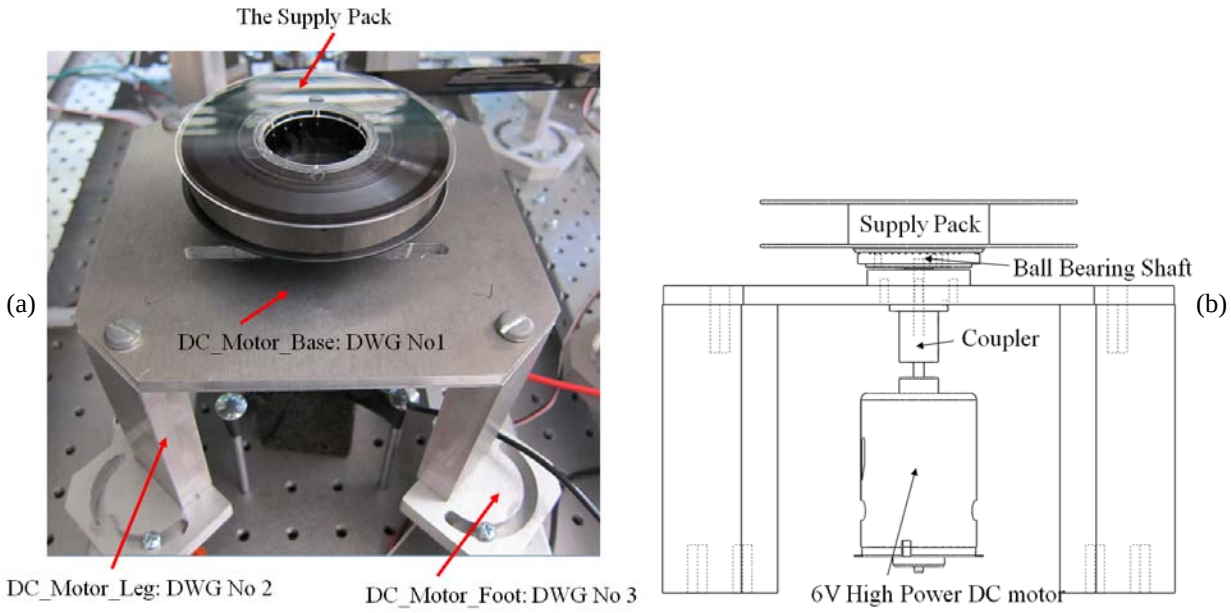

Fig. 2.9: A screenshot (a) and a schematic (b) of supply stand.

(C) Tape Take up Stand

The structure of the take up stand is the same as the supply stand. Table 2.3 shows the mechanical components that structure the take up stand, and Fig. 2.10 shows a photographic image and schematic of the take up stand. The take up pack is driven by a Maxon RE35 90W Graphite Brushed DC motor with a 3:1 ratio permanent gear head in order to increase the torque of the motor. A 10 bit Maxon magnet resistant encoder is also used in the motor to measure the angular speed of the motor in rpms. The motor is operated by a Maxon EPOS2 24/ 5 Digital motor controller and the angular speed of motor is controlled as prescribed based on the feedback from the encoder. Detailed descriptions of the motor controller and its operations are discussed in the descriptions of software development.

Tape Pack Stand	DC_Motor_Base: DWG No 1 (Appendix B) × 1 DC_Motor_Leg: DWG No 2 (Appendix B) × 4 DC_Motor_Foot: DWG No 3 (Appendix B) × 4
Ball Bearing Shaft	Diverted from a HP Commercial Tape Drive × 1
Coupler	Brass made 6mm to 6mm Female Coupler × 1
Driving Source	Maxon RE 35 DC Coreless Motor × 1
Gear Head	3:1 ratio Permanent Gear Head × 1
Encoder	Maxon 10bit Magnet Resistant Encoder × 1
Take up Pack	Diverted from a HP Commercial Tape Drive × 1

Table 2.3: Mechanical components of take up stand.

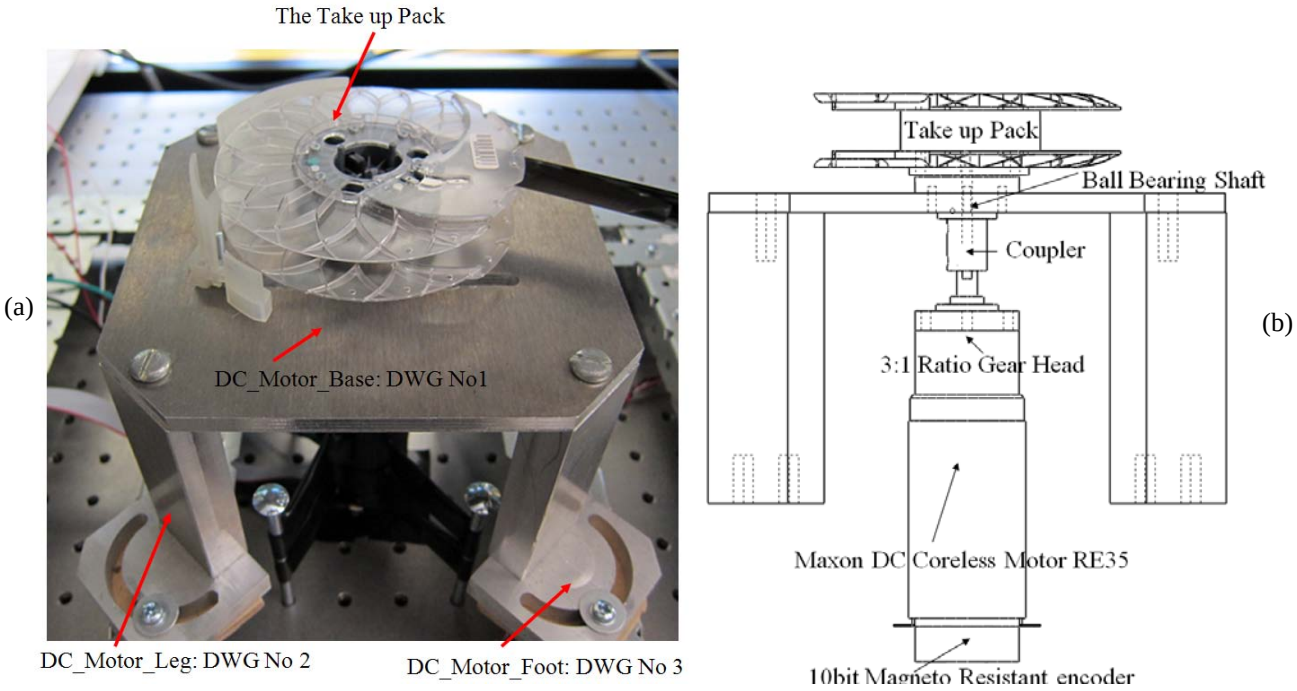

Fig. 2.10: A screenshot (a) and a schematic (b) of take up stand.

2.4.2 The Rotary Guider

The rotary guider is structured with a cylindrical flanged slider A, a cylindrical flanged guide B, and a rectangular rigid plate. The slider A and the guide B are mounted diagonally on each edge of the rigid plate. The rigid plate is mounted on a DC servo motor and is able to rotate; this sets the guide B as a rotation centre with its workspace between 0º and 180º horizontally. The diameter of both flanged slider A and flanged guider B are 10mm. The span between the flanged slider A and the flanged guide B is 100mm. A summary of the mechanical components used for the structure, a photographic image of, and a schematic of the rotary guider are shown in Table 2.4, Fig.2.11, and Fig. 2.12 respectively. The tension is

generated by the surface friction force between the tape and the slider A of the rotary guider in Fig. 2.11. The rotary guider actuates the amount of surface friction force between the tape and the slider A by rotating the rotary guider based on feedback from the tension sensor that is described in the next section. The DC servo motor is connected to the micro-control-unit-based homemade rotary guider controller which also drives the supply pack driving the DC motor, and rotates the guider using a PWM signal from the controller. Fig. 2.13 shows screenshots of the rotary guider with rotation angles of 0°, 20°, and 40° when the case of tape pack diameter is 96mm and 50mm.

Rotary Guider	Rigid Plate (TAMIYA Universal Plate) × 1 Probe_Holder_Base: DWG No 7 (Appendix B) × 1 Servo_Motor_Holder: DWG No 9 (Appendix B) × 1
Flanged Slider A	Diverted from a HP Commercial Tape Drive × 1
Flanged Guide B	Diverted from a HP Commercial Tape Drive × 1
Driving Source	5V Parallax Standard Servo Motor × 1

Table 2.4: Mechanical components of rotary guider.

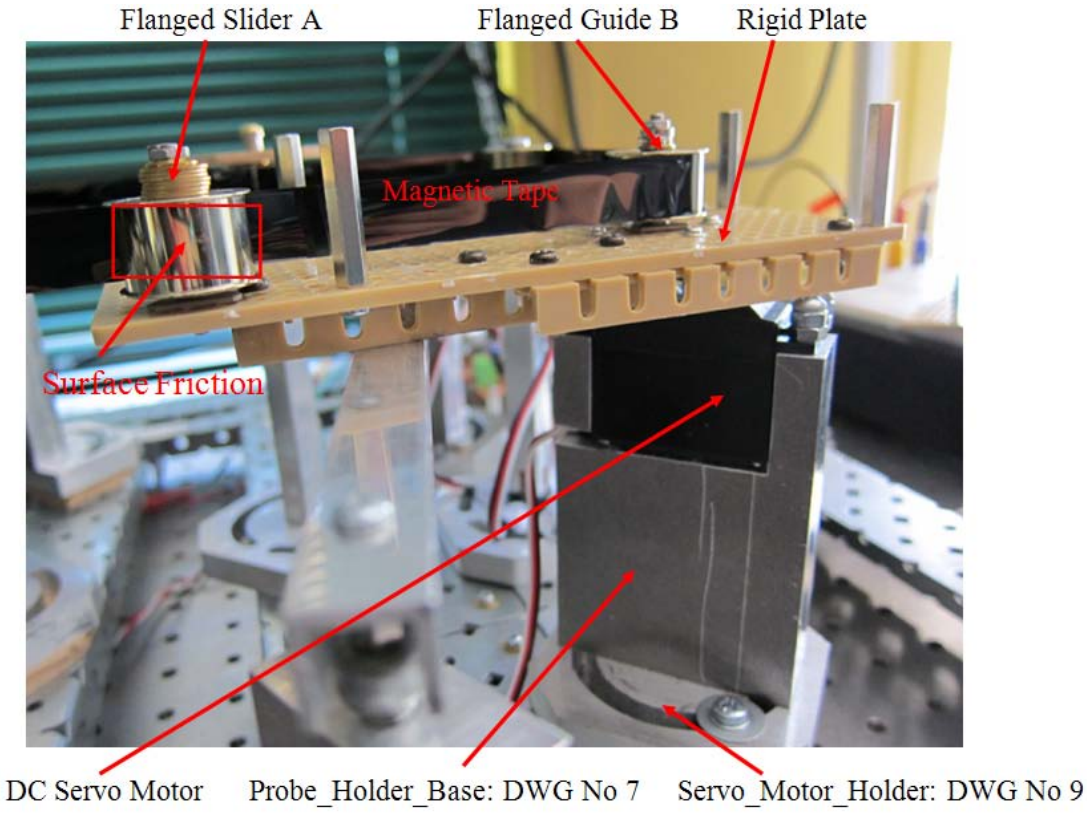

Fig. 2.11: A photographic image of developed rotary guider.

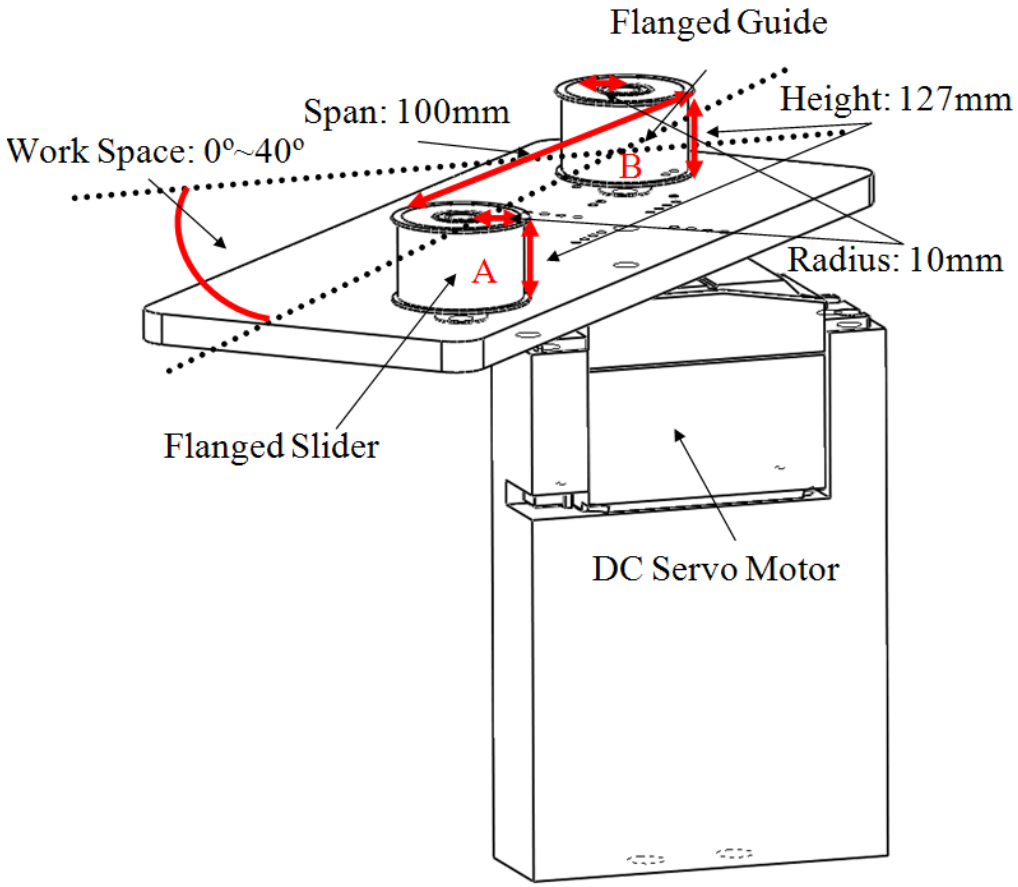

Fig. 2.12: A schematic of rotary guider.

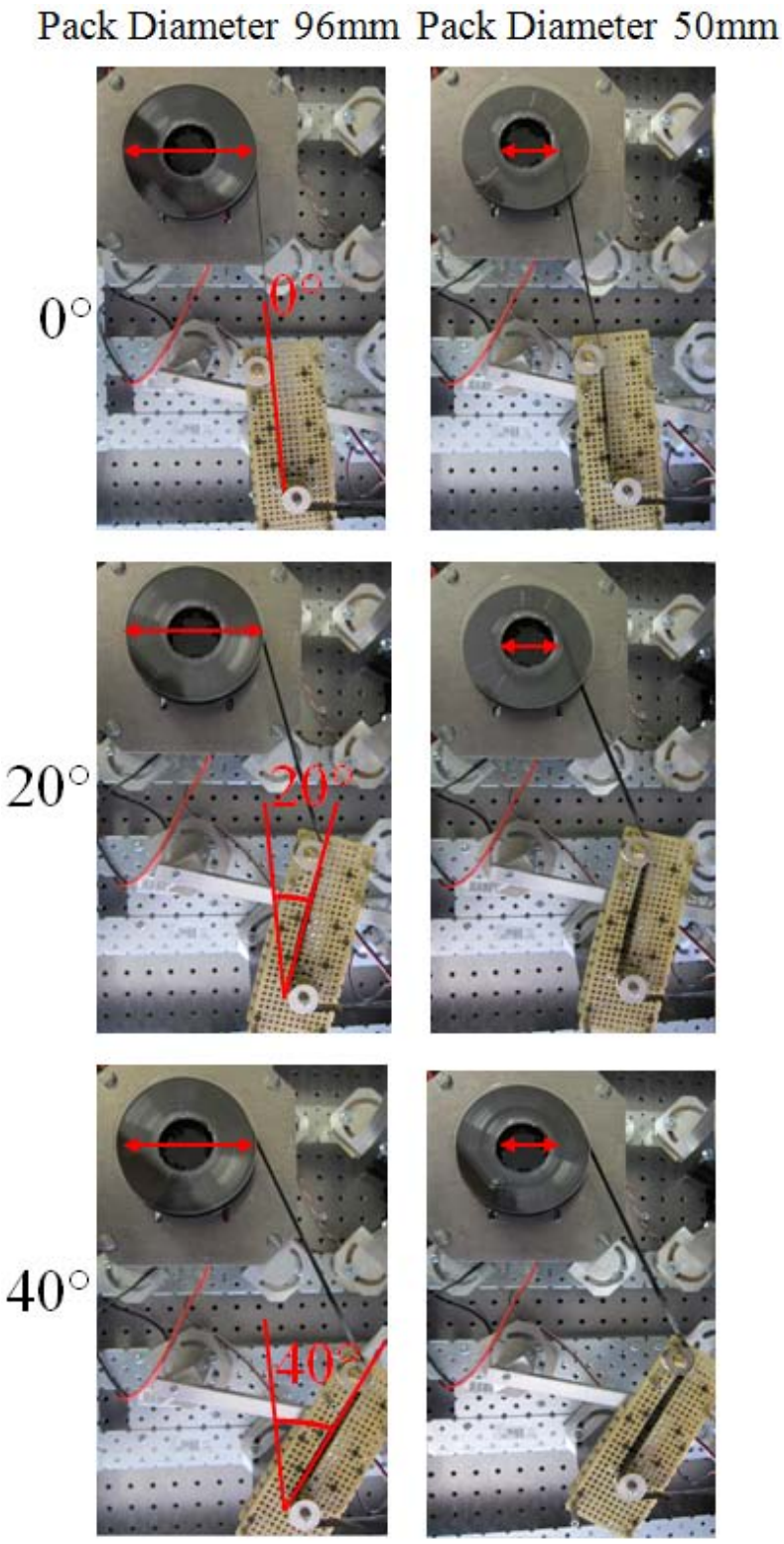

Fig. 2.13: Screenshots of rotation of rotary guider with rotation angle (a) 0°, (b) 20°, and (c) 40°.

2.4.3 Stationary Flanged Guide

The stationary flanged guide is structured with an aluminium body, a leg, and a rotatable cylindrical flanged guide that is diverted from the HP commercial tape drive. Table 2.5 below shows the mechanical components that are used to form a stationary flanged guide. Fig. 2.14 shows photographic images of flanged guides C and D. Flanged guide C is used to measure the tension, and tension sensor that is discussed in the next section are attached. Extra flanges were added to flanged guide D in order to prevent misalignment with the tape path.

Stationary Guide	Guide_Pole: DWG No 5 (Appendix B) × 2 Guide_Pole_Leg: DWG No 6 (Appendix B) × 2
Flanged Guide C & D	Diverted from a HP Commercial Tape Drive × 2

Table 2.5: Mechanical components of stationary guide.

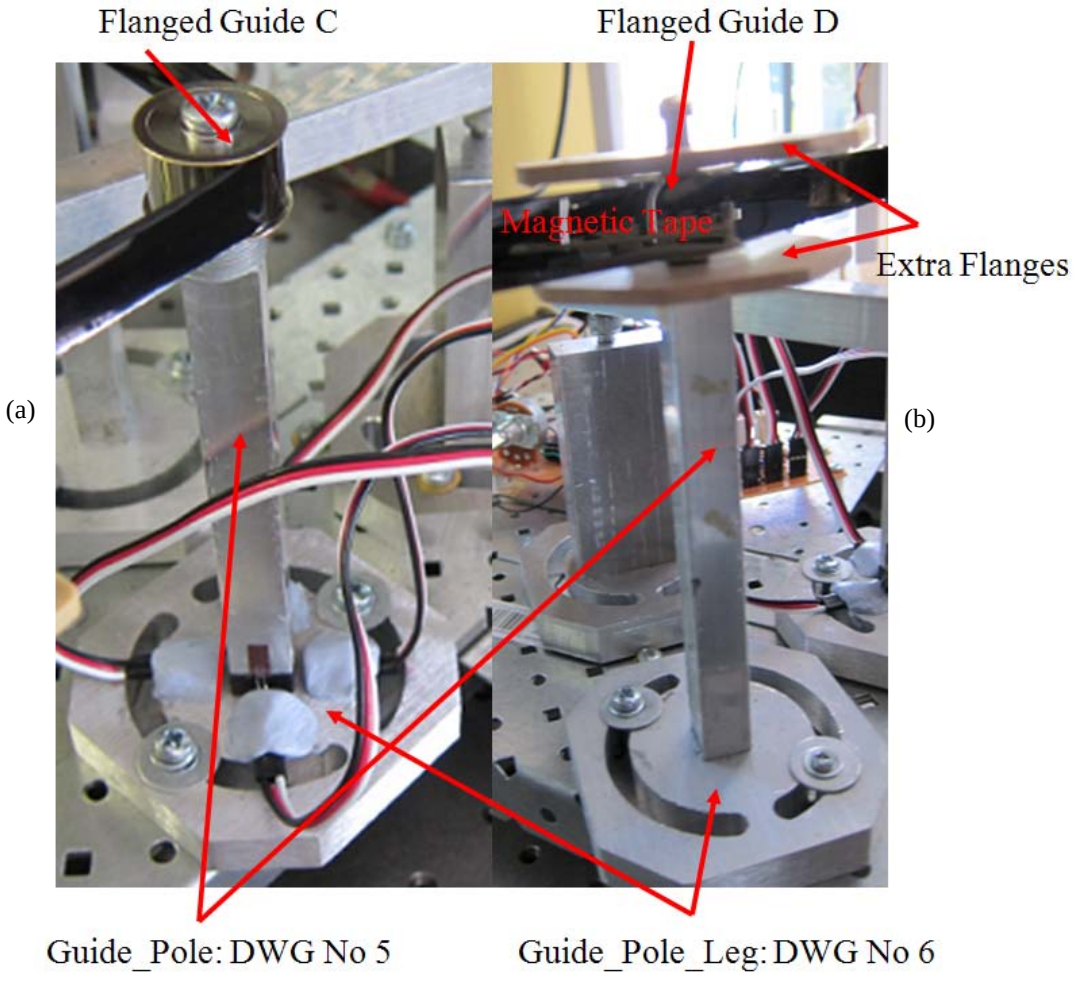

Fig. 2.14: Photographic image of stationary guides (a) flanged guide C and (b) flanged guide D.

2.4.4 Tension Sensor

In order to regulate the travelling tape tension, measuring current tape tension is essential. The developed magnetic tape drive system was designed to regulate travelling magnetic tape tension between guide posts B and C where the read/write head is normally placed in the tape drive products. This is shown in Fig. 2.4. Tape tension is measured by two sets of 2-active-gauge method employed strain gauges based tape tension sensors that are implemented on the guide post C in Fig. 2.4. A close up schematic of tape tension sensors is shown in Fig. 2.15. Each strain gauge set (Kyowa KFG-5-350-C1-11) is connected to the bridge circuit (Wheatstone bridge), and the output signal is amplified by the gauge amplifier with a gain of 1000 (BB INA101 High Accuracy Instrumentation Amplifier), then the amplified signal is conditioned by a 1Hz low pass filter. Finally, the signal is sent to the rotary guider controller (MCU) and goes through an analogue to digital conversion process. An electric circuit diagram and photographic images of the bridge circuit, amplifier, and low pass filter and are shown in Fig. 2.16 and 2.17 respectively. Fig. 2.18 shows a top view schematic of SG sets 1 and 2, and the applied load vector of each SG set. In a case where tape motion is static, tape tension Ta and Tb shown in Fig. 2.18 are equal amounts and the load "T" applied to flanged post "C" is on the axis of "T1" with θ as 0°. However, since magnetic tape is travelling, the strains on the pole that are measured by strain gauges are dynamic strain and the angle of axis of load "T" θ is changed depending on the difference between Ta and Tb; therefore, in order to measure tape tension accurately, the strain gauges must be placed on the axis of load "T". Hence, travelling tape tension is measured by using two sets of strain gauges. Load "T" is calculated by equation (3) using SG set 1 "T1" and SG set 2 "T2" as its elements.

$$T = \sqrt{T1^2 + T2^2} \quad \text{- (3)}$$

(Where T is the load applied to the guide (N) and T1 & T2 are elements of T (N).)

Tape tension is calculated based on measured load "T". Since tape travelling direction is as shown in Fig. 2.18 below, the relationship between Ta and Tb must be Ta > Tb, and tape wrap angle is fixed at 45º, the angle of load "F" θ is located between $0° \leq \theta \leq 45°$. Further 2-active-gauge method is applied in order to double the signal strength.

Tension Sensor	Strain Gauge (Kyowa KFG-5-350-C1-11 (350Ω)) × 4
Wheatstone Bridge	350Ω Resister × 4
Instrumentation Amplifier	BB INA101 High Accuracy Instrumentation Amplifier × 2 100KΩ Pot Resister × 2 10KΩ Variable Resister (40 Ω) × 2 0.1μF Capacitor × 2
Low pass Filter	1.6KΩ Resister × 2 100μF Capacitor × 2

Table 2.6: Electrical components of tension sensor.

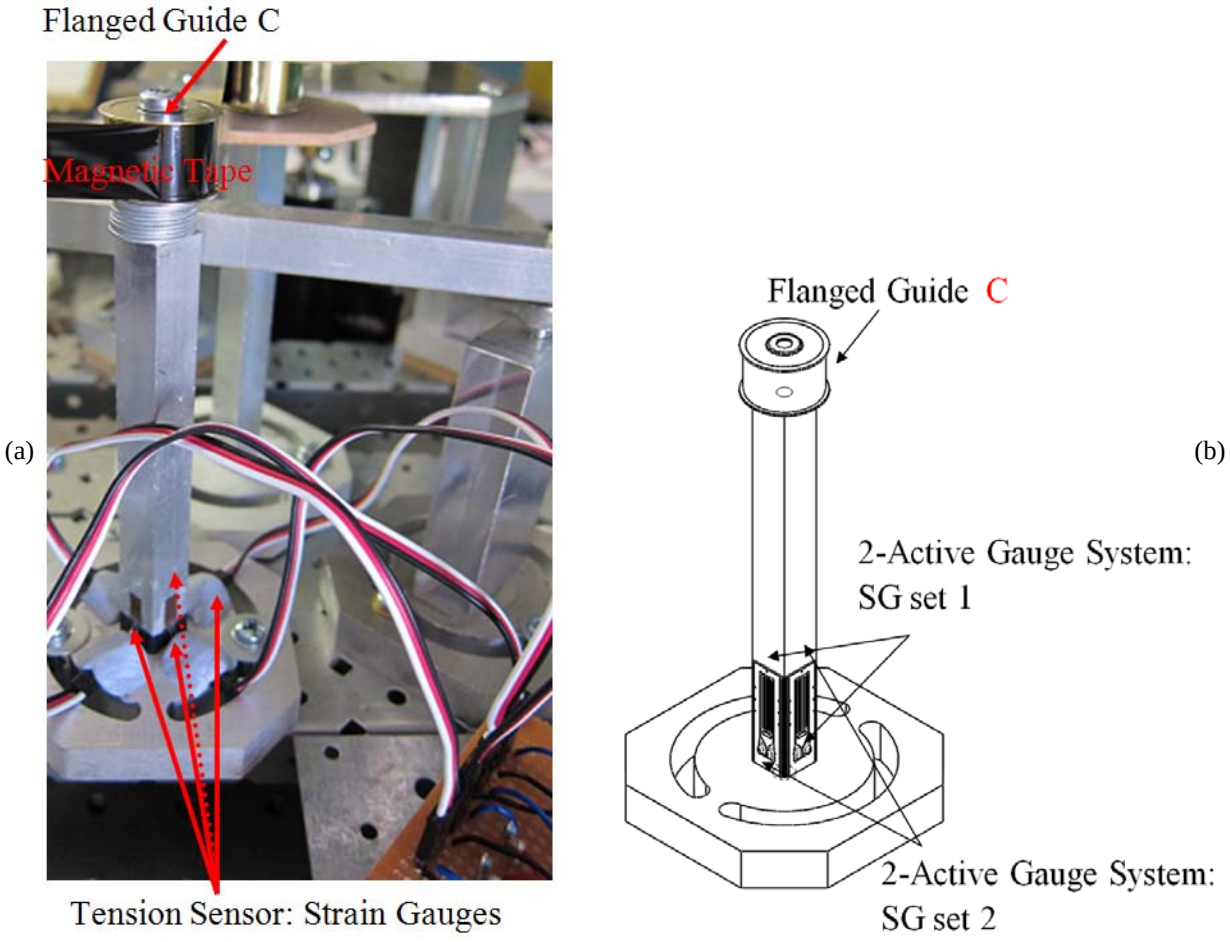

Fig. 2.15: A screenshot (a) and schematic (b) of strain gauges based tension sensors.

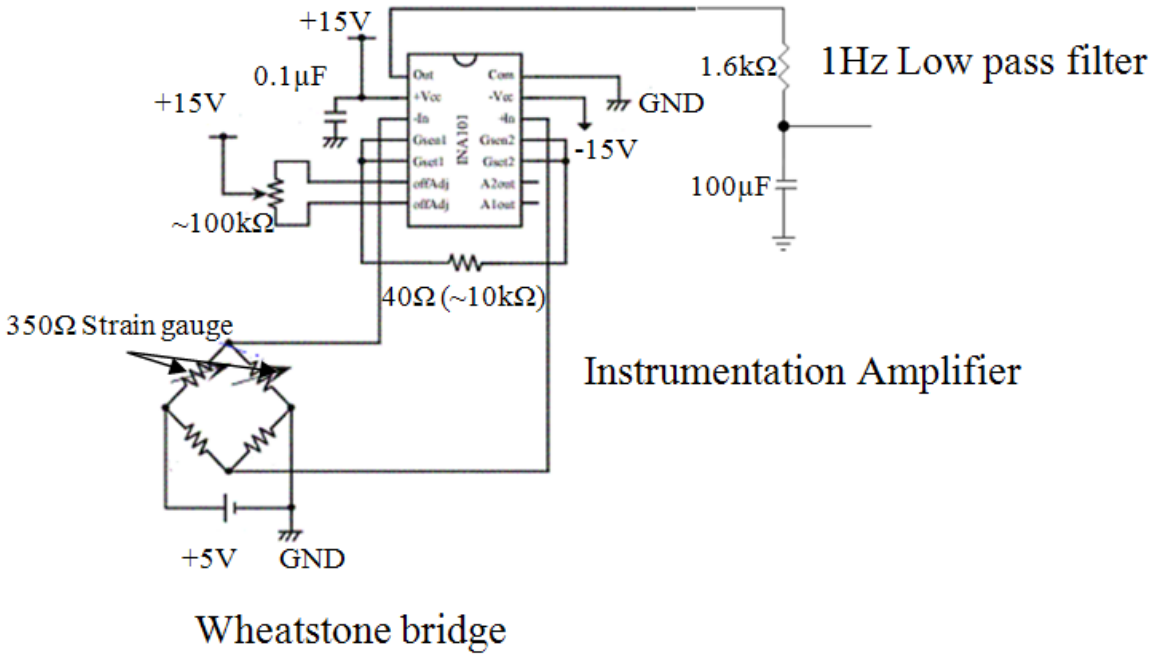

Fig. 2.16: A circuit diagram of bridge circuit and amplifier.

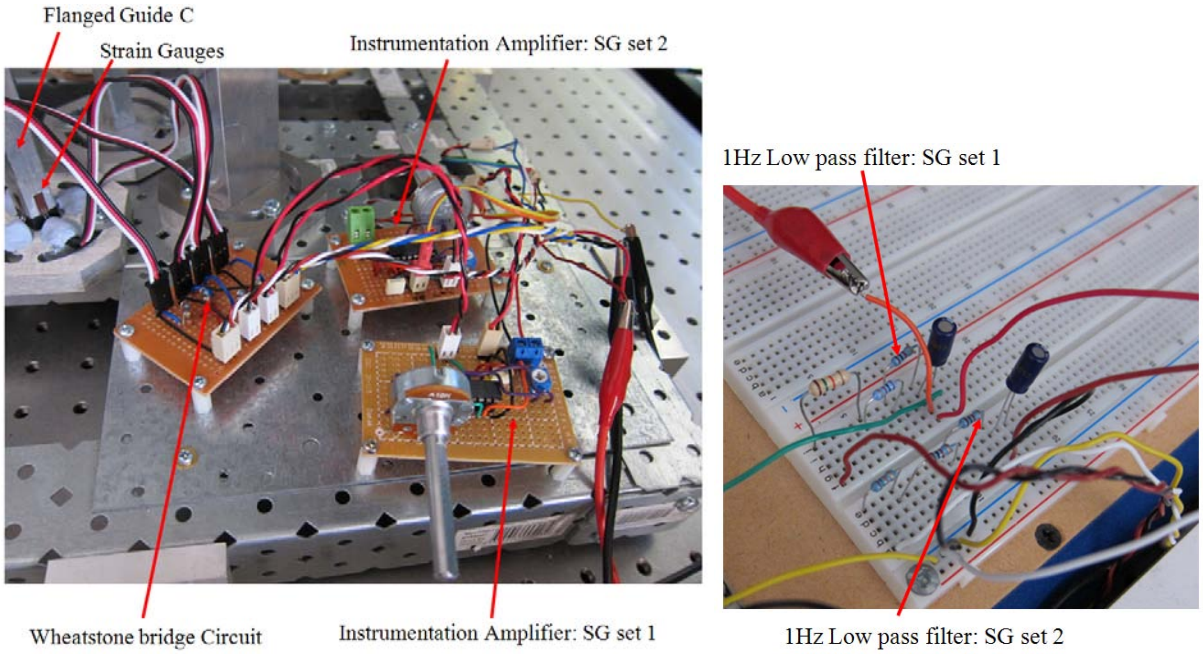

Fig. 2.17: Photographic images of developed bridge circuits, amplifiers, and low pass filters.

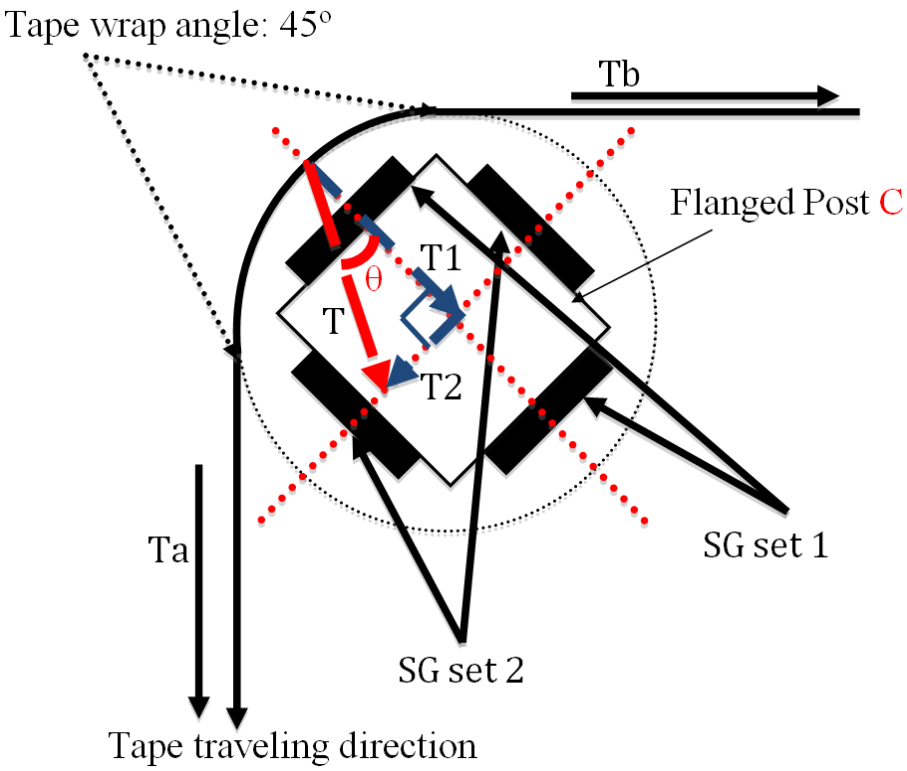

Fig. 2.18: A top view schematic of tension sensor placements.

(A) Strain Gauges Calibration

In order to convert outputs from strain gauges based tape tension sensors to tape tension, the calibration of sensors is required. Fig. 2.19 shows a photographic image and a schematic of the strain gauges calibration stand. This calibration is carried out with static tape motion. A certain length of magnetic tape is fixed on the rigid stationary wall and a weight is hung on the other side of the tape. The weight is initially 0g, and then it is increased by 10g up to 100g. One of the strain gauge set is attached on the axis of resultant force created by tension Ta and Tb with angle R_θ as 45°; a measured strain is created by the load "T1" ("T2") as shown in Fig. 2.18. The output voltage of strain gauges with each weight is recorded. The calibration of the other strain gauge set is also carried out with the same procedure. Fig. 2.20 shows the calibrated functions of both strain gauge sets with the relationship between output voltage of strain gauge (V) and weight (N). Both calibrated functions display linear characteristics. The gradient of each function is obtained by taking fitted curve; 0.0738 for SG set 1 and 0.0708 for SG set 2. The conversion equations of both SG set 1 and 2 from strain gauge output to load applied is shown in equation (4) and (5) respectively. "T1" and "T2" measure the load applied to flanged post C that is same

as tape tension. Therefore, from equation (3), the calculated load applied to flanged post C "T" in Fig. 2.18 equals the tape tension. Hence, tape tension is mentioned as "T" in the following sections.

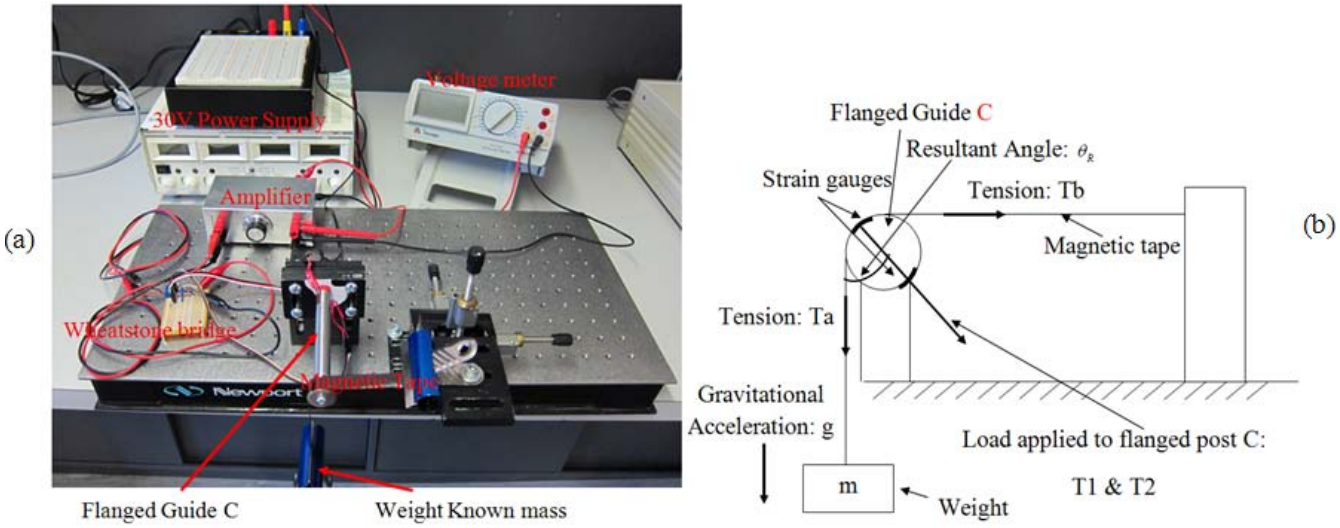

Fig. 2.19: A screenshot (a) and schematic (b) of tension sensor calibration stand.

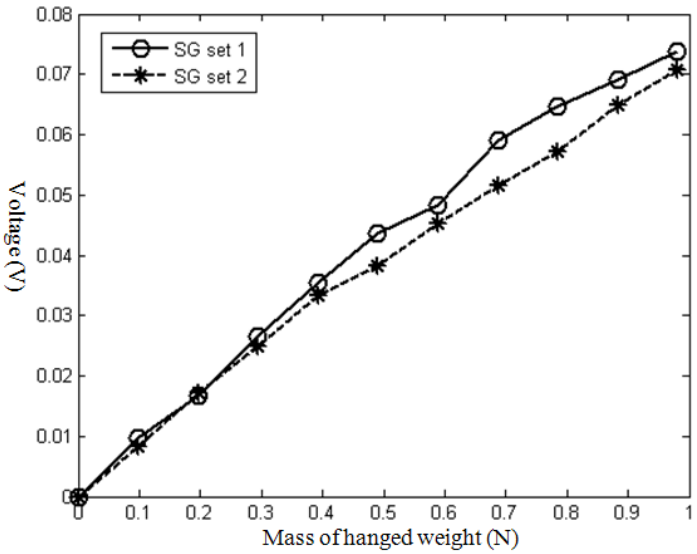

Fig. 2.20: Calibrated functions of both tension sensors SG set 1 and 2.

$$T1 = \frac{V_1}{0.0738} \text{ - (4)} \qquad T2 = \frac{V_2}{0.0708} \text{ - (5)}$$

(Where T1 (T2) is load applied to strain gauge set 1 (2) (N) and V1 (V2) is voltage out form strain gauge set 1 (2) (V).)

(B) Wrap Angle

The wrap angle of the stationary post increases as tape is transported due to an increase in the diameter of tape take pack up as shown in Fig. 2.21. In order to apply the calibrated results obtained in the previous section, the wrap angle of stationary guide C $2\theta_R$ must be maintained at 90°. However, the wrap angle $2\theta_R$ increases up to θ_α corresponding to the diameter of take up pack D as shown in Fig. 2.21. Therefore, it is essential to insert an extra stationary guide between the stationary guide C and the take up pack in order to maintain the wrap angle of statuary guide C at constant. An extra stationary guide D is inserted in the tape path, and Fig. 2.22 shows a photographic image of the extra stationary guide D.

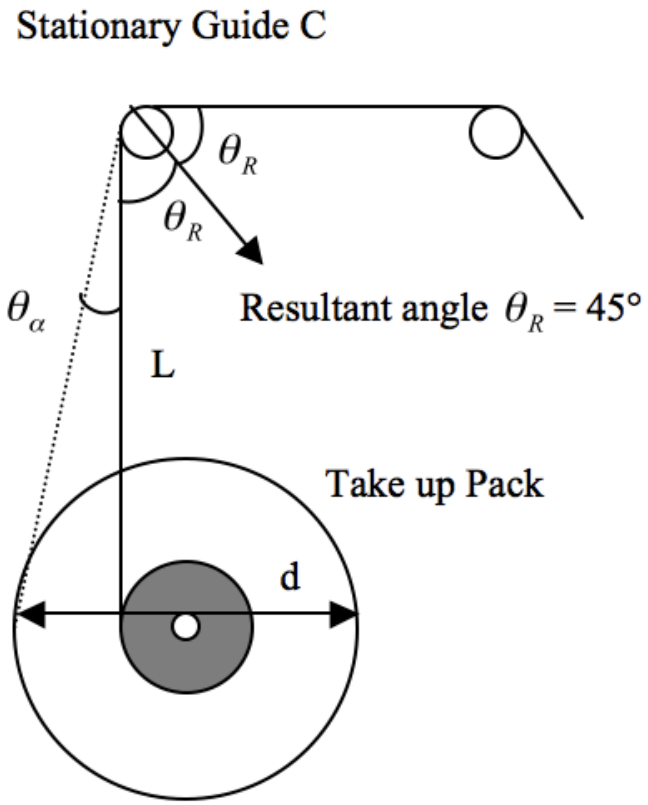

Fig. 2.21: A schematic of wrap angle change around stationary guide C.

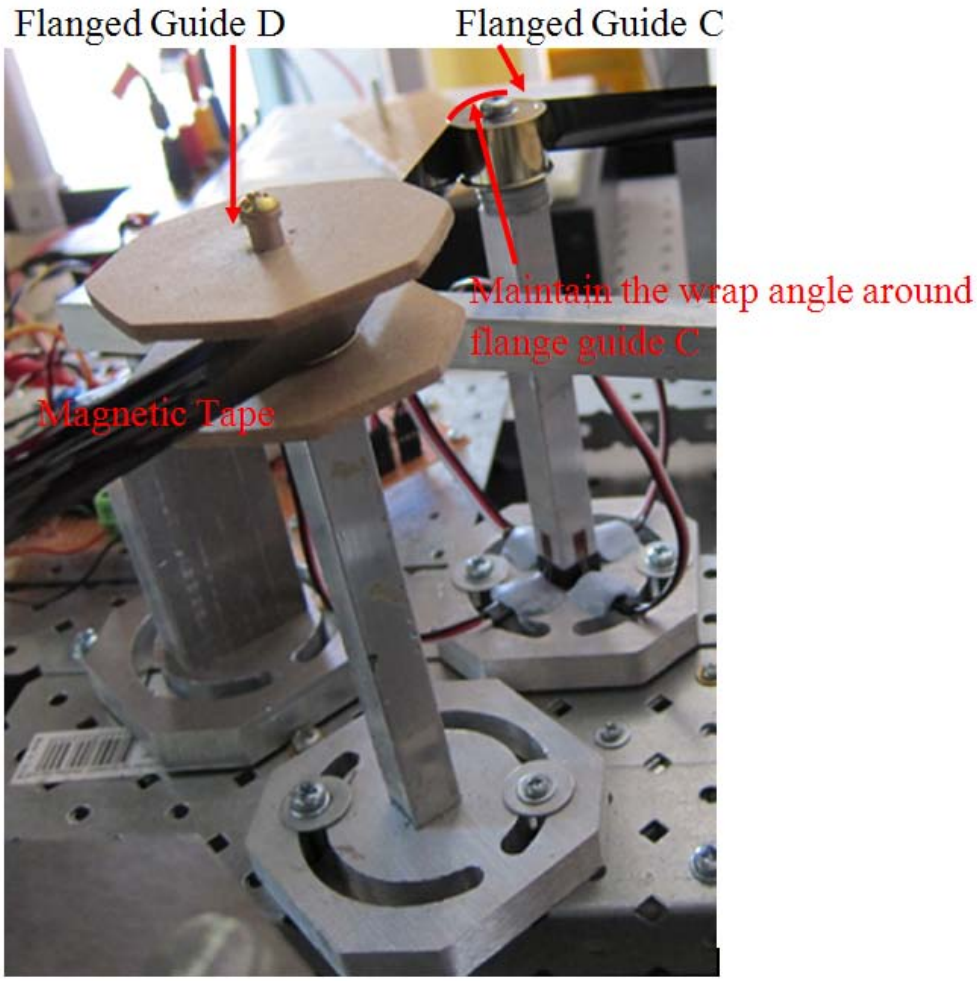

Fig. 2.22: A photographic image of extra stationary guide D.

2.5 Software Development

In this section, development of control units, the system driving software, and control GUI are described including connections of control units and control GUI. The tape transport system driver was developed in order to control elements of the developed system.

2.5.1 Control Elements, Instrumentations, and Software Development Environment

The developed tape transport system is required to control the following elements:

- Control the tape pack driving DC motor.
- Measure tape tension.
- Control rotation of rotary guider based on measured tape tension.
- Display logs and record measured tension and trajectory for rotary guider.

Table 2.7 below lists a control unit, motor controllers; software including GUIs are used to control the operations of tape transportation. The operations of the tape system are controlled by a micro-control unit (MCU). AKI H8/3052f that was chosen as a MCU for the developed tape system. AKI USB development board for the MCU is used in order to establish the serial communication line between MCU and the control PC. Both tape pack driving motors are controlled by a motor controller. The driving motor of the supply pack is controlled by a Parallax HB-25 motor controller, while the driving motor of the take up pack is driven using a Maxon EPOS2 24/5 digital motor controller. Operations of the system are commanded by the control PC through operation GUI. In this developed system, the forward pass operations are commanded by the EPOS Studio motor control GUI (Maxon motor ag, 2010); other operations such as control of rotary guider, tension measurement, and rewind operation of tape are commanded by a Windows HyperTerminal Based control GUI.

Fig. 2.23 shows photographic images of the MCU and both motor controller A and B are shown in Fig. 2.4. Technical specifications of control components are listed in Appendix A.

Micro Control Unit MCU	AKI-H8/3052f with USB Development Board × 1
Motor Controller A	Parallax HB 25 Motor Controller × 1
Motor Controller B	Maxon EPOS 2 24/5 Digital Motor Controller × 1
Development Software	Best Technology Inc GCC Developer Lite Ver2.36 × 1
GUI	Windows Hyper Terminal × 1 EPOS Studio Ver1.41 × 1

Table 2.7: A list of control components, instrumentations and GUIs.

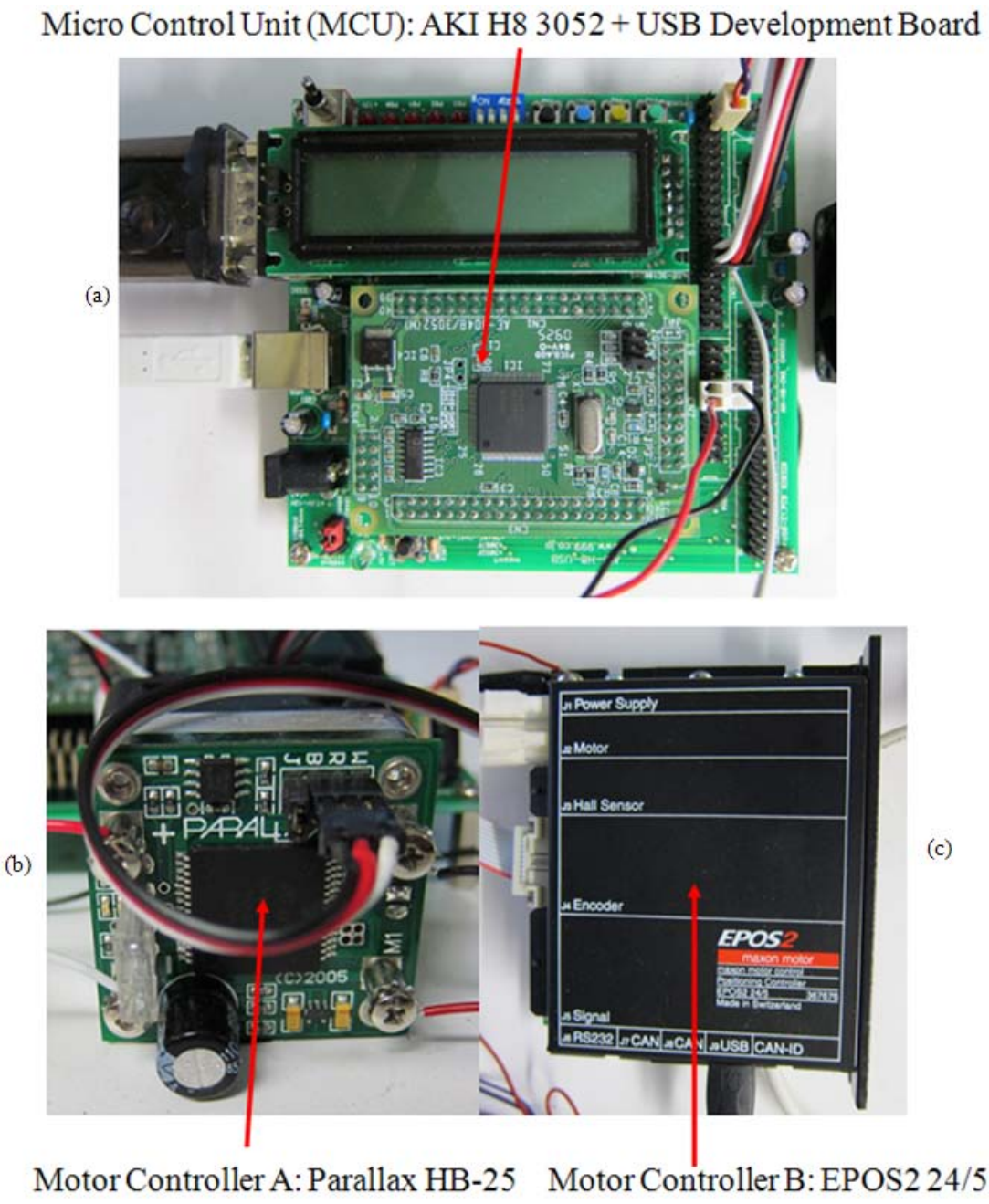

Fig. 2.23: Screenshots of (a) 16 bit micro control unit (MCU) with USB development board, (b) the motor controller A, and (c) the motor controller B.

The tape transport driving software for MCU was developed using C++ programming language in GCC Developer Lite Ver. 2.36 (BestTechnology Co., Ltd., 2010) environment. Fig. 2.24 shows a screenshot of the developing environment. Full program codes of the developed tape transport system drive are shown in appendix C.

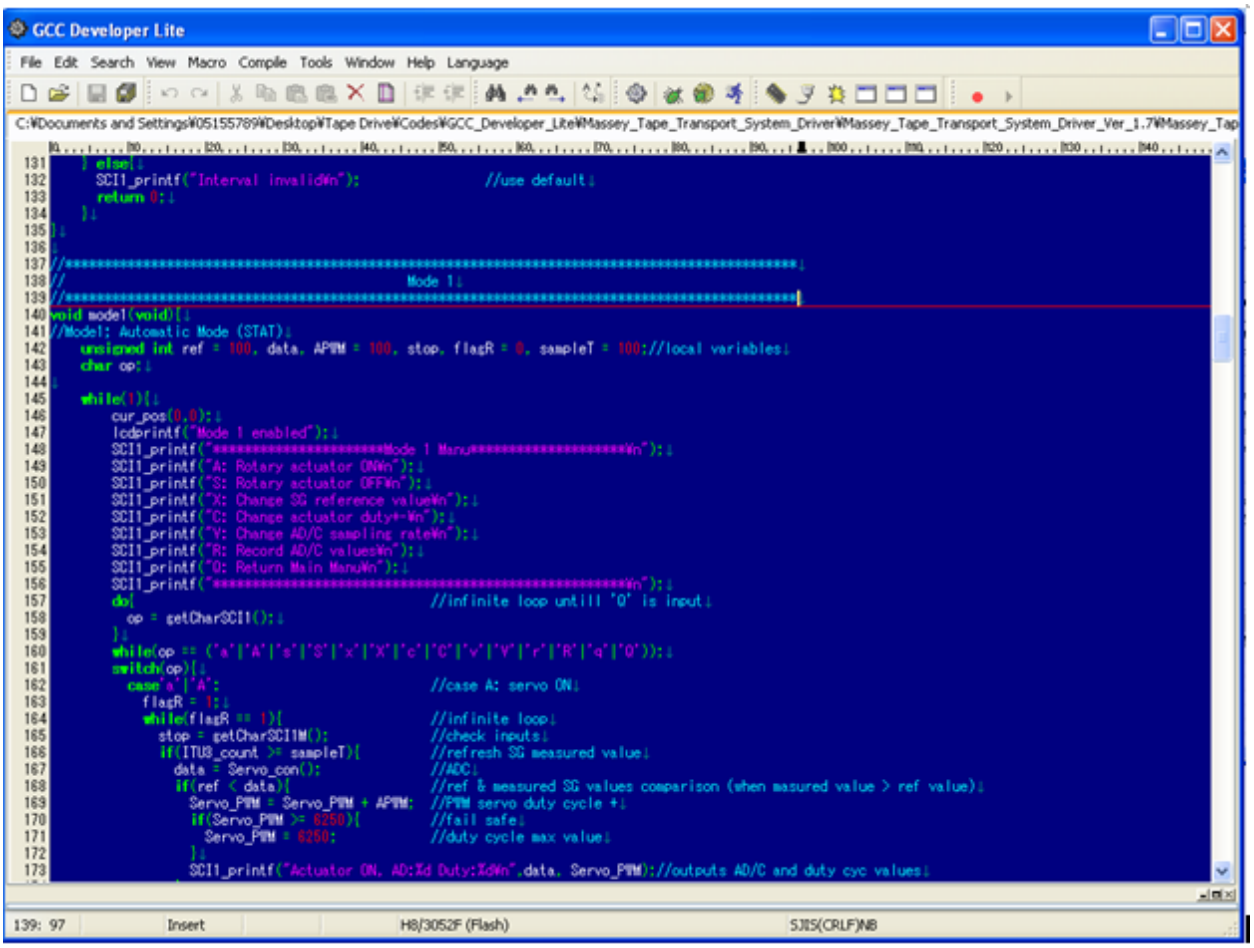

Fig. 2.24: A screenshot of GCC Developer Lite developing environment.

(BestTechnology CO., LTD., 2010)

2.5.2 The Tack up Stand Control

The take up pack is driven by a Maxon DC motor; the operation of the motor is controlled by an EPOS Studio graphical user interface (GUI) (Maxon motor ag, 2010) on a control PC through a motor controller (Maxon EPOS2 24/5). Fig. 2.25 shows connections between the controls PC (GUI), the motor controller, and DC motor. The operator inputs desired angular speed of motor in rpm with acceleration and declaration gain in rpm/sec. Motor controller controls the motor's rpm as desired by sending PWM signals to the motor based on the feedback encoder implemented within the motor. Measured rpm is also displayed on GUI as shown in Fig. 2.25.

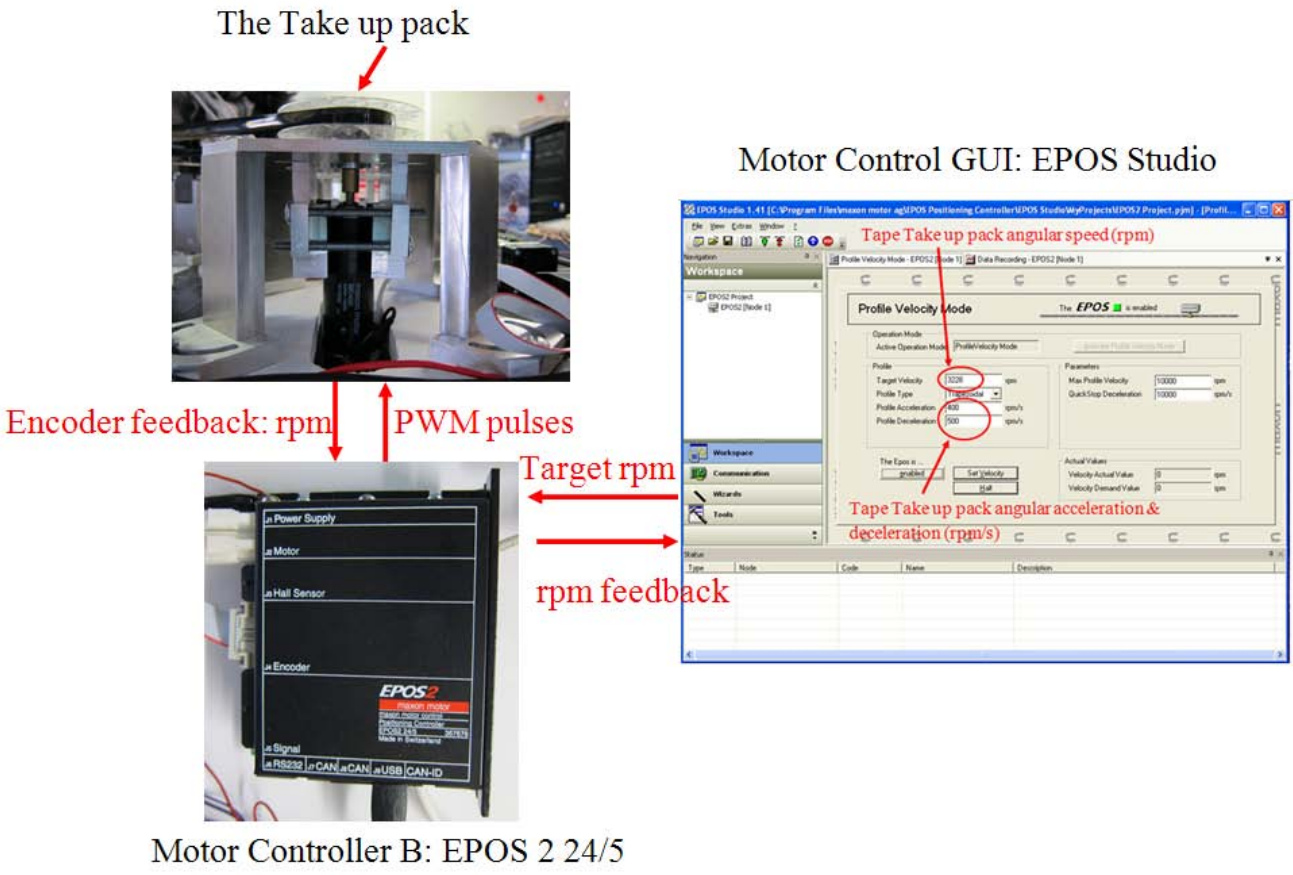

Fig. 2.25: A connection flowchart of the take up stand.

2.5.3 The Rotary Guider and the Supply Pack Control

AKI H8/3052f MCU control the operation of the tape supply pack driving motor and measures the travelling tape tension using the tension sensor. It then controls the rotary guider based on the measured tape tension. The driving motor for the supply pack is controlled by PWM of MCU and HB 25 motor controller. The motor controller amplifies the PWM signal generated from PWM port channel 1 of MCU to a stronger signal to drive the motor. Both measured analogue tension signal SG sets 1 and 2 are sent to the analogue-to-digital converter port channels 1 and 2 respectively and converted to digital signals. The resolution of the analogue signal is 10bit (1024). The converted digital signal is processed to calculate total tension within the MCU, and PWM port channel 2 sends a signal to the rotary guider to rotate the angle to regulate the tension. The operation of the system is commanded by the Windows Hyper Terminal based control GUI by establishing the serial communication line between the MCU and the control PC. MCU also replays responses to commands such as display the measured tape tension from both tension

sensors; the current angle of rotary guider from control GUI. Fig. 2.26 illustrates the connections between MCU and other control components.

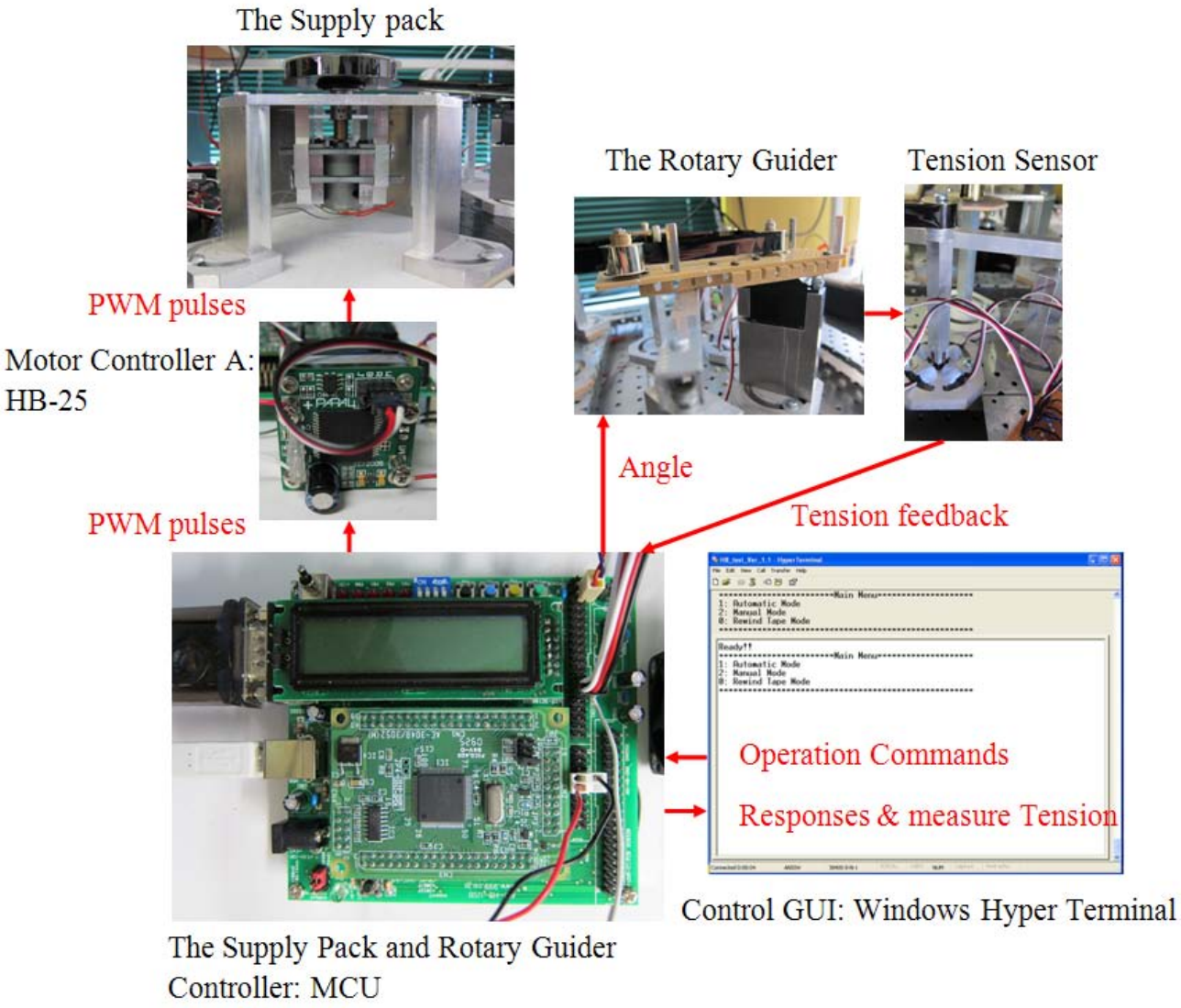

Fig. 2.26: A connection flowchart of the supply stand and rotary guider.

Fig. 2.27 shows the flowchart of the developed control GUI based on Windows Hyper Terminal. The control GUI initially opens up when the main menu is booted. To command the system, an operator chooses a mode from selections of automatic mode, manual mode, and rewinding mode. Automatic mode enables the tape tension regulation with dynamic tape path alternation. Manual mode enables the manual control of the rotary guider. Rewinding mode enables the reverse pass operation of tape transport. To enable each mode, input from a corresponding key is. For example, to enable Automatic Mode, pressing the 1 on the keyboard of the control PC.

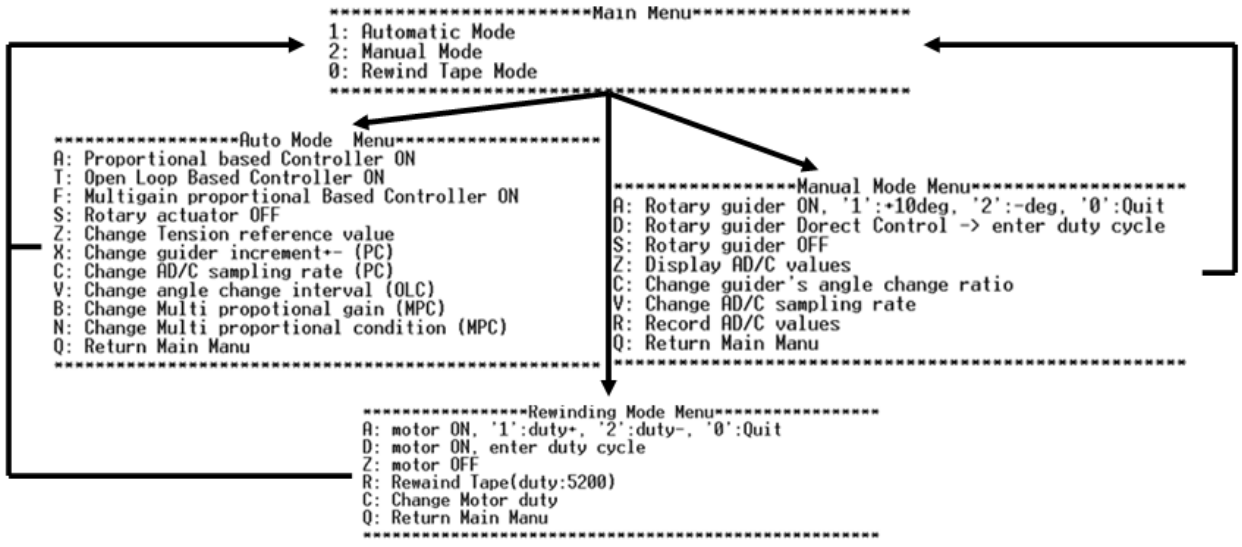

Fig. 2.27: A flowchart of developed Windows Hyper Terminal Based tape drives system control GUI.

2.6 Design Footsteps and Key Issues

Fig. 2.28 shows photographic images of early design and later design of the tape transport system; particularly the design of the rotary guider. In the early design of the rotary guider, the rotation centre of was not located at the flanged guide B when compared to its later design. The early design of the rotary guider had its workspace between 0° and 180° horizontally. However, the span between the flanged slider A and the flanged guide B differs corresponding to the rotation angle of rotary guider. That parameter increases the complexity of rotary guider dynamics; therefore, to reduce the parameter of rotary guider, the span between the flanged slider A and the flanged guide B are fixed by setting the rotation centre of the rotary guider as the flanged guide B as shown in the later design of the rotary guider in Fig. 2.28. Fig. 2.28: Screenshots of development steps of the tape transport system. A key issue of the developed tape transport system is the noise contained in the measured signal from the strain gauge based tension sensor. Fig. 2.29 shows the raw measured signal from the tension sensor SG set 1 with stationary tape. A huge amount of noise was observed. Therefore, conditioning of signal was essential to measure the tension accurately. An analogue low pass filter with its cut off frequency 1Hz is implemented as a simple signal condition after the bridge amplifier before the signal is converted to digital form at MCU. However, the effectiveness of low pass filter to noise is minor. Since the tape is axially moving the measured strain of the tension sensor is dynamic strain, appropriate signal conditioner is essentially required to clear the noises. In this tape system, the measured tension is recorded as a txt format file in digital form and offline analysis are performed using MATLAB environment with a digital low pass filter. However, for the real time processing of tension regulation at MCU, the noise of feedback signal degrades the accuracy of

tension measurement drastically. It is recommended that developing a signal conditioner and implementing it in the bridge circuit in order to clear the noise of the tension sensor signal.

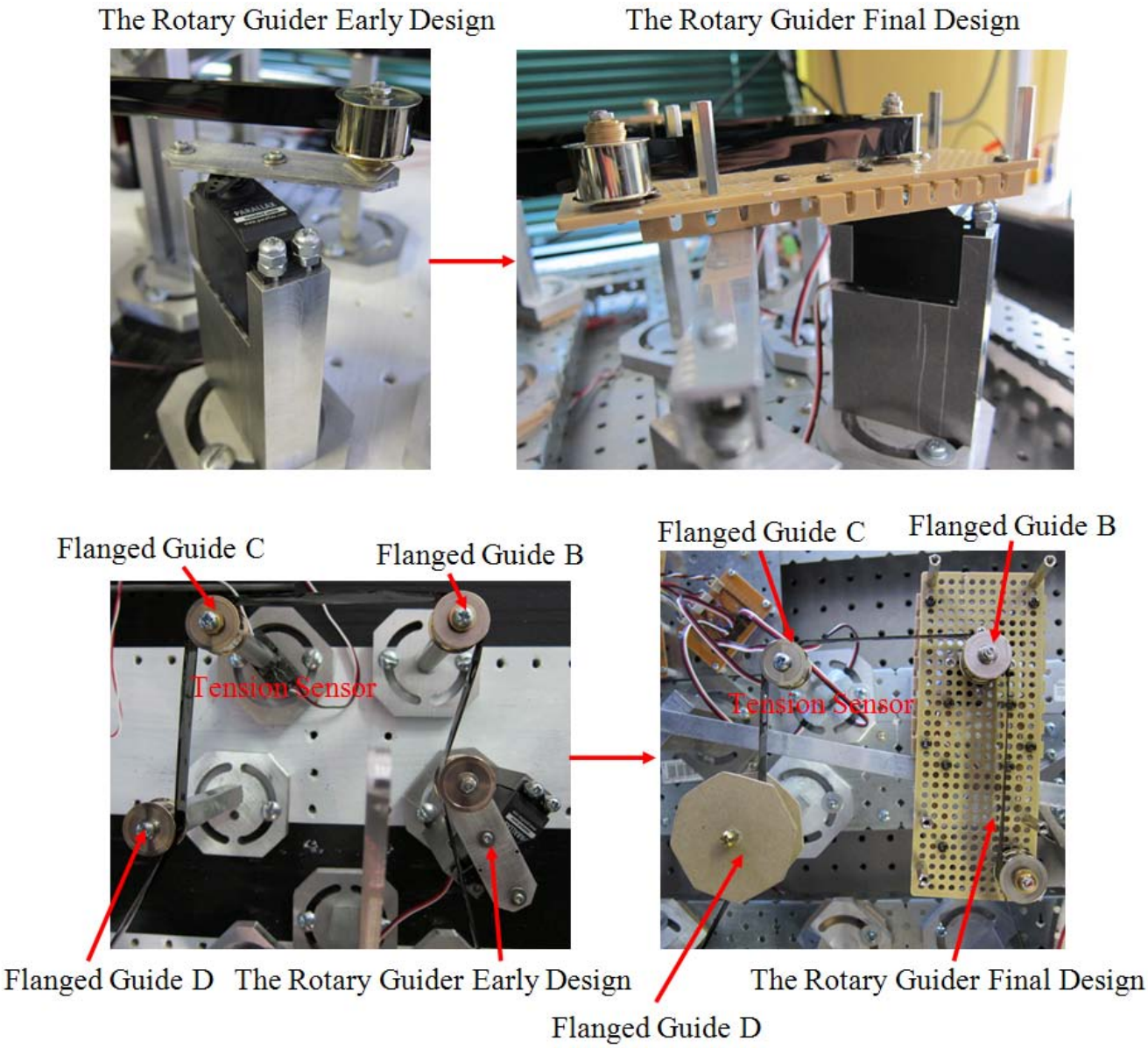

Fig. 2.28: Screenshots of development footsteps of tape transport system.

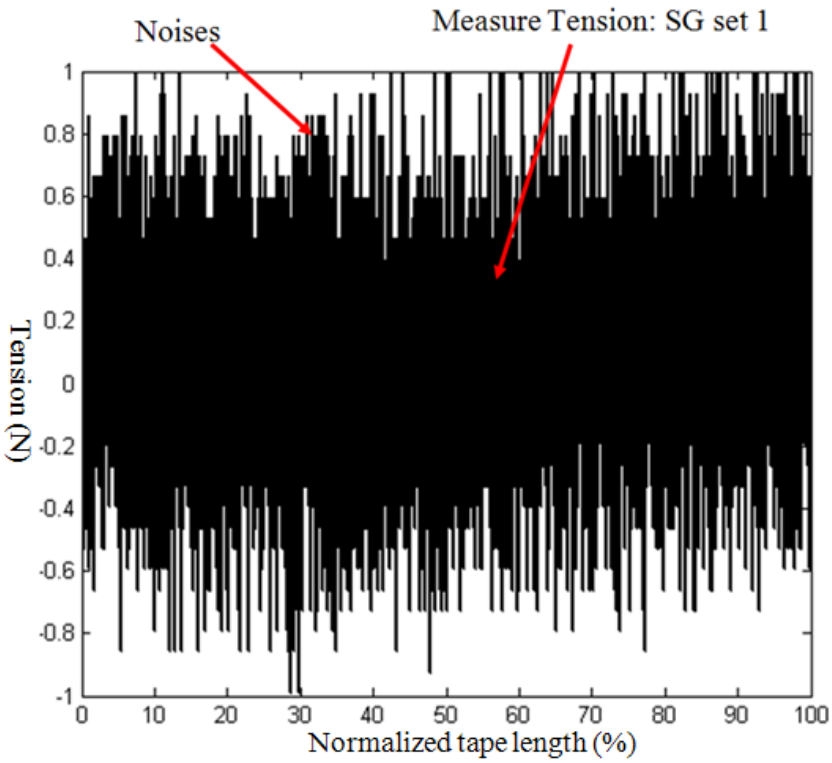

Fig. 2.29: Raw output signal of tension sensor (SG set 1).

2.7 Chapter Summary

This chapter presented a mechatronics integration of a linear high-density magnetic tape transport system that enables travelling tape tension regulation in closed loop control. The travelling tape tension is regulated by the rotary guider using feedback from the strain gauge based tension sensor. The tape is transported between the two tape packs over the guides as the tape packs are driven by high power DC motors. Operations of the developed tape transport system are commanded through the control PC with keyboard command input. However, the feedback signal from the tension sensor contains a huge amount of noise that degrades the accuracy of tension measurements. It is strongly recommended that condition the output signal of tension sensor be corrected before processing it as feedback of the closed loop control algorithm.

Chapter 3

Static Tape Path with Novel Rotary Guider

3.1 Chapter Overview

A homemade linear high-density magnetic tape transport system that enables the travelling tape tension regulation using the rotary guider in closed loop control was described in the previous chapter. Before investigating the effectiveness of tension maintainability of the developed system, the transitions of travelling tape tension during the tape transportation were calibrated in order to investigate the tension controllable region of the rotary guider. This chapter examines the transitions of travelling tape tension of the developed tape transport system through experimental studies. The parameter studies cover the travelling tape speed and the angle of the rotary guider. The tape path is altered depending on the angle of the rotary guider, and it is fixed during the tape transportation process. The tension increases as tape is transported. It was found that the state of change in tension heavily relies on the dynamics of the tape pack driving DC motor. The higher travelling speed of tape generates greater tension. The role of the angle of the rotary guider is to shift the level of tape tension and a higher rotation angle of the rotary guider generally generates a greater tape tension.

3.2 Test Apparatus and Experiment Procedure

A schematic of the test apparatus is shown in Fig. 3.1. The span between the flanged guides A, B, C, and D is fixed at 100mm. The wrap angle of tape around flanged guide C is fixed at 45º ($\theta_R = 45°$). The workspace of the rotary guider is set between 0º and 40º horizontally. The linear tape open 4 (LTO4) tape media is transported from the beginning-of-tape-position (BOT), to the end-of-tape-position (EOT), which are set at the diameter of the supply pack, 96mm and 55mm respectively, for all tests. The total length of tape transported from BOT to EOT is 660m. The tape travelling speed is set at 4m/s and 7m/s that correspond to the angular speed of the tape pack at 1004 rpm and 1756 rpm respectively. The tension is measured by using the strain gauge based tension sensor that is integrated into the flanged guide C. Outputs from the tension sensor are monitored and recorded through the data acquisition (DAQ) PC with the sampling frequency 500Hz. Recording is started once the tape pack driving motor is enabled. All tests were conducted in a 25° Celsius, normal atmosphere pressure laboratory environment. The summary of test conditions is shown in Table 3-1. The procedure to investigate the transition of tape tension in the function of length of transported tape contains the following steps:

(1) Initialize the tape transport system - Set the tape pack driving motor and the rotary guider at desired RPM (speed) and angle respectively. Tension the stationary tape and initialize the tension sensor.

(2) Start tape transportation - turn the motor on.

(3) Run the system for the time the desired length of tape is transported - monitor and record the outputs of tension sensor.

(4) Stop tape transportation - Rewind the tape from EOT to BOT.

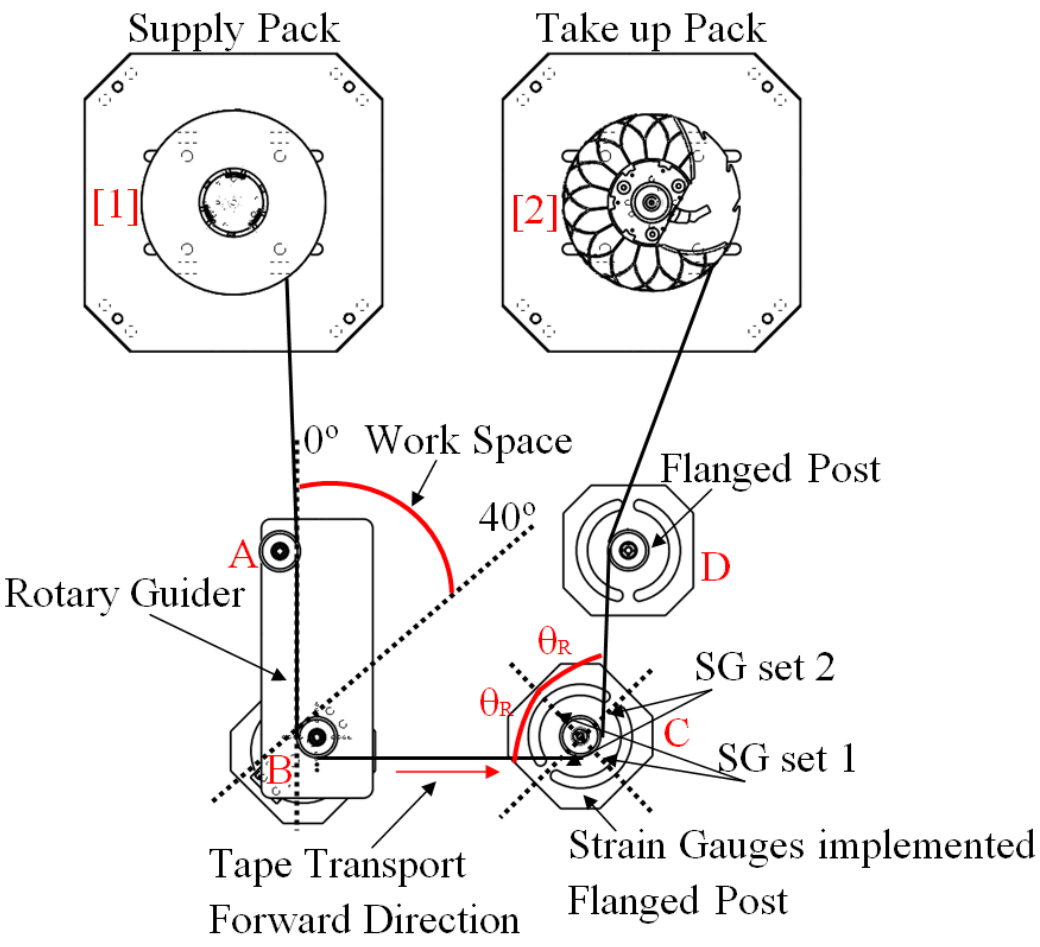

Fig. 3.1: A schematic of test apparatus.

Fixed test parameters	
Test ambient temperature	25°C
Tape span between each flanged guides A, B, C, and D	100 mm
Wrap angle around the flanged guide C	45º ($\theta_R = 45°$)
Diameter of the supply pack (LTO4)	96mm -> 55mm (BOT -> EOT)
Work space of rotary guider	0° to 40°
Sampling frequency	500Hz
Test parameters	
Target rpm of the tape pack (target average tape travelling speed)	1004 rpm (4m/s) 1757 rpm (7m/s)
Angle of rotary guider	0º, 10º, 20º, 30º, 40º

Table 3.1: Test conditions.

3.3 Tape Tension Transitions

Experimental studies were carried out with fixed rotary guider angles at 0º, 10º, 20º, 30º, and 40º to investigate the tension change in the length of transported tape. The transition of tape tension with removal of the rotary guider – the tape path is then formed by three flanged posts B, C, and D in Fig. 3.1 – is also examined in order to investigate the effective of the tape pack driving motor dynamics on the tape tension. As an example, measured output signals from SG set 1 (T1), 2 (T2), and tape tension (T) with fixed rotary guider angle at 30º at travelling tape speed at 4m/s and 7m/s are illustrated in Fig. 3.2 in the function of a normalized length of transported tape. During the first 3 percent of tape the transportation, the output signal level of SG set 1 (T1) ascends rapidly to approximately 0.32N at 4m/s and 0.68N at 7m/s due to the static torque of the tape pack driving motor. In tape speed at 4m/s, once the motor reaches a steady-state RPM at the point where approximately 10 percent of the tape is transported, T1 starts to decrease gradually; when approximately 30 percent of the tape is transported, it starts a quadric increase until the tape is fully transported. Tape speed at 7m/s performs a similar transition of tension. However, the drop level of tension is small as it is 4m/s; the level of tension is significantly higher in higher tape speed. The same tension transitions as T1 are observed for the output of T2 for both tested speeds during the first 3 percent of tape transportation. However, after this point, unlike the transition of T1, it oscillates around 0.1N at tape speed 4m/s and 0.2N at tape speed 7m/s for the remaining tape transportation. Comparing with T2 at tape speed, the tension changes for both tested speeds show similar trends, but the tape speed changes the level of tension. Higher tape speed generates greater tension. No matter which tape speed, it is apparent that the output signal level of T1 significantly

surpasses its T2 level, and the functions of T1 and T show similar tension transitions with the output signal level of T1 being slightly lower than its tape tension T. Fig. 3.3 shows the angle difference θ between the axis of T1 and the axis of tape tension T that is described in Fig. 2.18 of the previous chapter. At tape speed 4m/s, once the tape pack driving motor is turned on, it reaches 30º immediately and increases linearly to approximately 35º until 30 percent of the tape is transported; at this point, tape tension T starts to increase. After 30 percent of tape transportation, it decreases gradually and eventually approaches 15º. At tape speed 7m/s, the angle rises up to 28º when the tape pack driving motor starts, and then drastically reduces to 10º until 10 percent of tape is transported. For the remaining transportation process, it oscillates around 10º. It can be concluded that the transitions of angle are significantly related to the tension transitions of T1. Summarizing these observations, it is concluded that the output signal of T1 plays a major role in the measurement of tape tension T, and the output of T2 compensates for the level of tape tension; higher tape travelling speed generates greater tension, and the increase of torque during the tape transportation after the motor is tuned on reduces as the tape travelling speed increases.

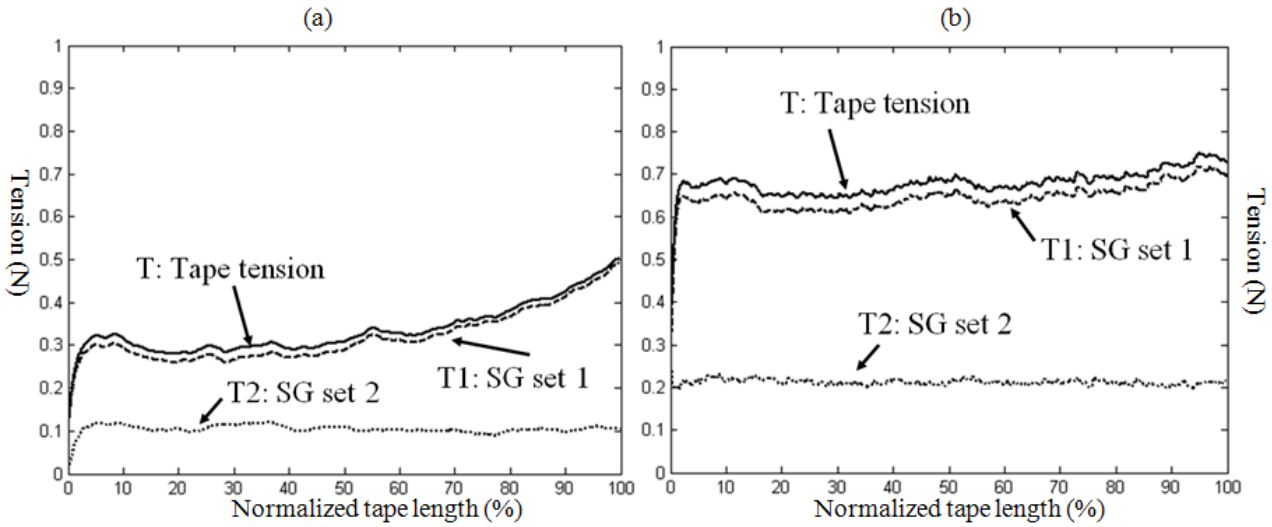

Fig. 3.2: Transitions of tension in the function of normalized length of tape transported with rotary guider angle at 30º (a) 4m/s, (b) 7m/s.

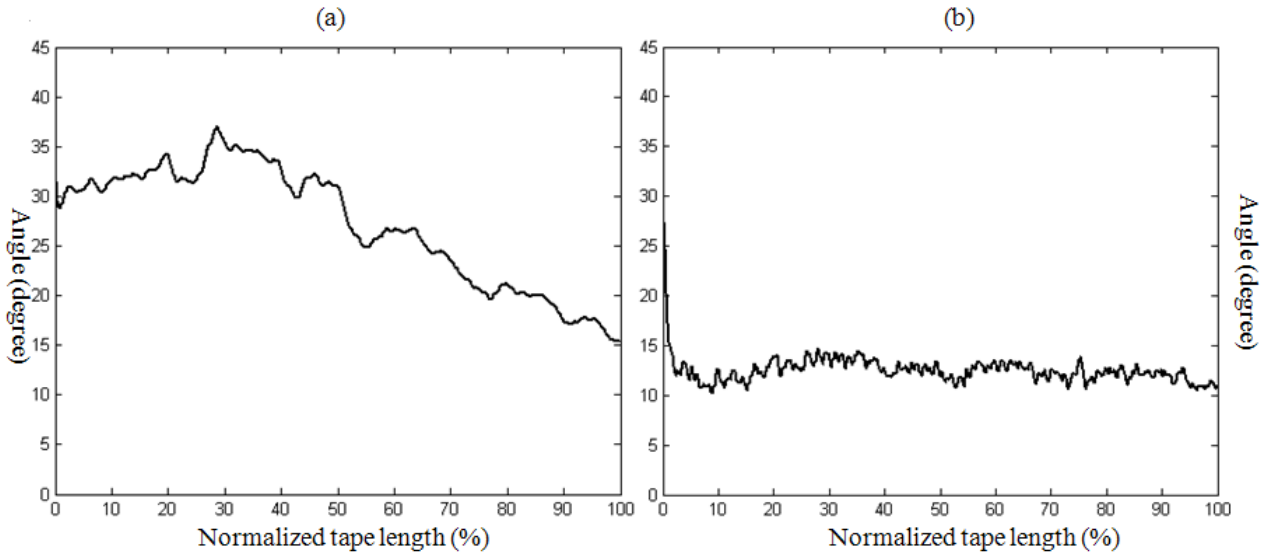

Fig. 3.3: Angle difference θ between axis of T1 and axis of T with fixed rotary guider angle at 30 (a) 4m/s, (b) 7m/s.

Measured nominal tape tension values of tested fixed rotary guider angles at the point of length of tape are transported α (3%), β (30%), and γ (100%) are shown in Table 3.2 for all tested conditions of the rotary guider. The general trend of tape tension change characteristics is similar to that mentioned previously in this section for all tested rotary guider conditions. From Table 3.2, comparing the tape tension changes of a fixed guider angle at 0º and the absence of rotary guider A, the similar transitions of tape tension during the tape transportation process was observed at both of the tested tape speeds. However, the tape tension level of the fixed angle at 0º is significantly higher than with the non-existence of rotary guider A for both tested speeds. It can be concluded that the dynamics of the tape pack driving DC motor (transitions of torque) is the primary element that decides the transitions of tape tension, and the existence of the rotary guider affects the tape tension level. In the comparisons of tape tension transitions between tested fixed rotary guider angles, it was found that the increment of the tape tension level due to the increase of the rotary guider angle by 10º is at constant 0.060N at 4m/s and 0.061N at 7m/s. Therefore, the tension shifting ability of the rotary guider is not influenced by the tape travelling speed. The level of tape tension significantly relies on the angle of the rotary guider, and it increases lineally in correspondence with the increase of the rotary guider angle. Equations that represent the tape tension level as corresponding to the angle of the rotary guider as a function of the normalized length of tape transported is calculated and shown as (6) for 4m/s and (7) for 7m/s below. Fig. 3.4 illustrates the nominal tape tension changes for each of the tested rotary guider conditions based on equations (6) and (7).

	α: 3% (N) 4m/s	α: 3% (N) 7m/s	β: 30% (N) 4m/s	β: 30% (N) 7m/s	γ: 100% (N) 4m/s	γ: 100% (N) 7m/s
Absence of rotary guider A	0.104	0.444	0.056	0.457	0.247	0.557
0º	0.161	0.500	0.084	0.501	0.260	0.590
10º	0.221	0.561	0.144	0.562	0.320	0.651
20º	0.281	0.622	0.204	0.623	0.380	0.712
30º	0.341	0.683	0.264	0.684	0.440	0.773
40º	0.401	0.744	0.324	0.745	0.500	0.834

Table 3.2: Measured nominal tape tension at three different points; α, β, and γ.

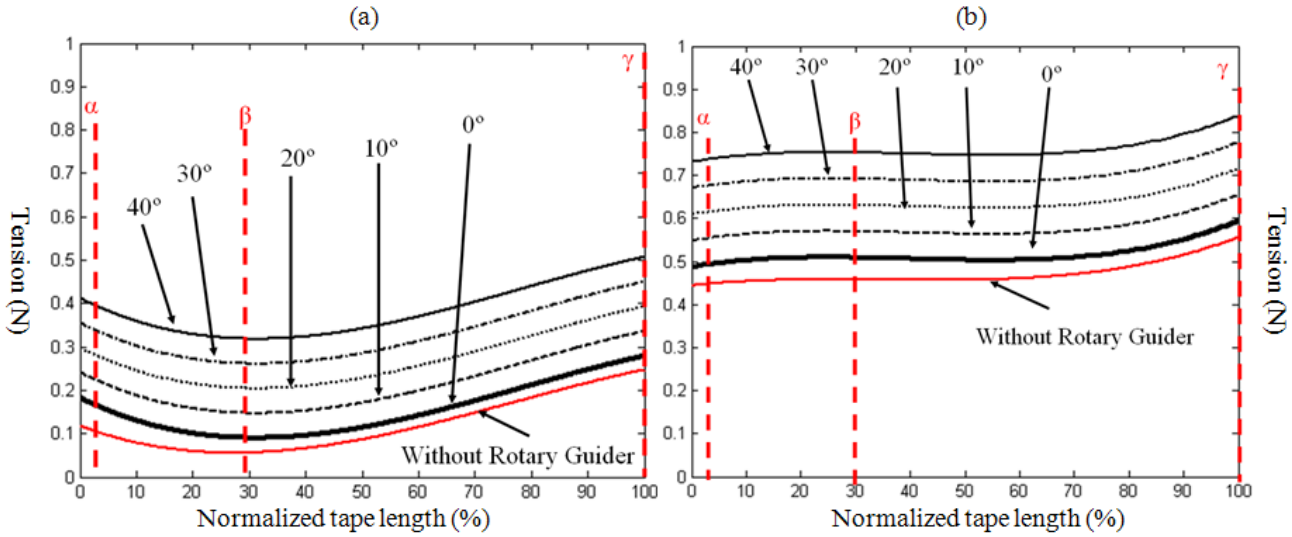

Fig. 3.4: Measured nominal tension in the function of normalized length of transported tape with rotary guider conditions (a) 4m/s, (b) 7m/s.

$$T = aL^3 + bL^2 + cL + d + 0.0060\theta_g \text{ - (6)}$$

$$(a = -5.6\times10^{-7},\ b = 1.3\times10^{-4},\ c = -6.6\times10^{-3}, \text{and}\ d = 0.18)$$

Where T is tape tension (N), L is normalized tape length (%), and θ_g is the angle of rotary guider (0º ~ 40º).

$$T = aL^3 + bL^2 + cL + d + 0.0061\theta_g \text{ - (7)}$$

$$(a = 5.0\times10^{-7},\ b = -6.0\times10^{-5},\ c = 2.0\times10^{-3}, \text{and}\ d = 0.49)$$

Where T is tape tension (N), L is normalized tape length (%), and θ_g is the angle of rotary guider (0º ~ 40º).

3.4 Validations

When the tape was transported from BOT to EOT with a fixed rotary guider angle, the transition of wrap angle at flanged slider A was investigated by measuring it at both BOT and EOT. It was found that the wrap angle increased from 0º to 7º during the test period at any rotary guider angle. The decrease rate of the supply pack's diameter and the span between the flanged slider A and flanged guide B were constant and fixed respectively. Therefore, the wrap angle of flanged slider A linearly increased through the test. Fig. 3.5 illustrates the initial wrap angles and their change characteristics with the fixed guider angle from 0º and 40º. From obtained results, it was found that the initial wrap angle of slider A increased by 15º as the guider angle increased by 10º, and the wrap angle of slider A increased 7º during the tape transportation process at any of the fixed rotary guider angles. Therefore, from the transition of tape tension with fixed rotary guider angles mentioned in the earlier section, the wrap angle increase of flanged slider A during the tape transportation process can be a minor effect on the tape tension change.

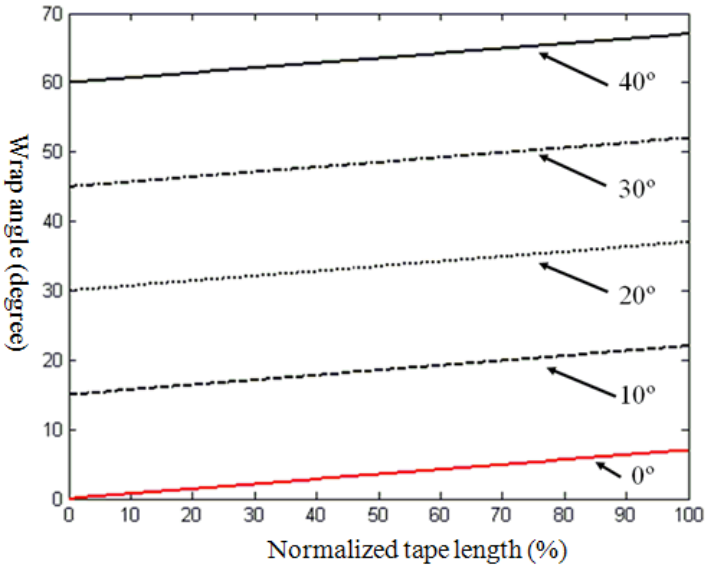

Fig. 3.5: The wrap angle changes of flanged slider A with multiple fixed angles of rotary guider.

The statistics of observed tension transitions for both tested tape-travelling speeds are calculated and summarized in Table 3.3. The differences of tensions at 30 percent and at 100 percent of tape transportation are calculated. The range of tension decreases when the rotary guider exists, and it reduces, at a higher tape travelling speed. It can be concluded that the existence of the rotary guider can reduce the influence of the dynamics of the tape driving DC motor on the tension. Comparing the standard divisions of presence and absence of a rotary guider, the existence of a rotary guider improves the standard deviation. In a comparison of tape travelling speeds, higher tape speed significantly improves the standard

deviation due to greater tape tension. It can be concluded that the existence of a rotary guider improves the standard deviation and higher travelling speed; in other words, higher tape tension improves the standard deviation significantly.

	Range of nominal tape tension 4m/s (γ - β) (N)	Range of nominal tape tension 7m/s (γ - β) (N)	Standard deviation 4m/s	Standard deviation 7m/s
No Rotary Guider	0.191	0.100	0.05957	0.02603
Rotary guider with fixed rotation angle	0.176	0.089	0.05703	0.02283

Table 3.3: Statistics of obtained tension transition functions.

The power spectrum of the measured tension signal with the absence of rotary guider A and the rotary guider angle of 20° at tape travelling speed 4m/s and 7m/s is illustrated in Fig. 3.6. In comparing the presence and absence of a rotary guider for each tested speed, the absence of the guider adds more power than its presence for both tested speeds. It can be concluded that the presence of the rotary guider and the greater number of guides present in the tape path reduces the amount of signal noise of. In comparison, the higher tape travelling speed contains a greater amount of power than a slower speed. The spikes as observed in Fig. 3.6 occur periodically; at tape speed 4m/s it occurs every 17 Hz. while at tape speed 7m/s it is observed every 29Hz. Since those spikes are observed periodically, they can be considered a dynamic of the tape pack motor. In this system, while one of the tape packs' driving motor is driving, the other motor is disabled, but still links to the driven tape pack. Therefore, spikes that are observed in Fig. 3.3 are the dynamics of tape driving DC motors. It can be concluded that the noises contained in the output signal of the tension sensor are caused by the dynamics of both tape pack driving brushed DC motors (DC turns).

3.5 Chapter Summary

The transitions of tension in the function of length of transported tape were investigated through experimental studies. It was found that the dynamics of the tape pack driving DC motor was the primary factor to affect tension transitions. Higher tape travelling speed, in other words a greater torque of motor, generates larger tension. The level of tape tension was able to be shifted by the rotary guider; a steeper rotation angle generates greater tension. The travelling speed of the tape did not affect the increment of tension corresponding to the rotation angle of the rotary guider. From power spectrum illustrations, the dynamics of tape pack driving brushed DC motors (DC turns) show a significant influence on the noise of the measured tension signal from the tension sensor. Therefore, it is recommended that replacement of tape pack driving motors from brushed DC motor to the motor will enable smooth turns such as those with a brushless DC motor.

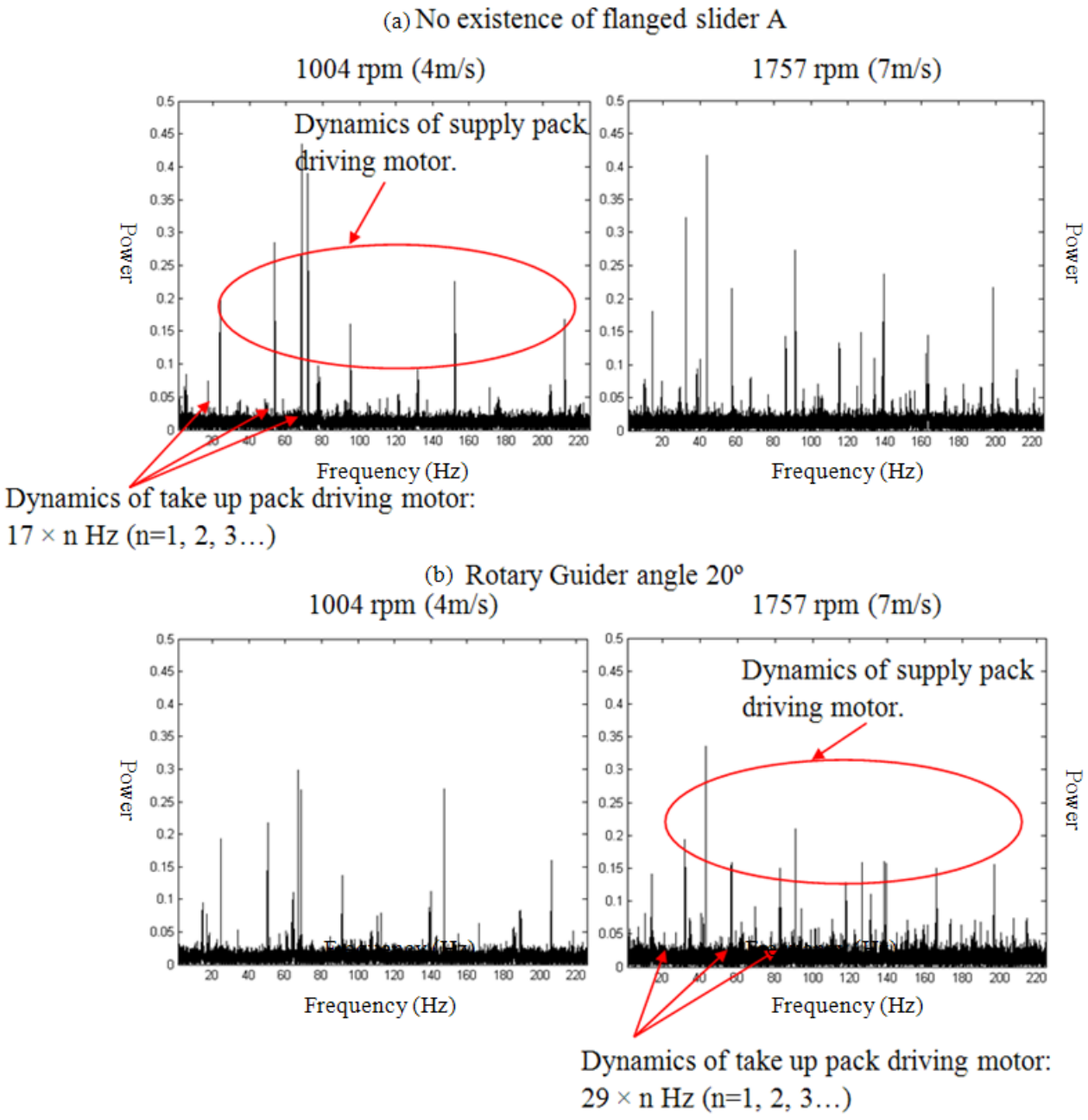

Fig. 3.6: Power spectrum density of (a) absence of rotary guider, (b) attendance of rotary guider.

Chapter 4

Dynamic Tape Path Alternation with Novel Rotary Guider

4.1 Chapter Overview

The tension transitions of the developed tape transport system in the function of length of transported tape with fixed tape path were investigated in the previous chapter. Based on the calibrated results, the tension controllable regions were found for each tested tape travelling speed. In this chapter, tension regulation using dynamic tape path alternation with the rotary guider of the developed tape transportation system is evaluated through experimental studies. A proportional gain controller is developed for the closed loop control. The designed controller is evaluated through parameter studies of the target tension and the tape travelling speed. Significant influences on the transitions of tension are observed and the tension is actuated as targeted. It can be concluded that the rotary guider with a closed loop control algorithm has an ability to actuate the travelling tape tension without relaying the dynamics of the tape pack driving motor.

4.2 Tension Controllable Regions and Experimental Procedure

The tape tension controllable region of the developed tape transport system is investigated based on the results of the fixed rotary guider angle in Fig. 3.3 in chapter 3; this is shown in Fig. 4.1 for both tape travelling speed 4m/s and 7m/s. The maintainable tape tension is approximately 0.04N between 0.28N and 0.32N for tape speed 4m/s, and is 0.12N between 0.60N and 0.72N for tape speed 7m/s. Based on the equation of normalized functions that were obtained in the previous chapter, the profiles of the rotary guider trajectory at three target tensions 0.28N, 0.30N, and 0.32N at tape speed 4m/s and 0.60N, 0.65N, and 0.70N at tape speed 7m/s are calculated and illustrated in Fig. 4.2. The obtained profiles of the rotary guider trajectory are within the workspace of the rotary guider and the tension can be controllable as targeted. In the previous chapter, the transition wrap angle around the rotary guider A is found to be 7º for any fixed rotary guider angle during the tape transportation process. An open loop algorithm that rotates the rotary guider back 7º through the tape transportation was developed in order to investigate the effectiveness of regulating the wrap angle around rotary guider A. A closed loop controlled proportional gain controller was developed to regulate the tension as targeted and evaluated through the experimental studies. In the experimental tests, the practical results of the rotary guider trajectory were expected to

follow as they are profiled in Fig. 4.2. Parameter studies were carried out on the speed of tape and the initial angle of the rotary guider for the open loop control algorithm and on the speed of tape and the target tension for the closed loop control algorithm. The same tape path setting is shown in Fig. 3.1 and fixed parameters as defined in the previous chapter were used during the experiment. The tension is recorded with a sampling frequency of 200Hz. A summary of experimental conditions is listed in Table 4.1. The experimental studies consisted of the following procedures.

(a) Initialize the tape transport system - Set the tape pack driving motor at desired tape travelling speed (rpm). Set initial angle of rotary guider at desired angle for open loop controller tests. Input the target tension for closed loop controller tests. Tension the stationary tape and initialize the tension sensor.

(b) Start tape transportation - turn the motor on.

(c) Run the system during the time the desired length of tape is transported - monitor and record the outputs of tension sensor.

(d) Stop tape transportation - Rewind the tape from EOT to BOT.

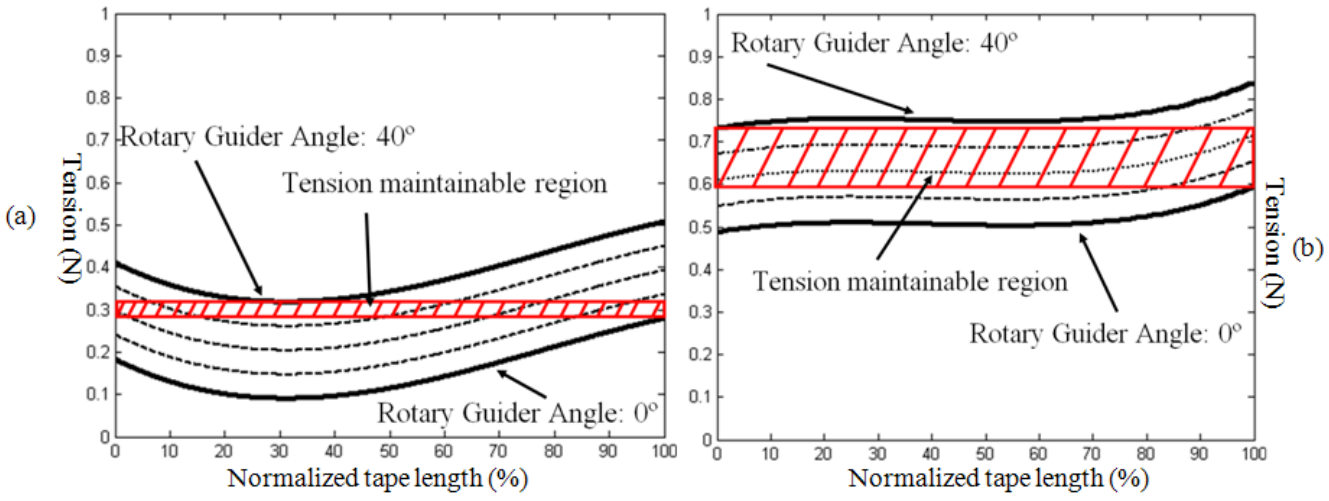

Fig. 4.1: Tension controllable region for (a) tape speed 4m/s (b) 7m/s.

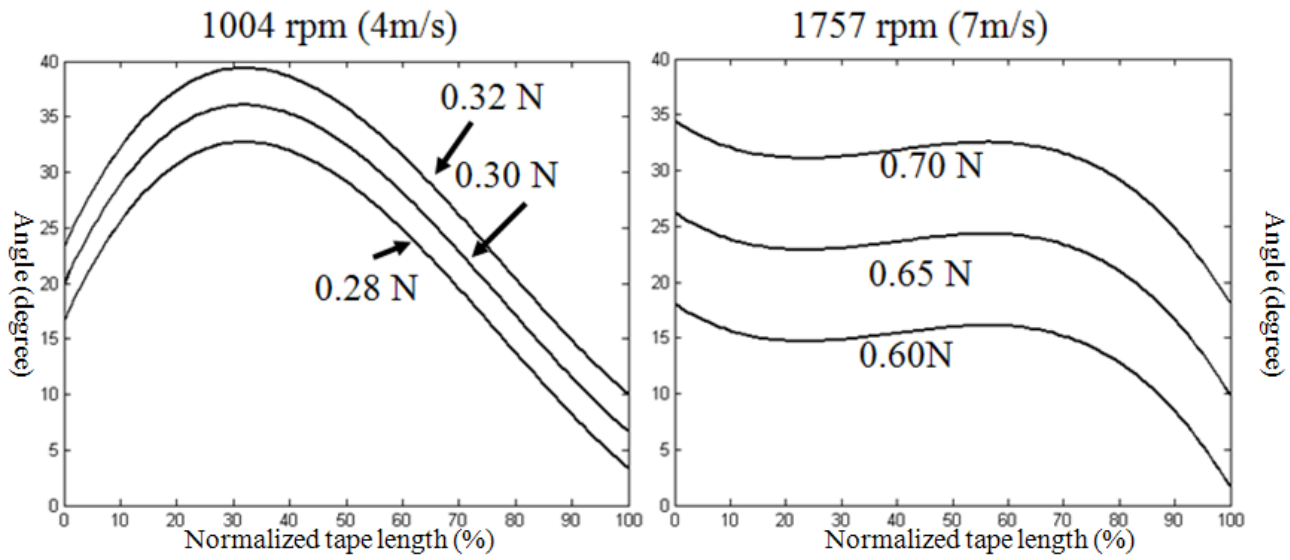

Fig. 4.2: The profiles of rotary guider trajectory for target tensions (a) tape speed 4m/s (b) 7m/s.

Fixed test parameters	
Test ambient temperature	25°C
Tape span between each flanged guides A, B, C, and D	100 mm
Wrap angle around the flanged guide C	45º ($\theta_R = 45°$)
Diameter of the supply pack (LTO4)	96mm -> 55mm (BOT -> EOT)
Work space of rotary guider	0° to 40°
Sampling frequency	200Hz
Test parameters	
Target rpm of the tape pack (target average tape travelling speed)	1004 rpm (4m/s) 1757 rpm (7m/s)
Open Loop Control	
Initial angle of rotary guider (4m/s and 7m/s)	10°, 20°, 30°, and 40°
Test period and Rotation interval (4m/s)	Period: 250 sec, Interval: 0.175sec
Test period and rotation interval (7m/s)	Period: 100 sec, Interval: 0.070sec
Closed Loop Control (Proportional Gain)	0.038º
Target Tension (4m/s)	0.28N, 0.30N, and 0.32N
Target Tension (7m/s)	0.60N, 0.65N, and 0.70N

Table 4.1: Test conditions.

4.3 Rotary guider with Open loop controller

In the previous chapter, the wrapping angle of rotary guider A increased 7° during the tape transportation process with any angle of rotary guider. Since the angular speed of the tape pack is regulated at a constant, the period of one rotation of tape pack is fixed with any diameter of tape pack. Therefore, the function of wrap angle change has a linear transition. An open loop logic rotary guider controller was developed in order to regulate the wrap angle at constant during the transportation process. Fig. 4.3 shows a block diagram of open loop control logic. The open loop control does not give any feedback. The system performs the pre-programmed actions. The plant of the system is the rotary guider and the controller of the system is MCU with an open loop control algorithm. The developed open loop controller decrements the angle by 0.036° with the interval t_{in} that is calculated based on the tape travelling speed until it rotates back 7°.

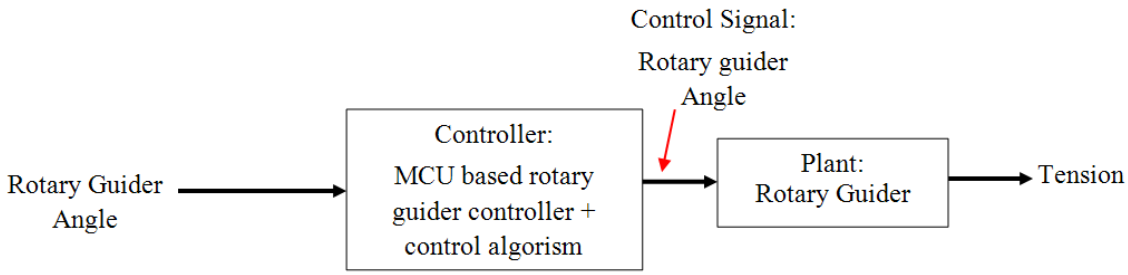

Fig. 4.3: A diagram of open loop control logic.

Fig. 4.4 shows a flowchart of the developed open loop control algorithm. The initial angle of the rotary guider and the test period are input to the system as prescribed at 250 seconds for 4m/s and 100 seconds for 7m/s. The controller calculates the rotation interval t_{in} based on the input test period. Once the system is started, the controller decrements the angle of the rotary guider by 0.036° with calculated interval of t_{in}, and measured tensions from both tension sensors SG set 1 (T1) and 2 (T2) are displayed on GUI and recorded in txt file format. The operation is looped until the rotary guider is rotated 7°.

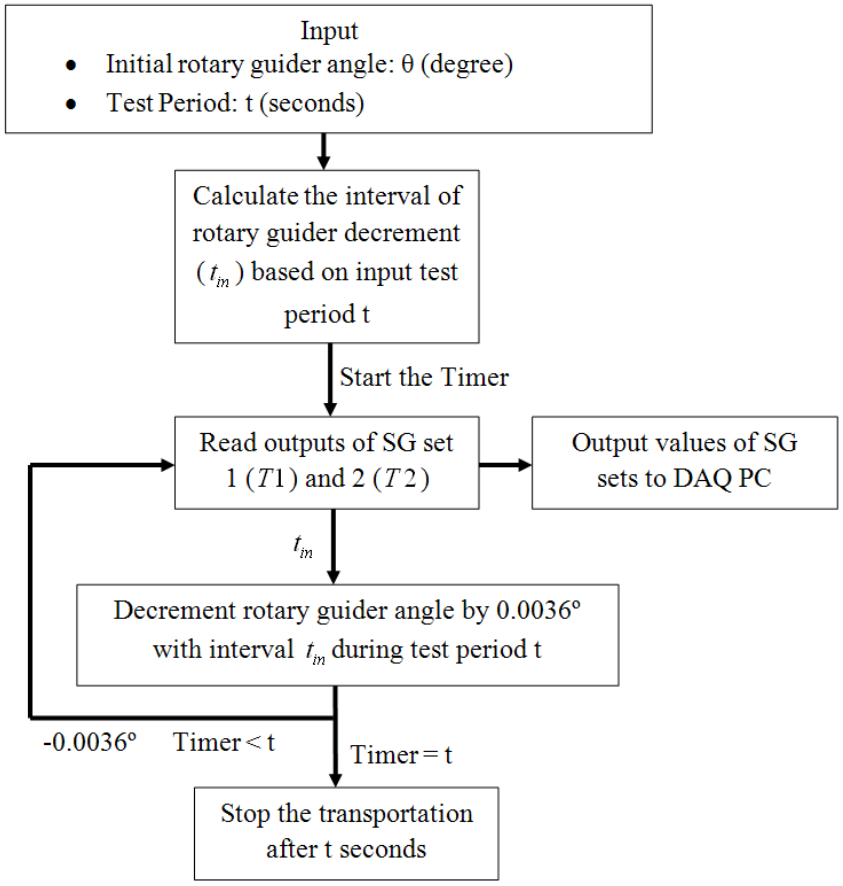

Fig. 4.4: A flowchart of open loop controller algorism.

The measured tensions were analysed using an offline MATLAB environment. Recorded tape tension T for all tested conditions were calculated and illustrated in Fig. 4.5. Angle trajectories of tested initial angles are also illustrated in Fig. 4.5 (c). The transitions of tension in the functions of normalized tape length showed similar transitions to the fixed tape path. However, at tape speed 4m/s, the gradient of the tension increase was significantly reduced compared to the fixed tape path. And a similar phenomenon was observed at tape speed 7m/s. The function of 7m/s contains periodic spikes. Since these spikes occurred at particular intervals, and the angle of rotary guider changed with certain times, the dynamics of the rotary guider could be causing these spikes. Table 4.2 lists the measured tape tension at three different points; α (3% of tape transport completion), β (30% of tape transport completion), and γ (100% of tape transport completion).

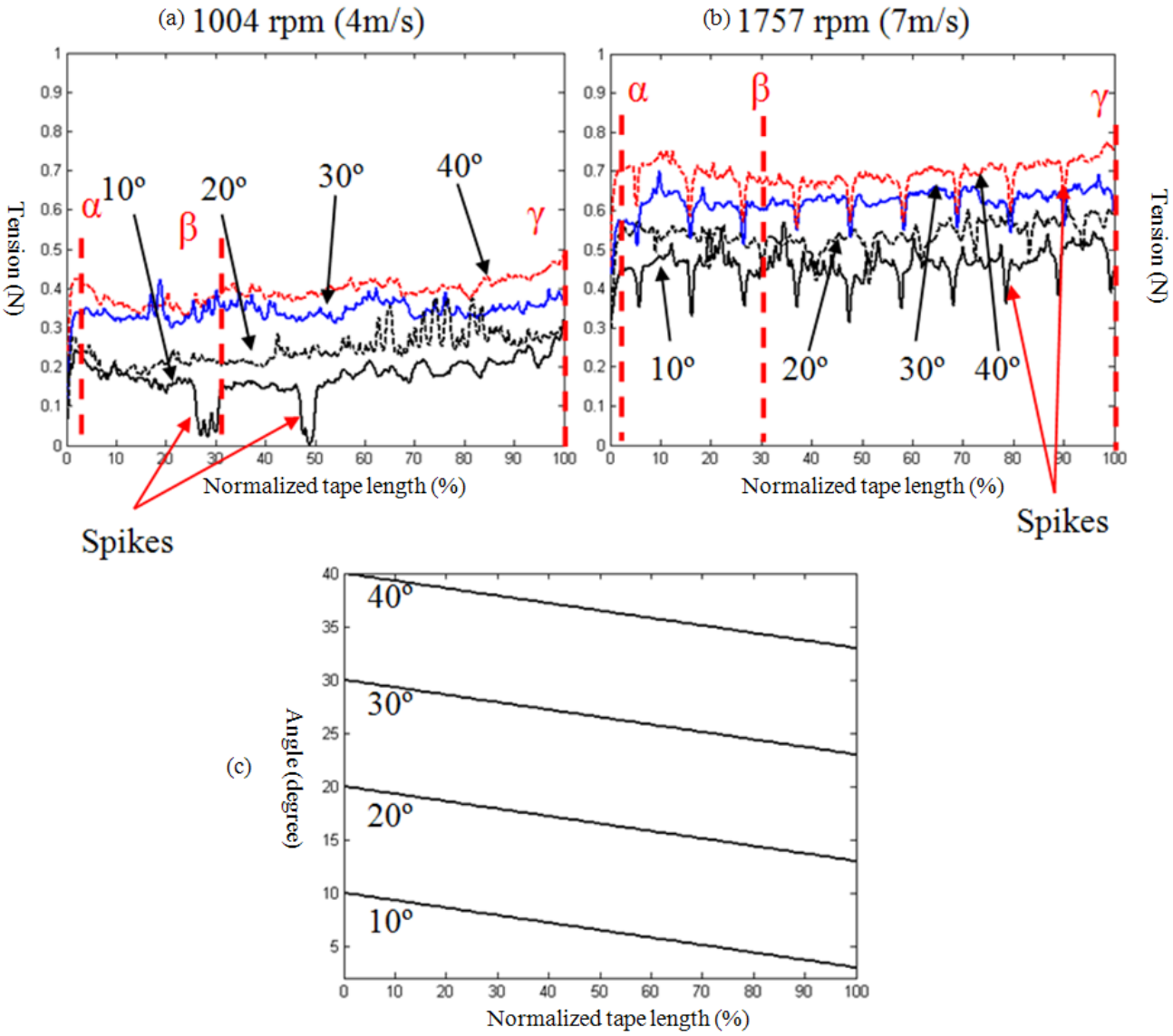

Fig. 4.5: The tape tension transitions (a) 4m/s and (b) 7m/s and (c) angle transitions in the functions of normalized tape length.

	α: 3% (N) 4m/s	α: 3% (N) 7m/s	β: 30% (N) 4m/s	β: 30% (N) 7m/s	γ: 100% (N) 4m/s	γ: 100% (N) 7m/s
Initial Rotary Guider Angle 10º	0.242	0.450	0.030	0.425	0.321	0.443
Initial Rotary Guider Angle 20º	0.280	0.555	0.215	0.470	0.310	0.587
Initial Rotary Guider Angle 30º	0.340	0.573	0.350	0.600	0.371	0.596
Initial Rotary Guider Angle 40º	0.426	0.700	0.353	0.667	0.483	0.748

Table 4.2: Measured tape tension at three different points; α, β, and γ.

The statistics of tension transitions were calculated for all tested conditions. The range of tension significantly decreased compared to the fixed tape path. Comparing the range at 4m/s and 7m/s, higher tape speed of range with all tested rotary guider angle had a significantly smaller range.

The standard deviations were calculated. At tape speed 4m/s, standard deviations improved compared to the standard deviations of the fixed tape path. While the standard deviations at 7m/s dropped significantly due to periodic spikes that are observed through the functions. It can be concluded that the designed open loop controller, in other words, the wrap angle regulation of rotary guider, produced a significant improvement of tension regulation at the lower tape transport speed. However, the transition of tension still increased overall and the performance of controller at tape travelling speed at 7m/s was significantly lower due to an increase of standard deviations. Development of an advanced rotary guider controller that is a rotary guider controller in closed loop is essential to improve the accuracy of tension regulation.

	Range of nominal tape tension 4m/s (γ - β) (N)	Range of nominal tape tension 7m/s (γ - β) (N)	Standard deviation 4m/s	Standard deviation 7m/s
Rotary guider with fixed rotation angle	0.176	0.089	0.05703	0.02283
Initial Rotary Guider Angle 10º	0.291	0.018	0.04883	0.04005
Initial Rotary Guider Angle 20º	0.095	0.117	0.04237	0.03691
Initial Rotary Guider Angle 30º	0.021	-0.004	0.02621	0.03276
Initial Rotary Guider Angle 40º	0.130	0.081	0.03244	0.03665

Table 4.3: Statistics of measured tension with open loop controller and fixed tape path.

4.4 Rotary Guider with Closed Loop Controller

The block diagram of closed loop control is shown in Fig. 4.6. The input of logic is the target tension. The plant of the system is the rotary guider, the feedback of the system is the tension sensor, and the controller of the system is the MCU with a proportional gain control algorithm. A proportional gain controller with the gain 0.036° was developed and implemented in the system.

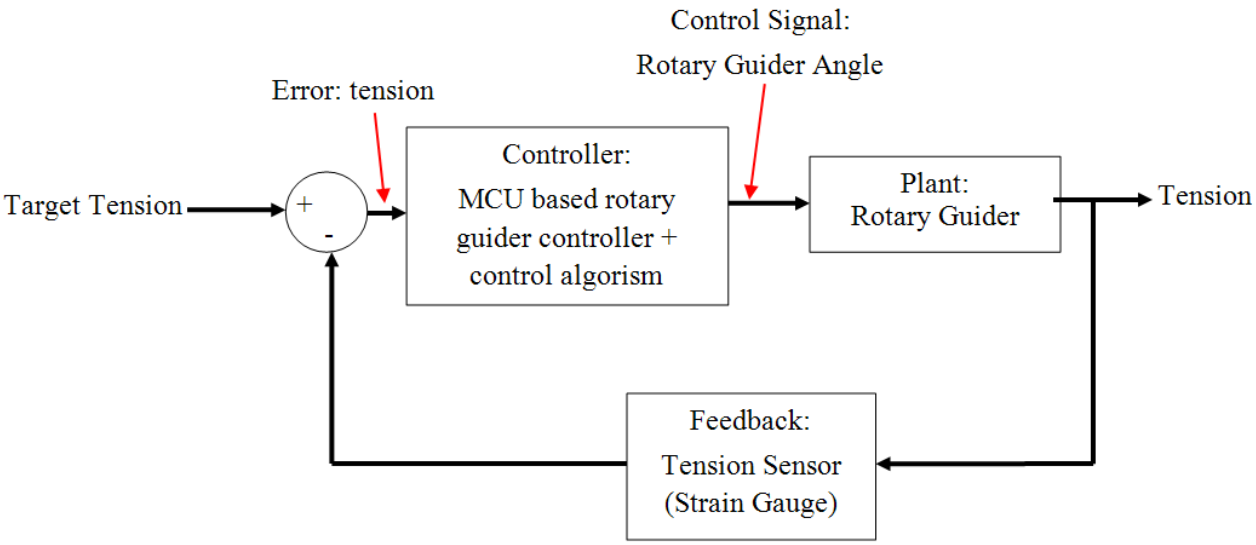

Fig. 4.6: A block diagram of closed loop control logic.

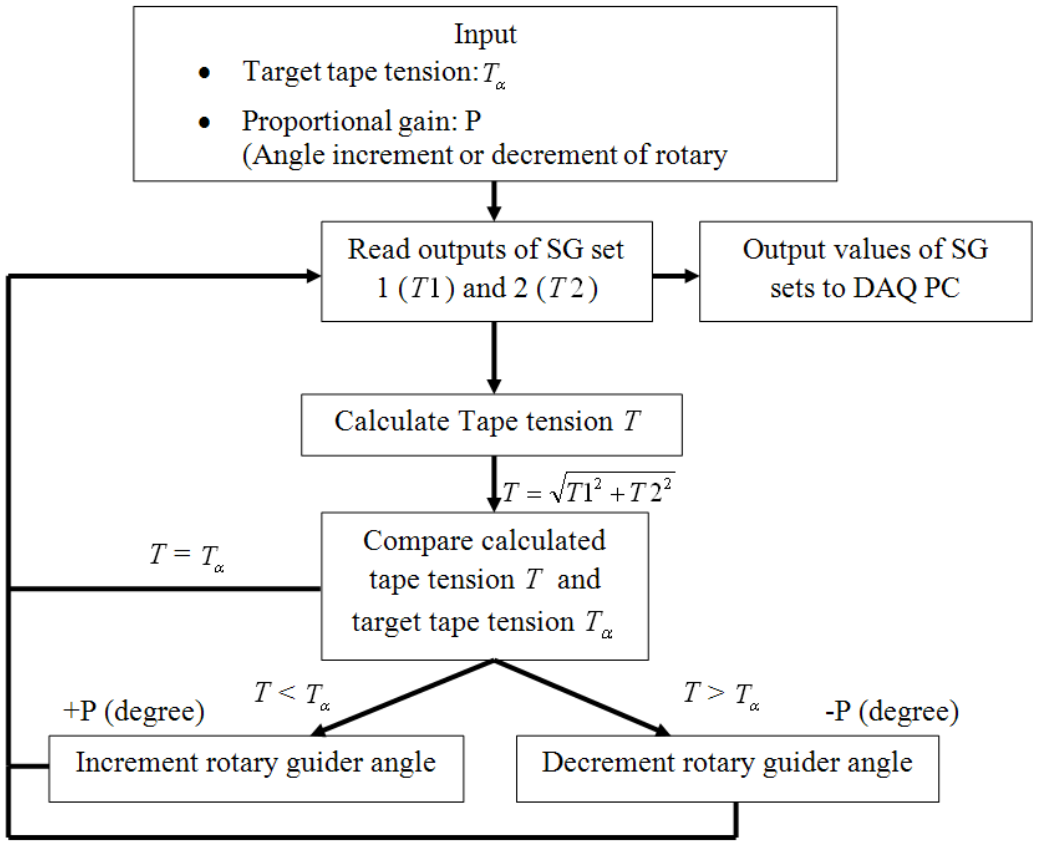

Fig. 4.7: A flowchart of proportional controller algorism.

Fig. 4.7 shows a flowchart of the proportional gain controller algorithm. The inputs of the algorithm are the target tension and the proportional gain. Once the transportation is started, the controller measures the initial tension of tape and uses this value as the reference tension. The controller reads the outputs of both tension sensors, SG set 1(T1) and SG set 2 (T2), and calculates the total tension (T). Obtained total tension (T) is compared with the reference tension. When the total tension is smaller than the reference tension, the rotary guider increases the angle corresponding to the input proportional gain, and decreases the angle in the other case. If the total tension (T) is equal to the reference tension, the angle of rotary guider is not to be changed. This routine is repeated until the completion of the transportation process. The measured tensions from tension sensors T1 and T2 and the trajectory of the rotary guider are displayed and recorded through the GUI on the control PC.

The measured tensions are analysed using an offline MATLAB environment. Table 4.4 shows measured nominal tape tension with tape speed 4m/s at the same points α (3%), β (30%), and γ (100%). Fig. 4.8 (a), (b), and (c) illustrate measured tape tension with the proportional gain based rotary guider controller in a function of the normalized length of tape transported. The transition of tension shows that the tension rises once the transportation is started due to the static torque of the motor. With the fixed tape path, the tension showed a slight drop once the speed of motor was stabilized, then the tension gradually increased corresponding to the increase of the tape pack driving motor's torque. With the dynamic tape path and the proportional controller, the transition of tension did not show the same phenomenon as with the transition of fixed tape path. Once the tape pack driving motor reached the desired speed, the tension began to oscillate around the target tension and produced overshoots and undershoots for the remaining transportation process. From Table 4.4, comparing the ranges of measured tension (γ - β), it is observed that the values of range with the proportional controller are significantly less than with its fixed tape path. The measured tension at point γ is close to the target tension for all three functions. Fig. 4.8 (a1), (b1), and (c1) represent trajectories of rotary guider rotation including the angle profile of target tension that is found in the previous section as a function of the normalized length of tape is transported. The trajectories of all three target tensions roughly follow the profiled trajectories. This could be due to the effectiveness of the dynamics of the tape pack driving DC motor and rotary guider; however, the angle trajectory of target tension 0.32N (c1) went out of control at a point between 13 and 50 percent of tape transportation. Therefore, it is recommended that in developing an advanced rotary guider controller such as a PID, a robust logic and fuzzy logic controller be used in order to improve performance of tape tension regulation.

Comparing the standard deviations of measured tension with a fixed tape path and a dynamic tape path, minor improvements of standard deviation are observed with dynamic tape path. Standard deviation of target tension 0.32N is significantly lower than other test conditions and fewer overshoots and

undershoots of tension transition are observed compared to the other two target tensions. However, target tension 0.32N goes out of control for approximately 40 percent of the transportation. It can be concluded that the designed proportional gain controller has an ability to regulate the tension as prescribed at 4m/s.

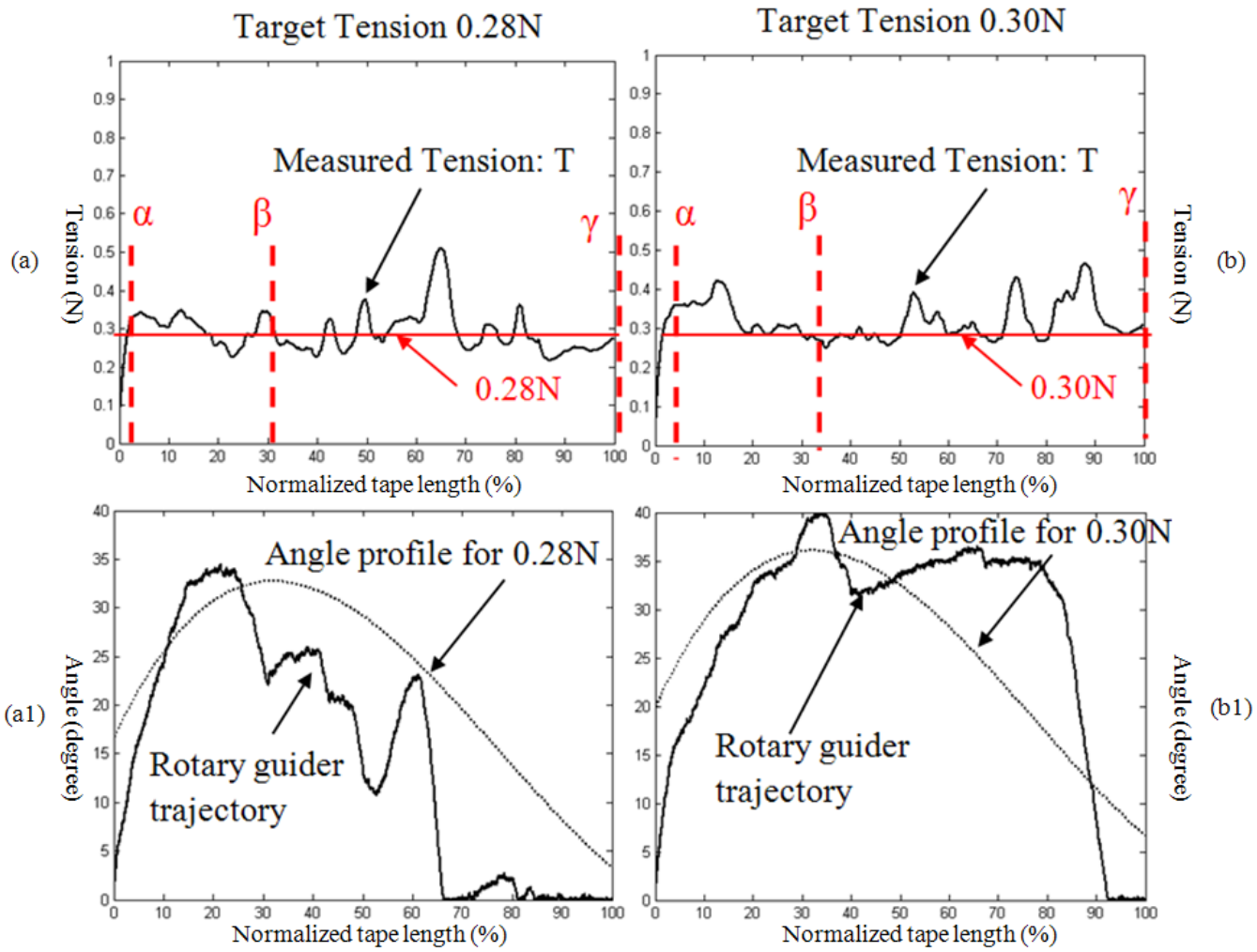

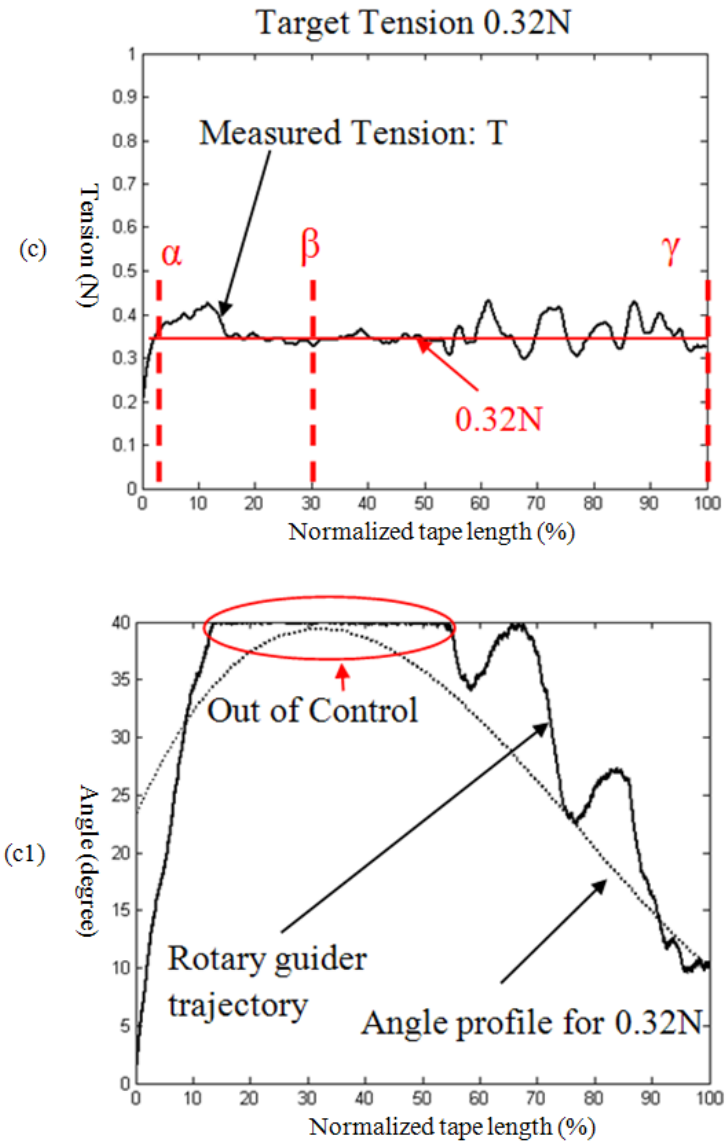

Fig. 4.8: Illustrations of tension transitions and trajectory of rotary guider in the functions of normalized tape length with proportional controller at tape travelling speed 4m/s.

	α: 3% (N) 4m/s	β: 30% (N) 4m/s	γ: 100% (N) 4m/s	Range of measured tape tension 4m/s (γ - β) (N)	Standard deviation 4m/s
Rotary guider with fixed rotation angle at 30°	0.341	0.264	0.440	0.176	0.05703
Target Tension 0.28N	0.334	0.344	0.275	-0.069	0.05661
Target Tension 0.30N	0.333	0.277	0.310	0.033	0.05276
Target Tension 0.32N	0.364	0.329	0.322	-0.007	0.03208

Table 4.4: Measured tape tension at three different points; α, β, and γ and statistics of proportional gain controller at 4m/s with three-target tensions and fixed tape path.

Table 4.5 shows measured tape tension with tape speed 7m/s at the same points α (3%), β (30%), and γ (100%). Fig. 4.9 (a), (b), and (c) illustrate measured tape tension with the proportional gain based rotary guider controller in a function of the normalized length of tape transported. The tension transitions are similar to the transitions of speed at 4m/s. Once the tape pack driving motor reached a desired speed, the tension begins to oscillate around the target tension. However, it was observed from all three tension functions of 7m/s, the overshoots of tension became significantly greater after 60 percent of the tape transportation process. Comparing the tension at point γ, the measured tension was far from the target tensions. Comparing the standard deviation of measured tensions, the value of standard deviation with dynamic tape path was three times larger than the standard deviation of the fixed tape path. This explains how the measured tension signal contained the large amount of noise. Fig. 4.9 (a1), (b1), and (c1) represent trajectories of rotary guider rotation including the angle profile of target tension. Trajectories of all three tested target tensions did not experience the out of control, unlike the trajectory of target 0.32N at tape speed 4m/s. However, the difference between the recorded trajectory of the rotary guider and its profiled trajectory for a specific target tension are significant. This could be caused by the dynamics of the rotary guider. Therefore, further studies of tension transition at high tape travelling speed are required in order to investigate the characteristics of dynamics of the rotary guider. The effectiveness of tension regulation with the designed proportional controller at tape speed 7m/s is not as significant as its effectiveness at tape speed 4m/s; however, the designed controller is still able to regulate the tension, but with low accuracy.

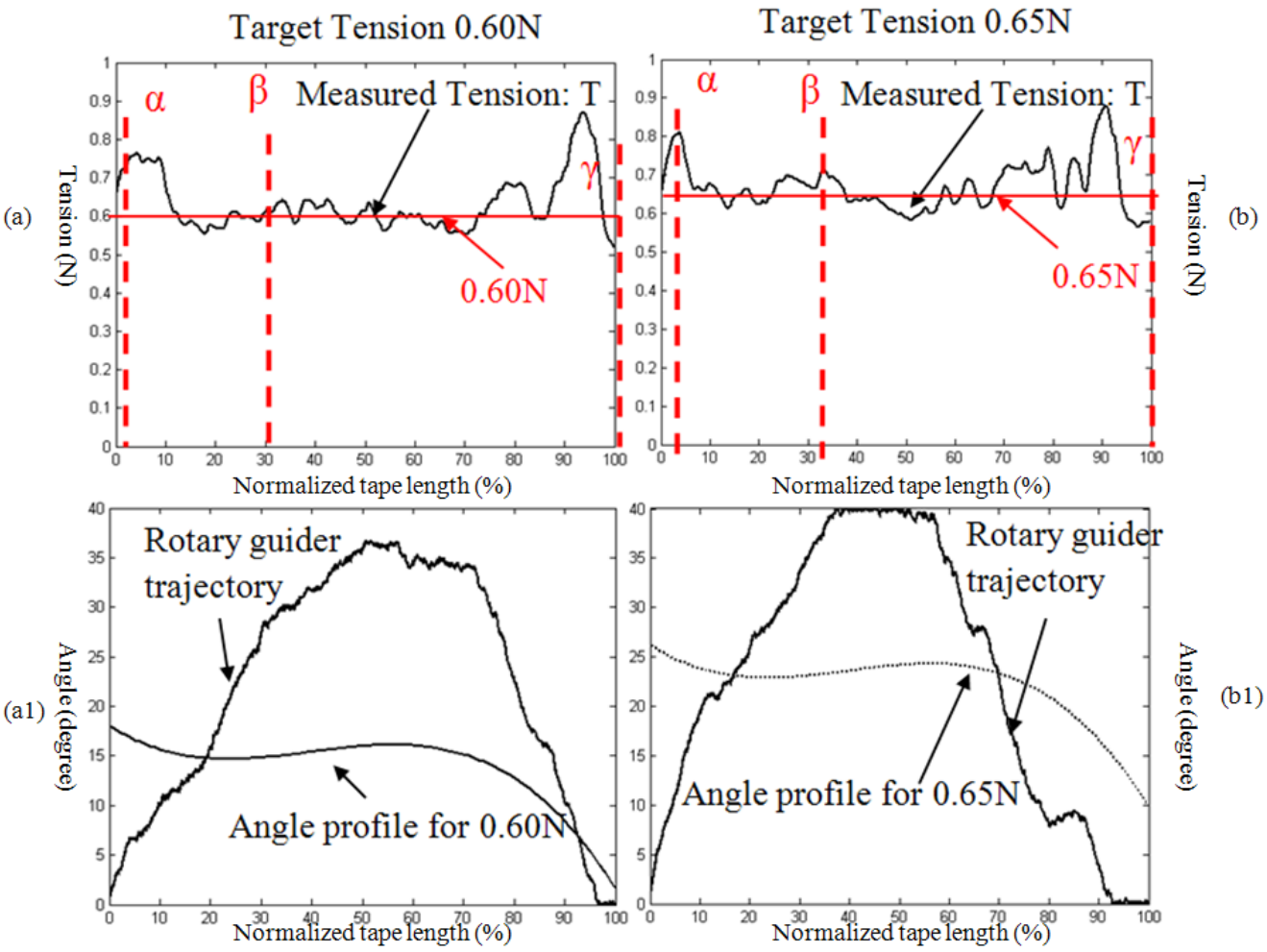
Target Tension 0.60N
Target Tension 0.65N
α
β
γ
Measured Tension: T
0.60N
0.65N
Tension (N)
Normalized tape length (%)
(a)
(b)
Rotary guider trajectory
Angle profile for 0.60N
Angle profile for 0.65N
Angle (degree)
(a1)
(b1)

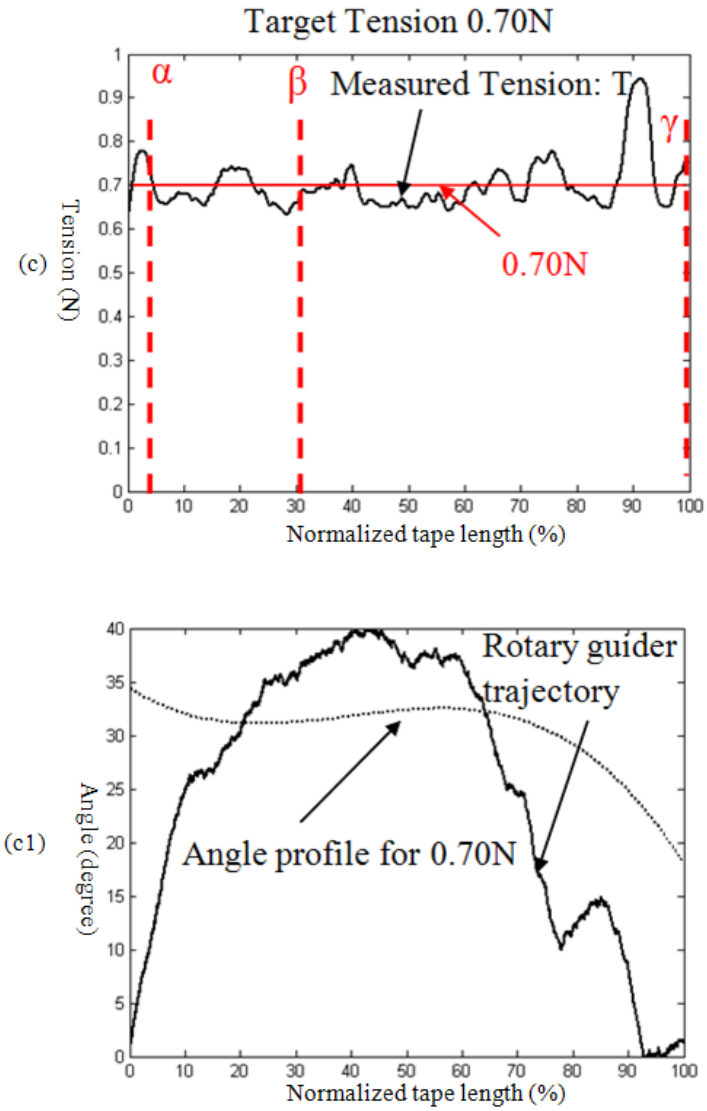

Fig. 4.9: Illustrations of tension transitions and trajectory of rotary guider in the functions of normalized tape length with proportional controller at tape travelling speed 7m/s.

	α: 3% (N) 7m/s	β: 30% (N) 7m/s	γ: 100% (N) 7m/s	Range of nominal tape tension 7m/s (γ - β) (N)	Standard deviation 7m/s
Rotary guider with fixed rotation angle at 30º	0.683	0.684	0.773	0.089	0.02283
Target Tension 0.60N	0.755	0.610	0.518	-0.092	0.07215
Target Tension 0.65N	0.804	0.671	0.579	-0.092	0.06295
Target Tension 0.70N	0.779	0.648	0.750	0.102	0.05878

Table 4.5: Measured tape tension at three different points; α, β, and γ and statistics of proportional gain controller at 7m/s with three-target tensions and fixed tape path.

4.5 Validation

Fig 4.9 illustrates the power spectrum density of the fixed tape path with the angle of rotary guider at 20° and the proportional controller with target tension 0.28N at tape speed 4m/s and 0.65N at tape speed 7m/s. In the fixed tape path, the dynamics of the tape pack driving motor is the major cause of noise in the measured tension signal. However, when the dynamic tape path is enabled, the amount of power is drastically increased and the power of dynamics of the rotary guider surpasses the power of dynamics of the tape pack driving motors. It was found that the dynamics of the rotary guider became the major disturbance of tension once the tape path is started and is altered dynamically; it is also the major source of noise generation for the tension sensor signal.

4.6 Chapter summary

The tension regulation with dynamic tape path alternation using open loop control logic and closed loop control logic were developed and evaluated through experimental studies. These experimental studies show that the rotary guider with suitable control logic can be regulated without relying on the dynamics of a tape pack driving motor. The designed controllers show superior performance of tension regulation at lower travelling speed of tape; however, the performance of tension regulation is degraded -significantly at the higher travelling speeds of tape. Further studies of the rotary guider especially at the higher tape travelling speeds are indicated. Development of an advanced rotary guider control algorithm such as fuzzy logic and a robust logic controller to enable precise actuation of travelling tape tension are also recommended.

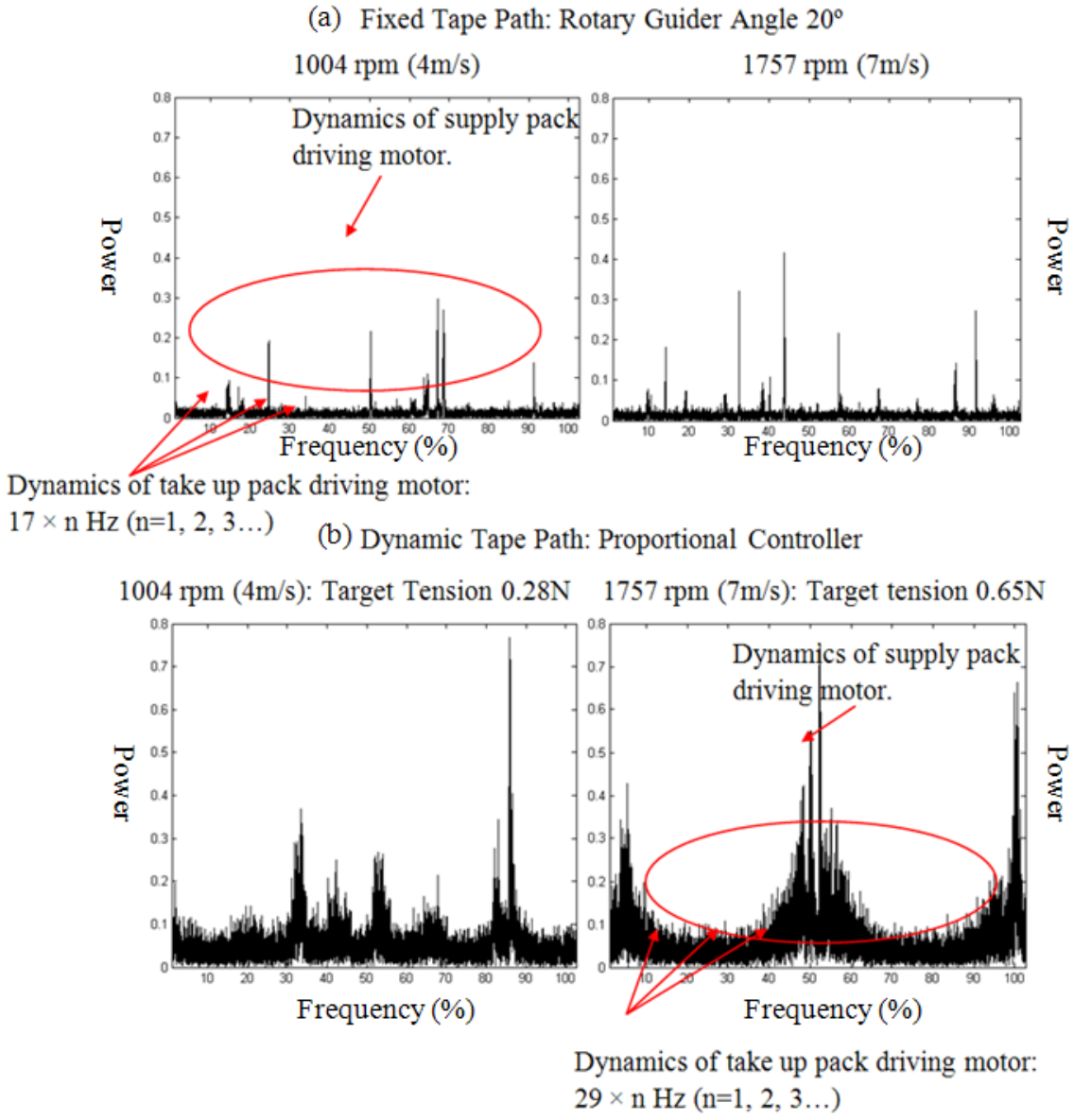

Fig. 4.10: The power of (a) fixed tape path with the guider angle 20° and (b) dynamic tape path alternation with proportional controller.

Chapter 5

Summary

This thesis has investigated the transverse force (tension) actuation technology of axially moving magnetic tape media. Specifically, the development of a prototype of a tape transportation system, a feasible proposed tension actuation mechanism, the investigation of transition of tension during the handing process, and validations of effectiveness of developed tension controllers through experimental studies. The following sections summarize the specific conclusions, recommendations, and limitations of the thesis including evaluation of technical feasibility of the developed tension actuation mechanism, and provide several possible directions of future work.

5.1 Conclusions and Recommendations

This thesis based research is concluded as

- A linear magnetic tape transport system which enables travelling tape regulation in closed loop control was developed.
- A rotary guider with dynamic tape path alternation was proposed and developed as a tension actuator. Strain gauge based tension sensor is developed and implemented to the system as the tension feedback.
- The transition of tension with the fixed angle of rotary guider (the fixed tape path) was investigated through experimental studies. The transition of tension was increasing as more length of tape was transported and it can be occurred due to the increase of torque of tape pack driving motor. It is concluded that the dynamics of tape pack driving motor is the primary factor to decide the state of change in tension. The angle of rotary guider shifts the level of tension. Higher travelling tape speed and angle of rotary guider generates generally greater tension.
- Rotary guider with dynamic tape path alternation in closed loop control (a proportional gain controller) enabled actuation of travelling tape tension and it is successfully regulated as prescribed. It is found that the dynamics of rotary guider is the major elements that influence to the state of change in tension, and they surpass the influence of tape pack driving motor dynamics to the tension.

Specific conclusions and recommendations of developed technology are listed below.

5.1.1 Development of Linear Magnetic Tape Transportation System

Both the hardware and the software of a linear magnetic tape transport system that enables the travelling tape tension actuation in closed loop control were developed. The travelling tape tension is actuated using the rotary guider using the surface friction guide between the tape and the rotary guider. The tension is measured using the strain gauge based tension sensor. The operations of the developed system including the tape transportation, rotary guider control, and monitoring and recording of measured tension from the tension sensor are commanded through GUIs on the control PC. However, the output signal of the tension sensor contains a significant amount of noise. Therefore, it is essential to implement a signal conditioner between the sensor and the MCU to eliminate the noise of the signal in order to measure the tension accurately.

5.1.2 Tension Transitions with Fixed Tape Path

The transitions of travelling tape tension during the handing process were investigated through experimental studies and measured using the combination of parameters in the travelling tape tension and the angle of the rotary guider. The angle of the rotary guider was fixed during the transportation process. The measured tensions were analysed using offline MATLAB. Through experimental studies, it was found that the transition of tape tension relies heavily on the dynamics of the rotary guider and the greater tension is applied to the travelling tape with a higher travelling speed. The level of tension can be shifted using the rotary guider. As a general trend, the higher rotation angle of the rotary guider generates greater tension. During the tape transportation from BOT to EOT, the wrap angle of tape around the rotary guider increased 7 degrees with any angle of rotary guider. However, the increase of wrap angle around rotary guider has a minor effect on the tension change;, this was figured out by comparing transitions of tension between the presence and absence of the rotary guider. In this system, the travelling speed was set as an averaged travelling speed and the actual speed increases as tape is transported during the transportation process. Therefore, it can be concluded that the regulation of the travelling speed of tape can reduce the gradient of tension and increase tension. Further, the driving source of tape packs are brushed DC motors and when the tape is transported, one of DC motors that correspond to the transporting direction is driven; the other motor is still connected to the tape pack, but disabled. Therefore, rotation of both DC motors can be affected by the tension change phenomena. For this reason, it is strongly recommended to replace the brushed DC motors with brushless DC motors to enable a smooth rotation of the tape pack driving motor and also to develop the travelling tape speed controller.

5.1.3 Dynamic Tape Path Alternation with Rotary Guider

Based on the calibration of tension transitions with a fixed tape path, the tension controllable regions of the rotary guider with travelling speed were calculated. A closed loop control algorithm for the rotary guider controller that is a proportional gain controller was designed and developed based on the calibrated tension controllable regions. An open loop control algorithm that rotates the guider to a certain angle with particular intervals was also developed in order to investigate the effectiveness of wrap angle regulation of the rotary guider. Experimental studies were carried out to evaluate the developed controllers. Through experiments, it was found that an open loop control algorithm reduces the increase of tape tension due to an increase of tape pack driving motor torque as the tape is transported, especially at lower travelling speeds of the tape. The closed loop control algorithm has an ability to regulate the tension as targeted without relying on the dynamics of the tape pack driving motor. The performance of tension regulation with designed controllers is significant at lower tape travelling speeds. While at higher travelling speed, the performance of the designed controller is degraded significantly. The advanced rotary guider controllers such as the robust logic controller need to be developed in order to improve the accuracy of tension regulation. Further, increasing the number of rotary guiders can e drastically improve the tension controllability of the rotary guider. However, since this tension actuation mechanism uses the surface friction between the tape and the rotary guider, higher tension might damage the tape; therefore, there is a trade-off between tension controllability and durability of tape.

5.2 Limitations

This thesis-based research contains several limitations due to a shortage of resources. The following issues for the developed tape transport system have been identified during this research.

1. The tape travelling speed control – In this developed system, the high power brushed DC motor has employed as the driving source of tape pack. During the transportation the angular speed of tape was regulated at constant in this system. Therefore, since tape pack performs circular motion, as the take up pack winds more tape the travelling speed of tape increases. Hence, it was observed that increase of tape travelling speed increases of tension. It is recommended that develop a control algorithm to regulate the travelling speed of tape.

2. The excitation and DC turn of tape pack driving motor – Since the developed tape system employs a brushed DC motor as the driving motor of tape pack, the excitation of the DC motor during the transportation process is problematic. It can affect the dynamics of in-plane and transverse vibration of tape when the developed tension regulation technology is integrated with

the advanced tape guiding mechanism that requires tension actuation in closed loop control. DC turn is also problematic in this system; while one of the tape pack-driving motors is operating, the other motor is disabled, but it is still connected to the tape pack. The DC turns heavily affect the tension shifting phenomena as was observed from the power spectrum of measured tension. Therefore, in order to solve these problems and enable smooth rotation of the motor, replacing the tape pack-driving brushed DC motor with the brushless DC motor is recommended.

3. The noise of the measured tension signal – The tension sensor was implemented in the system and is based on the strain gauges with gauge circuits and amplifiers. Since the tape is travelling, the tension that the sensor is measuring dynamically changes. Therefore, the measured signal contains a huge amount of noise, and that degrades the tension measurement accuracy drastically. In this study, the analysis of recorded signals was performed using MATLAB with off-line and the digital low pass filter was applied to condition the signal. However, in the system, a non-conditioned signal was used as the tension feedback for the rotary guider controller. Therefore, the control of the rotary guider performed inaccurately due to the noise of feedback signals. Therefore, to clear the feedback signal it is essential to implement an analogue signal conditioner between the sensor and the control unit (MCU) of the rotary guider.

5.3 Directions for Future Works

During the course of this research, the following problem areas were identified as potential topics for future work.

- Further studies of tension change characteristics with a rotary guider

Extra studies of tape dynamics with a rotary guider can be a possible topic for future work. The effectiveness of parameters such as properties, location, and number of rotary guiders, variety of tape spans between flanged guides, and different tape travelling speeds in terms of tension controllability of rotary guider and contribution of rotary guider to lateral tape motion (LTM) can be studied.

- Advanced controller design for the rotary guider

Developing an advanced rotary guider controller can be another potential topic for future work. From experimental studies carried out in this study, the dynamics of the rotary guider have significantly influenced the tension; therefore, advanced controllers such as robust logic and fuzzy logic controllers can be used to increase the accuracy of tension regulation.

- Integration with advanced tape guiding mechanisms

  Integrating the developed tension regulation technology with other developing advanced tape guiding mechanisms that disturb the tape tension irregularly and are not able to maintain the tension without closed loop controlled tension actuation mechanism such as the air breathing mechanism discussed by Nagao and Chang, (2009). The effectiveness and adaptability of tension regulation technology and other guiding mechanisms could also be studied.

The tension regulation technology developed in this research can provide practical insight for the design of tape transport systems for high-density data storage. Dynamic tape path alternation and friction guiding with the rotary guider proposed in this thesis supports further tape tension controller design in tape drives in the mass production phase.

References

1. Akizuki Denshi Tsusho Co., Ltd. (2002). *AKI H8/3052F Hardware Manual*. Akizuki Denshi Tsusho Co., Ltd.

2. BestTechnology Co., Ltd. (2010). GCC Developer Lite (Version 2.36.) [Computer software]. Tokyo, JAPAN: Best Technology CO., LTD.

3. Boyle, JM., & Bhishan, B. (2005). Vibration response due to lateral tape motion and impulse force in a linear tape drive. *Microsystem Technologies*, Vol11, pp.48–73.

4. EMC Corporation. (2010). *The Digital Universe Decade.* Retrieved Feb 26, 2011, from http://www.emc.com/collateral/demos/microsites/idc-digital-universe/iview.htm

5. Hewlett-Packard, IBM and Quantum. (2011). *ULTRIUM LTO Technology Overview LTO Roadmap*. Retrieved March 16, 2011, from http://www.lto.org/technology/index.html

6. Hitachi, Ltd. (2005). *Tape Library System.* Retrieved Feb 19, 2011, from http://www.hitachi.co.jp/Prod/comp/OSD/tplib/common/index.html

7. Jaycar Electronics. (2011). *6V 9000rpm DC Electric Motor*. Retrieved Feb 26, 2011, from http://www.jaycar.com.au/productView.asp?ID=YM2712&keywords=dc+motor&form=KEYWORD.

8. Jordan. S., & Chang. J.Y., (2008). Design and Active Guiding of Tape Lateral Motion with Traveling Wave Driven PZT Actuator. *ASME 18th Annual Conference on Information Storage and Processing Systems*, Santa Clara, CA, USA, 2008 June 16–17.

9. Kartik, V., (2006) *In-Plane and Transverse Vibration of Axially-Moving Media with Advanced Guiding and Actuation Elements*, Carnegie Mellon University, Pittsburgh.

10. Kartik. V., & Pantazi. A., & Lantz. M.A, (2010). High Bandwidth Track Following for Moving Media. *ASME Information Storage and Processing Systems Conference*, Santa Clara, CA, USA, 2010 June 14–15.

11. Keshavan, M.B., & Wickert, J.A., (1998). Transient Discharge of Entrained Air from a Wound Roll. *ASME Journal of Applied Mechanics*, Vol.65, Issue 4, pp.804–810.

12. Koseki, T., & Hayafune, K., & Masada, E., (1987). Lateral Motion of a Short-Stator Type Magnetic Wheel, *IEEE Transaction on Magnetics*, Vol.23, Issue 5, pp.2350–2352.

13. Kyowa Electronic Instruments Co., Ltd. (2011). *Gages for General Stress Measurement.* Retrieved Feb 19, 2011, from http://www.kyowa-ei.co.jp/product/pdf/kfg.pdf

14. Lakshmikumaran, A., & Wickert, J.A., (1998). Edge Buckling of Imperfectly Guided Webs, *ASME Journal of Vibration and Acoustics*, Vol.120, pp.346–352

15. Lu. Y., & Messner. W.V., (2001). Disturbance Observer Design for Tape Transport Control. *American Control Conference, Arlington,* VA, USA2001 June 25–27.

16. Lu. Y., & Messner. W.V., (2001). Robust Servo Design for Tape Transport. *IEEE International Conference on Control Applications*, Mexico City, Mexico, 2001 September 5–7.

17. Maxon motor ag. (2010). EPOS Studio (Version 1.41.)[Computer software]. Sachseln, Switzerland**:** Maxon motor ag.

18. Maxon Japan Corporation. (2011). *Encoder MR Type ML 128 -1000 Counts.* Retrieved Feb 19, 2011, from http://www.maxonjapan.co.jp/products/datasheets/262.pdf

19. Maxon Japan Corporation. (2011). *Maxon EPOS2 24/5 Digital Motor Controller.* Retrieved Feb 19, 2011, from http://www.maxonjapan.co.jp/product_mmc.htm

20. Maxon Japan Corporation. (2011). *Maxon RE 35, Graphite Brushes, 90 Watt.* Retrieved Feb 19, 2011, from http://www.maxonjapan.co.jp/products/datasheets/081.pdf

21. Ono. K., (1976). Lateral Motion of an Axially Moving String on a Cylindrical Guide Surface. *Journal of Applied Mechanics*, Vol.46, pp.905–912.

22. Ono. K., (1997). Lateral Motion Transfer Characteristics of Axially Moving Tape over Guide Post with Coulomb Friction. *Japanese Journal of Tribology*, Vol.42, Issue 5, pp.575–584.

23. Panda. S.P., & Engelmann. A.P., (2003). Control and operation of reel-to-reel tape drives without tension transducer. *Journal of Microsystem Technologies*, Vol.10, Number 53–59.

24. Pantazi. A., & Lantz. M., & Häberle. W., & Imaino. & W., & Jelitto. J., & Eleftheriou. E., (2010). ACTIVE TAPE GUIDING. *ASME Information Storage and Processing Systems Conference,* Santa Clara, CA, USA, 2010 June 14–15.

25. Parallax Inc. (2011). *HB-25 Motor Controller*. Retrieved Feb 19, 2011, from http://www.parallax.com/Portals/0/Downloads/docs/prod/motors/HB-25MotorController-V1.2.pdf

26. Parallax Inc. (2011). *Parallax (Futaba) Standard Servo.* Retrieved Feb 19, 2011, from http://www.parallax.com/Portals/0/Downloads/docs/prod/motors/900-00005StdServo-v2.1.pdf

27. Raeymaekers. B., & Talke. F.E., (2009). Attenuation of Lateral Tape Motion due to Frictional Interaction with a Cylindrical Guide. *Tribology International,* Vol.42, pp.609–614.

28. Richards, D.B., & Sharrock, M.P., (1998). Key Issues in the Design of Magnetic Tape for Linear Systems of High Track Density, *IEEE Transaction on Magnetics,* Vol.34, Issue 4, pp.1878–1882.

29. Shelton, J.J., & Reid, K.N., (1971). Lateral Dynamics of an Idealized Moving Web, *ASME Journal of Dynamic System, Measurement, and Control,* Vol.3, pp.187–192.

30. Shelton, J.J. & Reid, K.N., (1971). Lateral Dynamics of a Real Moving Web, *ASME Journal of Dynamic Systems, Measurement, and Control,* Vol.3, pp.180–186.

31. Taylor. R.J., & Talke. F.E., (2005). High Frequency Lateral Tape Motion and Dynamics of Tape Edge Contact. *Journal of Microsystem Technologies,* Vol.11, Number 8-10, pp.1166–1170.

32. Taylor. R.J., & Chung. M., Talke. F.E., (2006). Dynamic simulation of in-plane transverse displacement of tape. *Microsystem Technologies*, Vol12, pp.1117–1124.

33. Wicket. J.A., & Mote. C.D., (1990). Classical Vibration Analysis of Axially Moving Continua. *ASME Journal of Applied Mechanics,* Vol.57, pp.738–744.

34. Wicket. J.A., (1993) Analysis of Self-Excited Longitudinal Vibration of A Moving Media. *Journal of Sound and Vibration,* Vol.160 (3), pp.455–463.

35. Xu, P. (2009). *Mechatronics*, Unpublished lecture notes, School of Engineering and Advanced Technology, Massey University.

36. Zen, G., & Mu, F.S., (2006). Stability of an Axially Accelerating String Subjected to Frictional Guiding Forces. *Journal of Sound and Vibrations,* vol.289, pp.551–576.

Appendix A

A summary of mechanical and electrical components and GUI control software, specifications of electrical components, and a full electric circuit diagram of developed tape transport system are appended. Technical specifications of electrical components are listed following a full list of components. An electric circuit diagram that describes full connections of electric components and wiring is also appended.

A.1 Full List of Components and Instrumentations

Supply Pack Stand	
Tape Pack Stand	DC_Motor_Base: DWG No 1 (Appendix B) × 1
	DC_Motor_Leg: DWG No 2 (Appendix B) × 4
	DC_Motor_Foot: DWG No 3 (Appendix B) × 4
Ball Bearing Shaft	Diverted from a HP Commercial Tape Drive × 1
Coupler	Brass made 6mm to 6mm Female Coupler × 1
Driving Source	6V High Power DC Motor × 1
Supply Pack	Quantum LTO4 Tape Cartridge × 1
Take up Pack Stand	
Tape Pack Stand	DC_Motor_Base: DWG No 1 (Appendix B) × 1
	DC_Motor_Leg: DWG No 2 (Appendix B) × 4
	DC_Motor_Foot: DWG No 3 (Appendix B) × 4
Ball Bearing Shaft	Diverted from a HP Commercial Tape Drive × 1
Coupler	Brass made 6mm to 6mm Female Coupler × 1
Driving Source	Maxon RE 35 DC Coreless Motor × 1
Gear Head	3:1 ratio Permanent Gear Head × 1
Encoder	Maxon 10bit Magnet Resistant Encoder × 1
Take up Pack	Diverted from a HP Commercial Tape Drive × 1
Rotary Guider	
Rotary Guider	Rigid Plate (TAMIYA Universal Plate) × 1
	Probe_Holder_Base: DWG No 7 (Appendix B) × 1
	Servo_Motor_Holder: DWG No 9 (Appendix B) × 1
Flanged Slider A	Diverted from a HP Commercial Tape Drive × 1
Flanged Guide B	Diverted from a HP Commercial Tape Drive × 1
Driving Source	5V Parallax Standard Servo Motor × 1
Stationary Guide	
Stationary Guide	Guide_Pole: DWG No 5 (Appendix B) × 2
	Guide_Pole_Leg: DWG No 6 (Appendix B) × 2
Flanged Guide	Diverted from a HP Commercial Tape Drive × 2

Tension Sensor	
Tension Sensor	Strain Gauge (Kyowa KFG-5-350-C1-11 (350Ω)) × 4
Wheatstone Bridge	350Ω Resister × 4
Instrumentation Amplifier	BB INA101 High Accuracy Instrumentation Amplifier × 2
	100KΩ Pot Resister × 2
	10KΩ Variable Resister (40 Ω) × 2
	0.1μF Capacitor × 2
Low pass Filter	1.6KΩ Resister × 2
	100μF Capacitor × 2
Control Units	
Micro Control Unit (MCU)	AKI-H8/3052f with USB Development Board × 1
Motor Controller A	Parallax HB 25 Motor Controller × 1
Motor Controller B	Maxon EPOS 2 24/5 Digital Motor Controller × 1
GUI	Windows Hyper Terminal × 1
	EPOS Studio Ver1.41 × 1
Cables	RS232 Cable × 1
	USB to Miniport B Cable × 2

Table A-1: Full list of mechanical and electrical components, instrumentations, and software.

A.2 Technical Specifications of Instrumentations

Technical specifications of driving sources, encoder, strain gauge, micro control unit, and motor controllers are listed in following lists.

Driving Source Technical Specifications

- Maxon RE 35 90W DC Coreless

Power Rate	90W
Nominal Voltage	15V
No Load Speed	7070 rpm
Torque	77.7mNm

Table A-2: Technical specifications of take up pack driving motor.

(Maxon Japan Corporation, 2011)

- 6V High Power DC Motor

Power Rate	5.96W
Nominal Voltage	6V
No Load Speed	9000 rpm
Torque	18mNm

Table A-3: Technical specifications of supply pack driving motor.

(Jaycar Electronics, 2011)

- Parallax (Futaba) Standard Servo

Workspace	0° - 180°
Torque	304mNm
Nominal Voltage	6V
Pulse Input	20 ms

Table A-4: Technical specifications of rotary guider driving motor.

(Parallax Inc, 2011)

Encoder Technical Specifications

- Maxon Encoder Magnet Resistant

Resolution	10bit (1000)
No. Channel	3ch
Maximum Frequency	200Hz
Maximum Measurable rpm	12000

Table A-5: Technical specifications of encoder.

(Maxon Japan Corporation, 2011)

Strain Gauge Technical Specifications

- Kyowa KFG-5-350-C1-11; General-purpose foil strain gauge

Gauge Length	0.5mm
Resistance	350Ω
Gauge Factor	2

Table A-6: Technical specifications of strain gauge.

(Kyowa Electronic Instruments Co., Ltd., 2011)

Micro Control Unit (MCU) Technical Specifications:

- Hitachi H8/3052F (AKI H8/3052F)

Crystal Frequency	25 MHz
ROM	512 KB
RAM	8 KB
ITU	16bit timer × 5ch
TPC	4ch pulse outputs
WDT	Watch Dog Timer
SCI	2ch
A/D	10bit resolutions × 8
D/A	10bit resolutions × 2
I/O Ports	78

Table A-7: Technical specifications of micro control unit.

(Akizuki Denshi Tsusho Co., Ltd., 2002)

Motor Controller Technical Specifications

- Parallax HB 25 Motor Controller (Motor Controller A)

Motor Supply	6.0 VDC – 16.0 VDC
Load Current	25 A Continuous, 35A Peak
PWM Frequency	9.2 kHz
Pulse Input	1.0ms (Full Reverse) – 2.0ms (Full Forward) 1.5ms (Neutral)

Table A-8: Technical specifications of motor controller A.

(Parallax Inc, 2011)

- Maxon EPOS2 24/5 (Motor Controller B)

Motor Supply	11 VDC – 24 VDC
Load Current	5A Continuous, 10A Peak

Table A-9: Technical specifications of motor controller B.

(Maxon Japan Corporation, 2011)

A.3 Full Electric Circuit Diagram

Fig. A-1 shows a full electric circuit diagram of tape transport system including the connections between MCU and the other electric components. All electric components are connected setting the MCU (AKI H8/3052f) as the hub. The pin 78 and 79 of MCU are connected to the tension sensors. Each tension sensor is structured from two strain gauges, a Wheatstone bridge, an instrumentation amplifier, and a low pass filter. The measured analogue tension signals from both tension sensors are sent to MCU through analogue to digital converters. The supply pack and the rotary guider are connected to Pulse Width Modulation (PWM) channel 1 and channel 2 that are pin 93 and 94 of MCU respectively. Control PC and MCU is connected through RS232 communication line to command the operations of tape transport system and receive responses through Graphical User Interface (Windows Hyper Terminal).

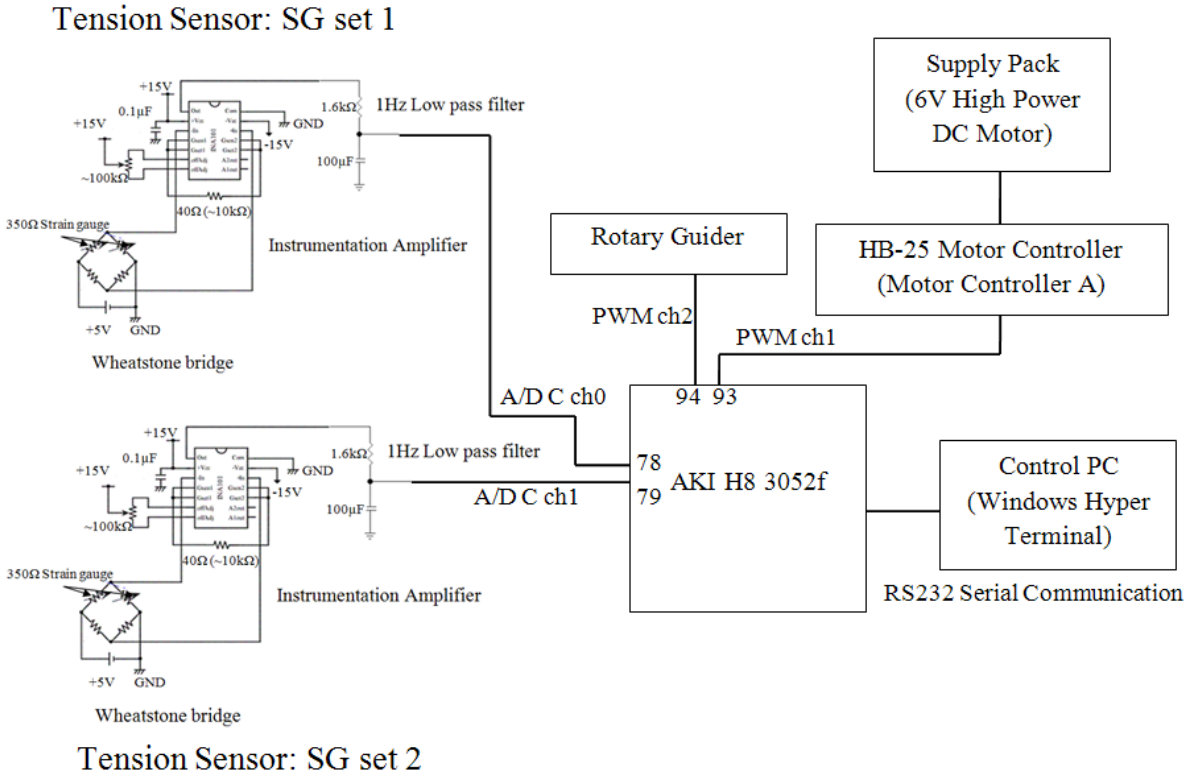

Fig. A-1: A full electric circuit and connections of electrical components.

Appendix B

Mechanical components structure developed tape transport system were designed using, SolidWorks 2009 SP4, 3 dimensional mechanical computer aided design (3D CAD) environment and manufactured by Massey University Workshop Albany with top quality. Following 2D drawings are shown designed mechanical components with dimensions.

Tape Pack Stand

B-1 Tape Pack Stand – Base

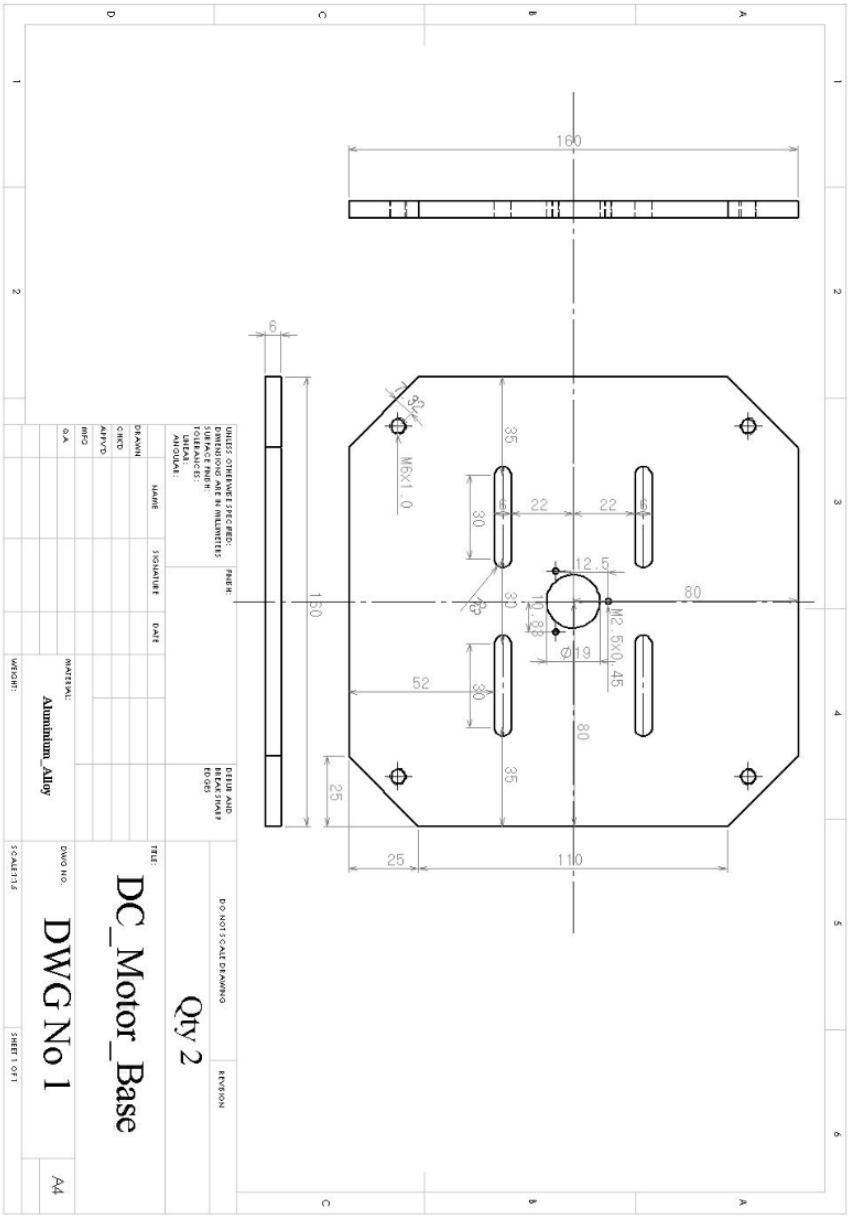

B-2 Tape Pack Stand - Leg

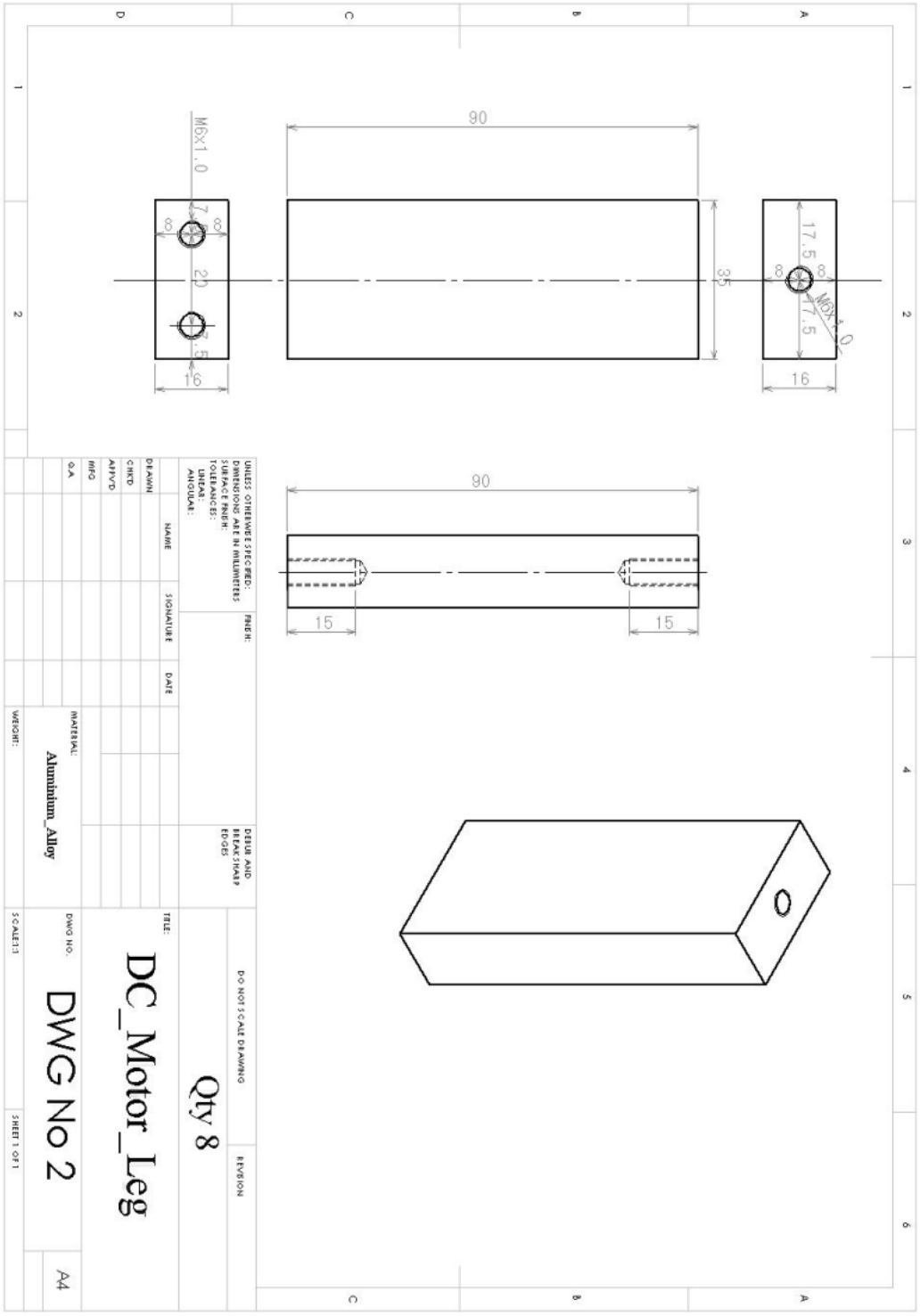

B-3 Tape Pack Stand - Foot

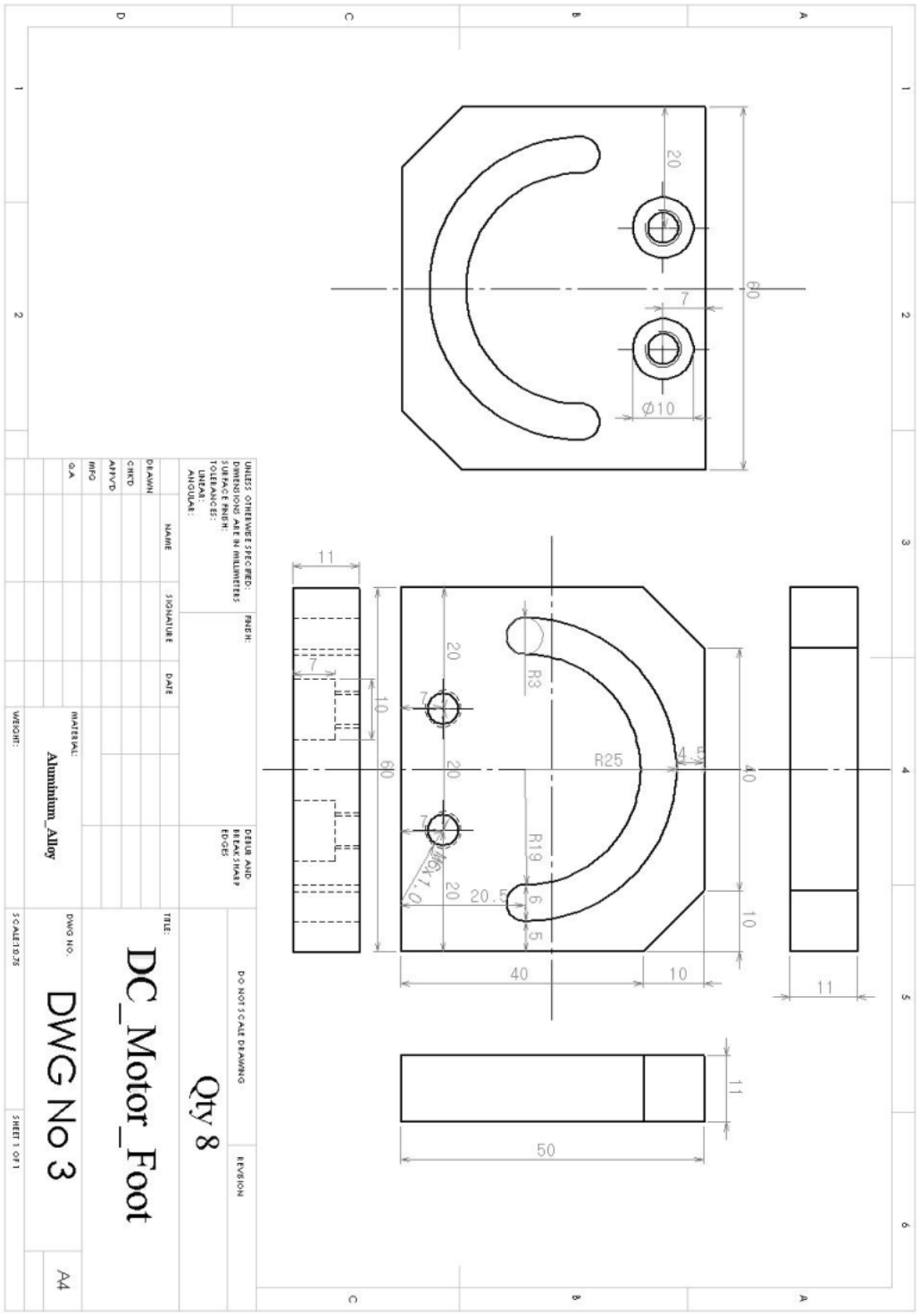

Stationary Guide

B-4 Stationary Guide - Pole

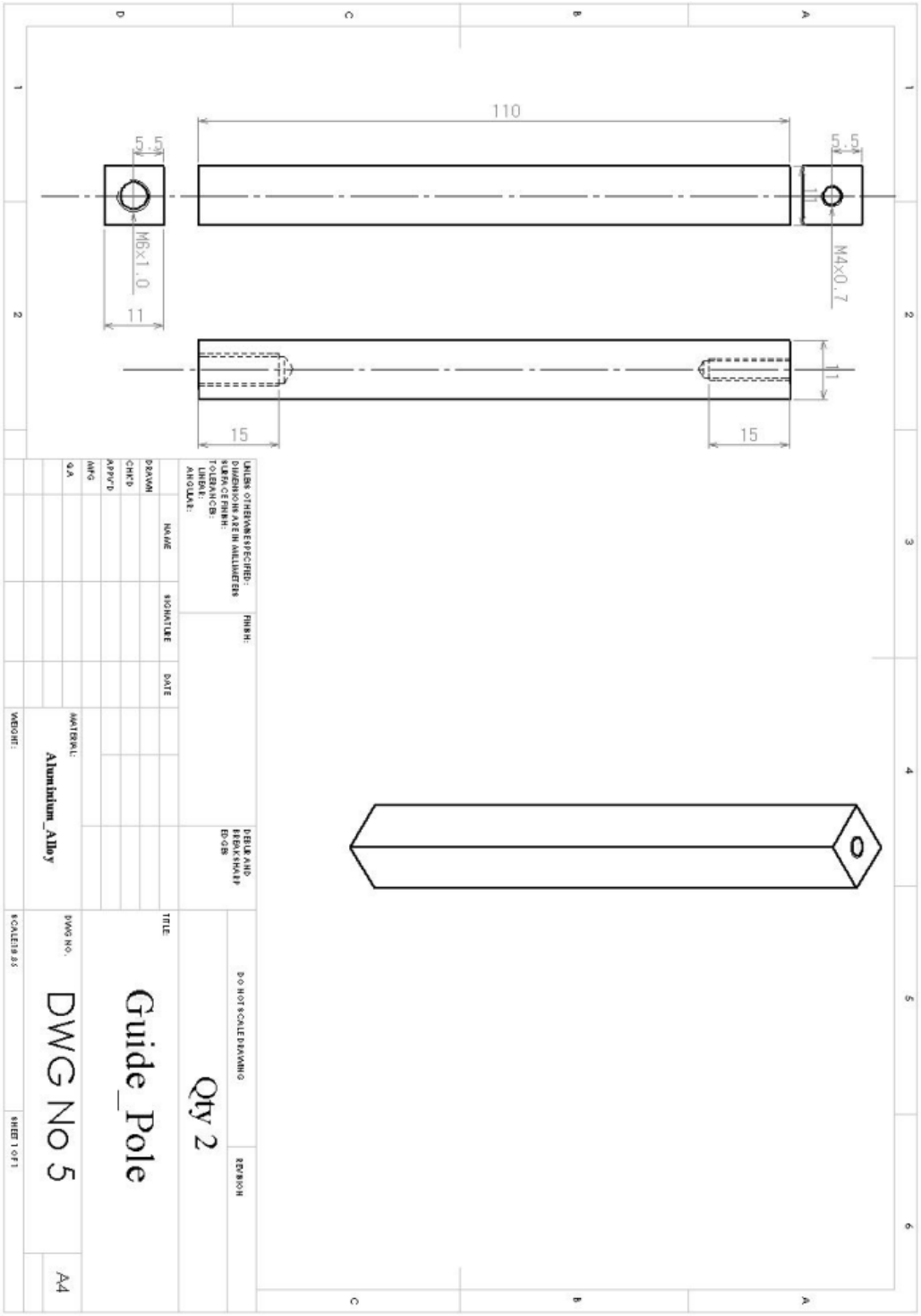

B-5 Stationary Guide - Leg

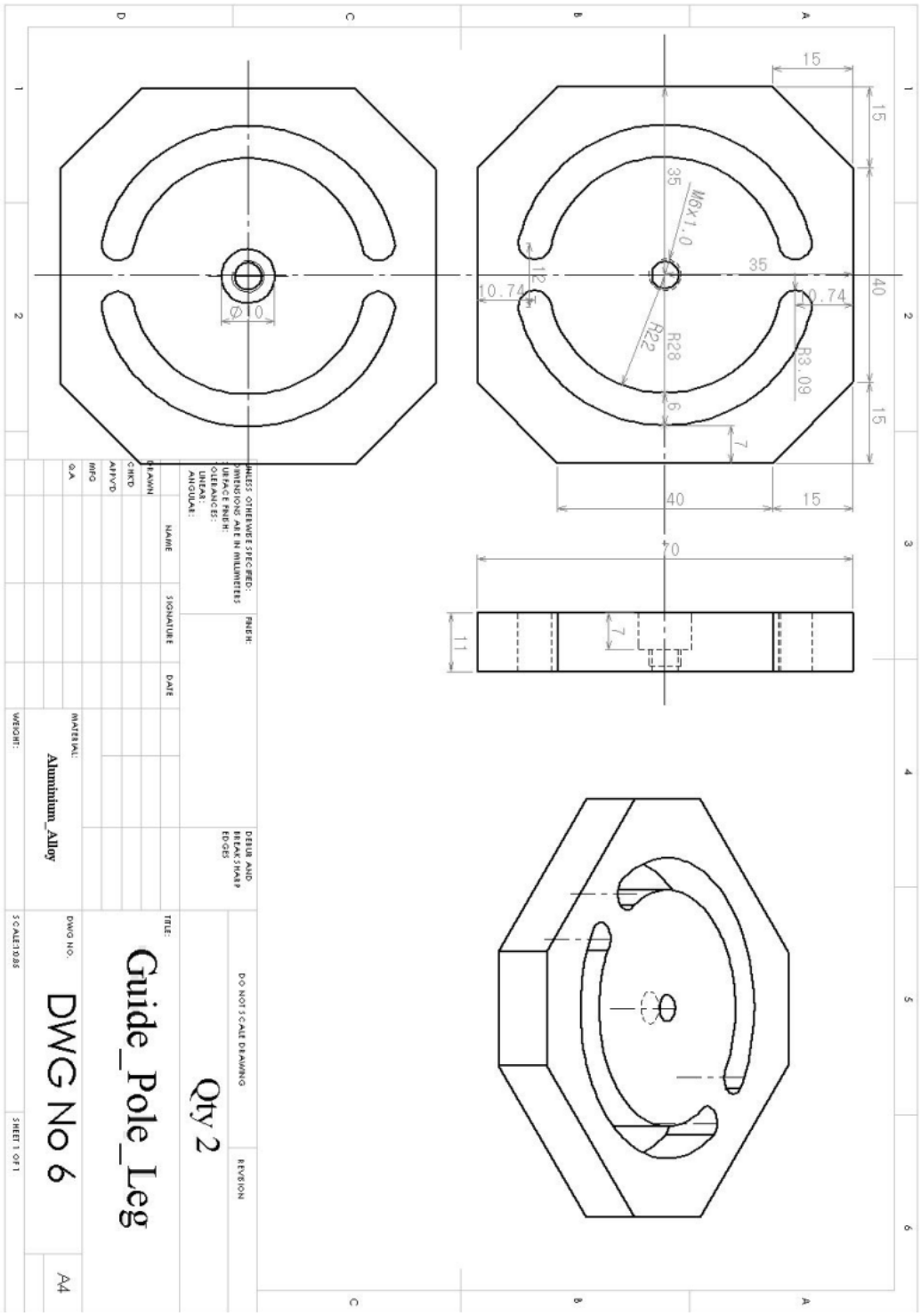

Rotary Guider

B-6 Rotary Guider - Base

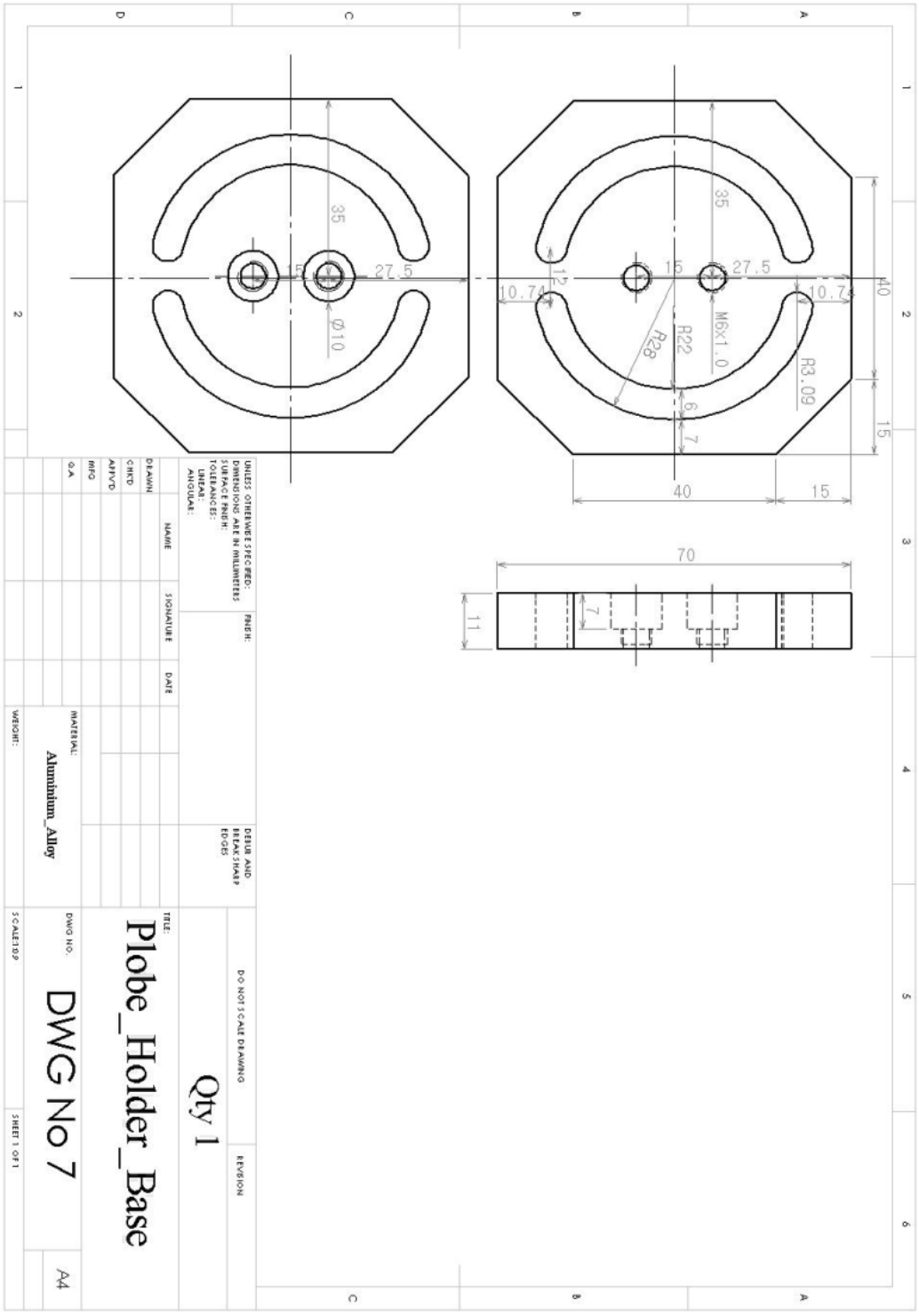

B-7 Rotary Guider - Body

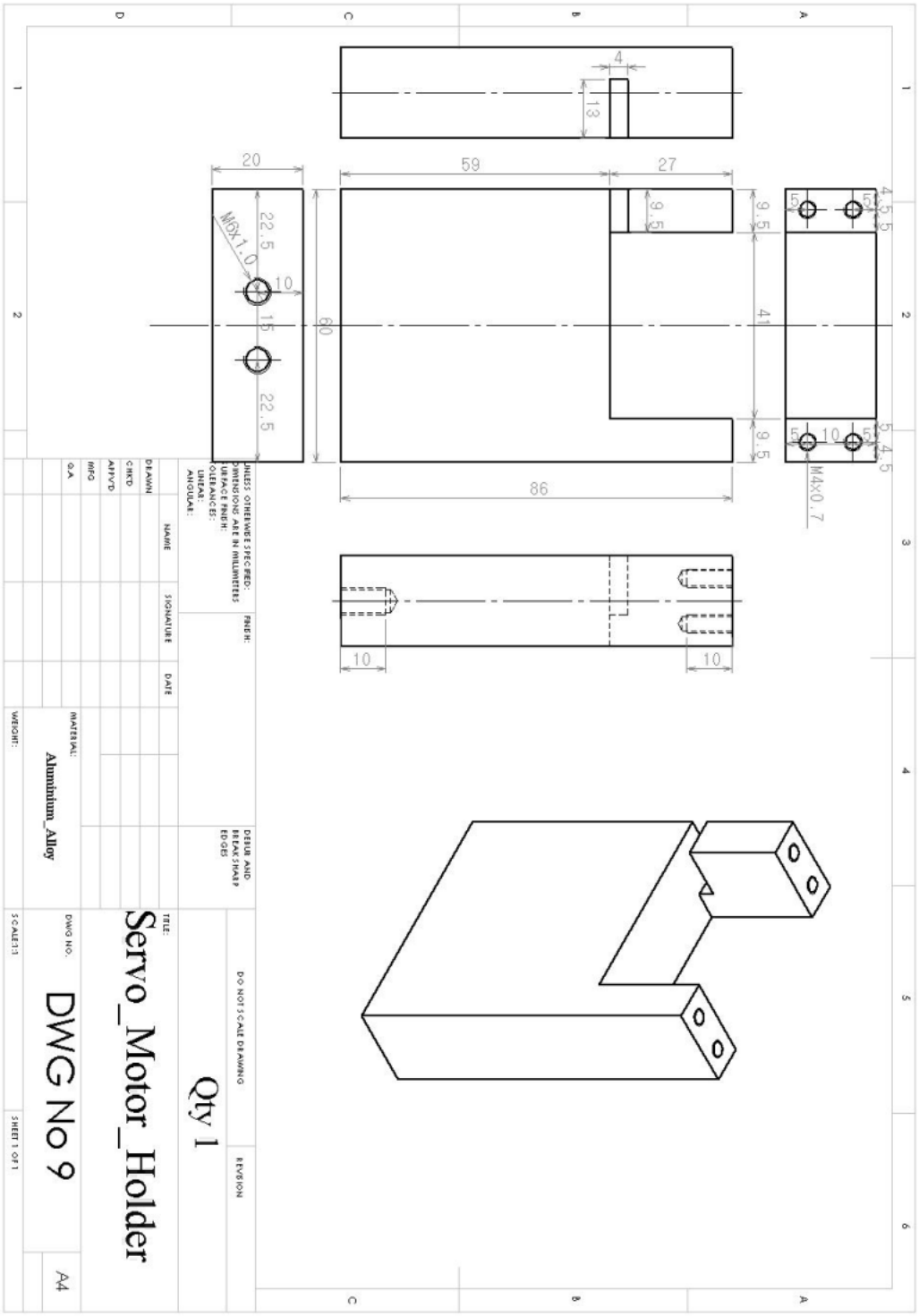

Appendix C

The tape transport driving software for control MCU (AKI H8/3052f) of developed tape transport system was developed using GCC Developer Lite version 2.36 (BestTechnology Co., Ltd., 2010) in C++ computing language. Full codes of system driving software are shown below.

Tape Transport System Driver (Coding Language: C++, Developing environment: GCC Developer Lite)

```
//*****************************************
Massey_Tape_Transport_System_Driver_Ver_2_0
BY RIICHI 2010.12.13
For AKI-H8/3052F CPU board with USB
development board
This program drives Massey tape transport system.

Features: rewind tape and tape tension regulation
-> Proportional based controller, open loop based
controller, and multi-gain proportional based
controller

Functions: 10bit ADC, PWM (RPM & angle), SCI
controlled, and AD/C data recordable
//*****************************************
#include <3052.h>
#include <stdio.h>
#include <math.h>
#include "functions_Ver_2.1.h"
//*****************************************
//                    Global variables
//*****************************************
int SG1, SG2;
unsigned int i, diff, DC_PWM, Servo_PWM,
Servo_PWM_max, PWM_valD, PWM_valS, ref = 0,
ref1, ref2, init1 = 0, init2 = 0;
unsigned long int ITU3_val, ITU3_count;
unsigned char g[11] = {0,1, 5, 10, 20, 50, 80, 100,
150, 200, 250};
unsigned char inter[11] = {0, 1, 5, 10, 15, 25, 35, 45,
55, 65, 75};

//*****************************************
//        Interruption setting (IMFA and IMFB)
//*****************************************
void int_imia1 ()
{
  ITU1.TSR.BIT.IMFA = 0;
                    //clear IMFA of ITU1(PWM1)
}

void int_imib1 ()
{
  ITU1.TSR.BIT.IMFB = 0;  //clear IMFB of ITU1
  ITU1.GRB = Servo_PWM;       //get ITU1.GRB
value for Servo_PWM duty cycle
}

void int_imia2 ()
{
  ITU2.TSR.BIT.IMFA = 0;
                     //clear IMFA of ITU2(PWM2)
}

void int_imib2 ()
{
  ITU2.TSR.BIT.IMFB = 0;  //clear IMFB of ITU2
  ITU2.GRB = DC_PWM;        //get ITU2.GRB
value for DC_PWM duty cycle
}

void int_imia3 ()
{
  ITU3.TSR.BIT.IMFA = 0;//clear IMFB of ITU3
  ITU3_count++;
}
```

```
//*****************************************
//                  Start ITU3
//*****************************************
void statITU3 (void)
{
   ITU3.GRA = ITU3_val;        //1 cycle time (10us)
   ITU.TSTR.BIT.STR3 = 0;                //stop timer
   ITU3.TCNT = 0;                //clear timer count
   ITU.TSTR.BIT.STR3 = 1;                //start timer
}

//*****************************************
//                  Servo duty controller
//*****************************************
int Servo_con(void)      //Obtain SG total ADC value
{
   int Servo_duty, Servo_duty0, Servo_duty1;
                                    //local variables

   ADconv();                //get AD converted value
   SG1 = addra();           //SG 1 ADC
   SG2 = addrb();           //SG 2 ADC
   Servo_duty0 = addra() - ref1;//calculate SG 1 error
   Servo_duty1 = addrb() - ref2;//calculate SG 2 error
   Servo_duty = (pow(Servo_duty0,2)) +
(pow(Servo_duty1,2));          //calculate total tension
   return (Servo_duty);
}

//*****************************************
//          SG reference value obtaining (Display)
//*****************************************
void SGval(void)             //Obtain SG 1 & 2ADC
value
{
   ADconv();               //get AD converted value
   SG1 = addra();          //SG 1 ADC
   SG2 = addrb();          //SG 2 ADC
   SCI1_printf("%d %d\n", SG1, SG2);
                           //display on PC
}

//*****************************************
//              SG value obtaining (Display)
//*****************************************
void SGval1(void)          //Obtain SG 1 & 2ADC
value
{
   ADconv();               //get AD converted value
   SG1 = addra();          //SG 1 ADC
   SG2 = addrb();          //SG 2 ADC
}

//*****************************************
//              Tension reference value setup
//*****************************************
unsigned int Tref(){
   unsigned int tref;                   //local variable

   tref=getIntSCI1("Enter Tension ref value ^ 2 (0 -
1023): ");//Obtain a ref val for tension ^ 2
   if(tref >= 0 && tref <= 1023){    //limit tref range
     SCI1_printf("Tension ref value ^ 2 is %d\n",
tref);                                  //display on PC
     return(tref);
   } else{
     SCI1_printf("%d: SG ref value invalid\n", tref);
                                 //fail safe: use default
     return 0;
   }
}

//*****************************************
//          Rotary guider's angle change ratio setup
//*****************************************
unsigned int AcDuty(){
   int acang, acduty;                   //local variables

   acang=getIntSCI1("Enter Guider Angle(0 - 40
degree): ");//Obtain guider angle change ratio
   if(acang >= 0 && acang <=
40){                                    //limit acang range
     acduty = acang * 28;//convert from duty to angle
     SCI1_printf("Guider angle is %d\n", acang);
```

```
                                        //display on PC
    return(acduty);
   } else{
    SCI1_printf("%d: Input guider angle is invalid\n",
acang);                                 //fail safe: use default
    return 0;
   }
}

//*****************************************
//          Rotary guider's duty change ratio setup
//*****************************************
unsigned int AcDuty1(){
   int acang;                           //local variable

   acang=getIntSCI1("Enter duty change ratio(0 -
1023): ");//Obtain guider duty change ratio
   if(acang >= 0 && acang <=
1023){                                  //limit acang range
    SCI1_printf("Duty change ratio is %d\n", acang);
                                        //display on PC
    return(acang);
   } else{
    SCI1_printf("%d: Input duty change ratio is
invalid\n", acang);             //fail safe: use default
    return 0;
   }
}

//*****************************************
//                    ADC sampling rate
//*****************************************
unsigned ADsample(){
   int ads;                             //local variable

   ads=getIntSCI1("Enter AD/C sampling rate (1 -
60000): up to 0.6sec");         //Obtain sampling rate
   if(ads >= 1 && ads <=
60000){                                 //limit ads range
    SCI1_printf("AD/C sampling rate is %d\n", ads);
                                        //display on PC
    return(ads);
   } else{
    SCI1_printf("%d: Sampling rate invalid\n", ads);
                                        //fail safe: use default
    return 0;
   }
}

//*****************************************
//                    Rotary guider angle set up
//*****************************************
unsigned int Angle(){
   unsigned int angle, angle1;          //local variable

   angle = getIntSCI1("Set rotary guider angle: ");
                                        //obtain guider angle
   if(angle >= 0 && angle <= 40){ //limit angle range
    angle1 = 2400 - angle * 28;
                                        //set guider at input angle
    SCI1_printf("Rotary guider was set at %d
degree\n", angle);                      //display on PC
    return(angle1);
   } else{
    SCI1_printf("%d: guider angle is invalid\n",
angle);                                 //fail safe: use default
    return 0;
   }
}

//*****************************************
//                    Angle change interval setup
//*****************************************
unsigned long int Period(){
   unsigned long int period, interval, angle_change =
70000, angle_change_duty = 3570000;//local
variables

   period = getIntSCI1("Enter test period (1 - 300 sec;
default 170)): ");                      //Obtain test period
   if(period >= 1 && period <=
300){                                   //limit test period
    SCI1_printf("Interval is %lu\n", period);
                                        //display period on PC
```

```
    interval = angle_change / period;
                                    //interval calculation 1
    interval = angle_change_duty / interval;
                                    //interval calculation 2
    SCI1_printf("Interval is %lu\n", interval);
                                   //display interval on PC
    return(interval);
   } else{                                  //fail safe
    SCI1_printf("Invalid period\n");    //use default
    return 0;
   }
}

//*****************************************
//    Multi-gain proportional controller gain set up
//*****************************************
void Multi_gain(void){
   int t;
   unsigned char gainT, gainMAX = 0, limit1 = 1,
limit2 = 255;                           //local variables

   for(t = 1; t < 11; t++){              //loop 10 times
    gainT = getIntSCI1("Enter gain (1 - 255): ");
                                        //Obtain gains
    if((gainT < limit1) || (gainT >
limit2)){                              //limit gainT range
     if(gainMAX >= g[t]){                 //fail safe 1
      g[t] = gainMAX;          //g[t] gets gainMAX
      if(g[t] >= limit2){
       g[t] = limit2;
              //if gainT > 255 -> set gainT at 255
      }
      SCI1_printf("%d: input gain %d is invalid ->
set to %d\n", gainT, t, g[t]);       //set gainT at max
     }
     else{
      SCI1_printf("%d: input gain %d is invalid ->
set to default %d\n", gainT, t, g[t]);      //use default
      gainMAX = g[t];
     }
    }
    else if(gainT < gainMAX){
                                   //fail safe 2: new < max
     if(gainMAX >= g[t]){
      g[t] = gainMAX;          //g[t] gets gainMAX
      if(g[t] >= limit2){
       g[t] = limit2;
              //if gainT > 255 -> set gainT at 255
      }
      SCI1_printf("%d: input gain %d is invalid ->
set to %d\n", gainT, t, g[t]);       //set gainT at max
     }
     else{
      SCI1_printf("%d: input gain %d is invalid ->
set to default %d\n", gainT, t, g[t]);    //use default
      gainMAX = g[t];          //refresh gainMAX
     }
    } else{
      g[t] = gainT;                    //change gain
      if(gainT >= gainMAX){
       gainMAX = gainT;      //refresh gainMAX
      }
      SCI1_printf("Gain %d is set at %d\n", t, g[t]);
                                   //display on PC
    }
   }
   for(t = 1; t < 11; t++){              //loop 10 times
    SCI1_printf("Gain %d is set at %d\n", t, g[t]);
                           //display all gains on PC
   }
}

//*****************************************
//Multi-gain proportional controller conditions set up
//*****************************************
void Multi_con(void){
   int t;
   unsigned char conT, conMAX = 0, limit1 = 1,
limit2 = 255;                           //local variables

   for(t = 1; t < 11; t++){                //loop 10 times
    conT = getIntSCI1("Enter condition (1 - 255): ");
                                   //Obtain conditions
```

```
    if((conT < limit1) || (conT > limit2)){                    //limit conT range
      if(conMAX >= inter[t]){                 //fail safe 1
       inter[t] = conMAX;       //g[t] gets gainMAX
       if(inter[t] >= limit2){
        inter[t] = limit2;
                  //if gainT > 255 -> set gainT at 255
       }
       SCI1_printf("%d: input condition %d is invalid -> set to %d\n", conT, t, inter[t]);  //set conT at max
      }
      else{
       SCI1_printf("%d: input condition %d is invalid -> set to default %d\n", conT, t, inter[t]); //use default
       conMAX = inter[t];
      }
    }
    else if(conT < conMAX){//fail safe2 : new < max
     if(conMAX >= inter[t]){
      inter[t] = conMAX;          //g[t] gets gainMAX
      if(inter[t] >= limit2){
       inter[t] = limit2;
                  //if gainT > 255 -> set gainT at 255
      }
      SCI1_printf("%d: input condition %d is invalid -> set to %d\n", conT, t, inter[t]);   //set conT at max
     }
     else{
      SCI1_printf("%d: input condition %d is invalid -> set to default %d\n", conT, t, inter[t]); //use default
       conMAX = inter[t];           //refresh gainMAX
     }
    } else{
      inter[t] = conT;                      //change gain
      if(conT >= conMAX){
       conMAX = conT;
                                    //refresh gainMAX
      }
      SCI1_printf("Condition %d is set at %d\n", t, inter[t]);                                  //display on PC
    }
   }
   for(t = 1; t < 11; t++){                 //loop 10 times
    SCI1_printf("Condition %d is set at %d\n", t, inter[t]);                 //display all conditions on PC
   }
}

//*****************************************
//          Multi-gain proportional logic controller
//*****************************************
void Logic(void){

   if((inter[2] > diff) && (diff >= inter[1])){                                  //condition 1
     i = 1;
   }
   if((inter[3] > diff) && (diff >= inter[2])){                                  //condition 2
     i = 2;
   }
   if((inter[4] > diff) && (diff >= inter[3])){                                  //condition 3
     i = 3;
   }
   if((inter[5] > diff) && (diff >= inter[4])){                                  //condition 4
     i = 4;
   }
   if((inter[6] > diff) && (diff >= inter[5])){                                  //condition 5
     i = 5;
   }
   if((inter[7] > diff) && (diff >= inter[6])){                                  //condition 6
     i = 6;
   }
   if((inter[8] > diff) && (diff >= inter[7])){                                  //condition 7
     i = 7;
   }
   if((inter[9] > diff) && (diff >= inter[8])){                                 //condition 8
     i = 9;
   }
```

```
   if((inter[10] > diff) && (diff >=
inter[9])){                              //condition 9
     i = 10;
   }
   if((inter[11] > diff) && (diff >=
inter[10])){                             //condition 10
     i = 11;
   }
}

//*****************************************
//                SG value initialization
//*****************************************
void SGinit(void)
{
   int t;                                //local variable

   for(t = 0; t < 10; t++){              //loop 10 times
     ADconv();                                 //get AD
converted value
     init1 = addra();                    //SG1 ADC
     ref1 = ref1 + init1;
                  //store obtained values for average
     init2 = addrb();                    //SG2 ADC
     ref2 = ref2 + init2;
                  //store obtained values for average
   }
}

//*****************************************
//                System starting sequence
//*****************************************
void get_ready(void){
   int ready = 5, timer = 5;
   unsigned long int count = 100000;
                                    //local variables

   ITU3_count = 0;              //ITU3 count refresh
   ref1 = 0;                          //set ref1 to 0
   ref2 = 0;                          //set ref 2 to 0
   SCI1_printf("System starting in\n");
//display on PC
   while(ready >= 0){              //start count down
    if(ITU3_count >= count){
     if(timer >= 1){
      SCI1_printf("%d\n",    timer);
                          //display remaining count
      SGinit();             //obtain SG initial values
     } else{
      SCI1_printf("GO!\n");
      ref1 = ref1 / 50;   //average SG1 initial value
      ref2 = ref2 / 50;   //average SG2 initial value
      SCI1_printf("ADC value init SG set one:%d,
SG set two:%d\n", ref1, ref2);
                          //display SG initial values
     }
     timer--;                         //decrement timer
     ready--;                         //decrement ready
     ITU3_count = 0;             //ITU3 count refresh
    }
   }
}

//*****************************************
//                          Auto Mode
//*****************************************
void Amode(void){
                    //Mode1; Automatic Mode (STAT)
   int t, u = 0, angle = 0;
   unsigned int data, APWM = 1, stop, flagR = 0,
flagS = 1, sampleT = 1;         //(10us)//local variables
   unsigned long int interval = 8686;
   char op;

   while(1){
     cur_pos(0,0);
     lcdprintf("AMode enabled");
     SCI1_printf("******************Auto Mode
Menu*********************\n");
     SCI1_printf("A: Proportional based Controller
ON\n");
     SCI1_printf("T: Open Loop Based Controller
ON\n");
```

```
      SCI1_printf("F: Multi-gain proportional Based
Controller ON\n");
      SCI1_printf("S: Rotary actuator OFF\n");
      SCI1_printf("Z: Change Tension reference
value\n");
      SCI1_printf("X: Change guider increment+-
(PC)\n");
      SCI1_printf("C: Change AD/C sampling rate
(PC)\n");
      SCI1_printf("V: Change angle change interval
(OLC)\n");
      SCI1_printf("B: Change Multi proportional gain
(MPC)\n");
      SCI1_printf("N: Change Multi proportional
condition (MPC)\n");
      SCI1_printf("Q: Return Main Menu\n");

SCI1_printf("**********************************
**********************\n");
      do{                    //infinite loop until 'Q' is input
        op = getCharSCI1();            //obtain command
      }
      while(op ==
('a'|'A'|'t'|'T'|'f'|'F'|'s'|'S'|'x'|'X'|'c'|'C'|'v'|'V'|'b'|'B'|'n'|'N'|'z'|'
Z'|'r'|'R'|'q'|'Q'));
      switch(op){
        case'a'|'A':     //case A: proportional controller
          ITU3_count = 0;            //ITU3 count refresh
          get_ready();
          cur_pos(0,1);          //cursor position on LCD
          lcdprintf("Guider enabled");    //print on LCD
          SCI1_printf("SG val, Servo Duty cycle, angle,
Sampling time:%d\n", sampleT);
          flagR = 1;

          while(flagR == 1){               //infinite loop
            stop = getCharSCI1M();
                        //check input for escape loop
            if(ITU3_count >= sampleT){
                        //refresh SG measured value
              data = Servo_con();                  //ADC
              if(ref < data){
//ref & measured SG values comparison (when
measured value > ref value)
                Servo_PWM = Servo_PWM + APWM;
                            //PWM servo duty cycle +
                if(Servo_PWM >= 2400){        //fail safe
                  Servo_PWM = 2400;
                                //duty cycle max value
                }
                angle = (2400 - Servo_PWM) / 28;
                        //obtain output current angle
                SCI1_printf("%d %d %d %d %d\n",SG1,
SG2, data, Servo_PWM, angle);
                    //outputs AD/C and duty cycle values
              }
              if(ref > data){
//ref & measured SG values comparison (when
measured value < ref value)
                Servo_PWM = Servo_PWM - APWM;
                            //PWM servo duty cycle -
                if(Servo_PWM <= 1280){        //fail safe
                  Servo_PWM = 1280;
                                //duty cycle min value
                }
                angle = (2400 - Servo_PWM) / 28;
                        //obtain output current angle
                SCI1_printf("%d %d %d %d %d\n",SG1,
SG2, data, Servo_PWM, angle);
                    //outputs AD/C and duty cycle values
              }
              ITU3_count = 0;        //ITU3 count refresh
            }
            if(stop == '0'){
                    //when '0' was input quit the loop
              flagR = 0;                    //set the flag to 0
              cur_pos(0,1);      //cursor position on LCD
              lcdprintf("Guider disabled");//print on LCD
            }
          }
        break;

        case't'|'T':
              //case T: Open loop based control mode
```

```
ITU3_count = 0;            //ITU3 count refresh
u = 0;                              //refresh u
flagS = 1;
Servo_PWM = Angle();
                  //input initial guider angle
Servo_PWM_max = Servo_PWM + 196;
                    //set guider stop angel
if(Servo_PWM_max >= 2400){
              //limit max servo_PWM_max
 Servo_PWM_max = 2400;
}
SCI1_printf("Ready! -> press 0 to start\n");
            //pause program till 0 is pressed
while(flagS == 1){
 stop = getCharSCI1M();//check input "0"
 if (stop == '0'){
  flagS = 0;
 }
}
get_ready();
cur_pos(0,1);     //cursor position on LCD
lcdprintf("Guider enabled");//print on LCD
flagR = 1;

while(flagR == 1){            //infinite loop
 stop = getCharSCI1M();
            //check input (emergency stop)
 if(ITU3_count >= interval){//rotate guider
  u++;
  if(u >= 10){
   SGval1();                          //ADC
   Servo_PWM = Servo_PWM + 1;
                  //decrement guider angle
   angle = (2400 - Servo_PWM) / 28;
                    //obtain current angle
   u = 0;
  }
  ITU3_count = 0;   //ITU3 count refresh
 }
 SGval1();                          //ADC
        SCI1_printf("%d %d %d %d\n",SG1, SG2,
Servo_PWM, angle);
       //outputs AD/C, duty cycle values, and angle
        if(Servo_PWM_max <= Servo_PWM){
         flagR = 0;                    //escape loop
        }
       if(stop == '0'){
            //when '0' was input escape the loop
        flagR = 0;//set the flagR to 0 (escape loop)
        cur_pos(0,1);      //cursor position on LCD
        lcdprintf("Guider disabled");//print on LCD
       }
      }
      break;

      case'f'|'F':  //multi-gain proportional controller
       ITU3_count = 0;           //ITU3 count refresh
       get_ready();
       cur_pos(0,1);          //cursor position on LCD
       lcdprintf("Guider enabled");    //print on LCD
       SCI1_printf("SG val, Servo Duty cycle, angle,
logic No, Sampling time:%d\n", sampleT);
       for(t = 1; t < 11; t++){
        SCI1_printf("Gain:%d is set at:%d\n", t,
g[t]);                                  //display all gains
       }
       SCI1_printf("\n");
       for(t = 1; t < 11; t++){
        SCI1_printf("Condition:%d is set at:%d\n", t,
inter[t]);                          //display all conditions
       }
       flagR = 1;

       while(flagR == 1){                //infinite loop
        stop = getCharSCI1M();
                        //check input for escape loop
        if(ITU3_count >= sampleT){
                        //refresh SG measured value
         data = Servo_con();                    //ADC
         if(data < ref){
    //compare current tension and reference tension
         diff = ref - data;
```

```
        //perform operation based on comparison result
            Logic();                    //switch conditions
            Servo_PWM = Servo_PWM - g[i];
            if(Servo_PWM <= 1280){          //fail safe
              Servo_PWM = 1280;
                                  //duty cycle min value
            }
            angle = (2400 - Servo_PWM) / 28;
                          //obtain output current angle

SCI1_printf("%d %d %d %d %d %d\n",SG1, SG2,
diff, Servo_PWM, angle, i);
       //outputs AD/C and duty cycle values, and logic
          }
          if(data > ref){
       //compare current tension and reference tension
            diff = data - ref;
       //perform operation based on comparison result
            Logic();                    //switch conditions
            Servo_PWM = Servo_PWM + g[i];

            if(Servo_PWM >= 2400){        //fail safe
              Servo_PWM = 2400;
                                  //duty cycle max value
            }
            angle = (2400 - Servo_PWM) / 28;
                          //obtain output current angle

SCI1_printf("%d %d %d %d %d %d\n",SG1, SG2,
diff, Servo_PWM, angle, i);
     //outputs AD/C and duty cycle values, and logic
          }
          ITU3_count = 0;      //ITU3 count refresh
        }
        if(stop == '0'){
              //when '0' was input escape the loop
          flagR = 0;//set the flagR to 0 (escape loop)
          cur_pos(0,1);      //cursor position on LCD
          lcdprintf("Guider disabled");//print on LCD
        }
      }
      break;

      case's'|'S':                    //case S: Servo OFF
        Servo_PWM = 2400;
                          //set PWM servo duty cycle
        angle = 0;
        SCI1_printf("Guider disabled angle:%d\n",
angle);                                 //print on display
        cur_pos(0,1);         //cursor position on LCD
        lcdprintf("Guider disabled"); //print on LCD
      break;

      case'z'|'Z'://case Z: change SG reference value
        ref = Tref();         //rewrite tension reference
value
      break;

      case'x'|'X':
   //case X: change servo's duty cycle changing ratio
        APWM = AcDuty1();
              //rewrite servo duty cycle change ratio
      break;

      case'c'|'C'://case C: change ADC sampling time
        sampleT = ADsample();
                          //rewrite ADC sampling time
      break;

      case'v'|'V':
     //case V: open loop based angle change interval
        interval = Period();
                          //obtain angle change interval
      break;

      case'b'|'B':
              //case B: Multi-gain proportional gain
        Multi_gain();
              //change Multi-gain proportional gain
      break;

      case'n'|'N':
         //case N: Multi-gain proportional condition
        Multi_con();
```

```
        //change Multi-gain proportional conditions
        break;

      case'q'|'Q':                    //back to main menu
        return;
      }
   }
}
//Mode1; Automatic Mode (END)

//*****************************************
//                    Manual Mode
//*****************************************
void Mmode(void){
                    //Mode2; Manual Mode (STAT)
   int angle = 0, data, stop, flagR = 0, flagA = 0,
APWM = 280, APWM1 = APWM / 28, dutyS = 0,
sampleT = 1, wait = 0;          //(10us)local variables
   char op, duty;

   while(1){
      cur_pos(0,0);
      lcdprintf("MMode enabled");
      SCI1_printf("******************Manual
Mode Menu*********************\n");
      SCI1_printf("A: Rotary guider ON, '1':+10deg,
'2':-deg, '0':Quit\n");
      SCI1_printf("D: Rotary guider Direct Control ->
enter duty cycle\n");
      SCI1_printf("S: Rotary guider OFF\n");
      SCI1_printf("Z: Display AD/C values\n");
      SCI1_printf("C: Change guider's angle change
ratio\n");
      SCI1_printf("V: Change AD/C sampling
rate\n");
      SCI1_printf("R: Record AD/C values\n");
      SCI1_printf("Q: Return Main Menu\n");

SCI1_printf("**********************************
**********************\n");
      do{               //infinite loop until 'Q' is input
         op = getCharSCI1();
      }
      while(op ==
('a'|'A'|'d'|'D'|'s'|'S'|'t'|'T'|'z'|'Z'|'c'|'C'|'v'|'V'|'r'|'R'|'q'|'Q'));
        switch(op){
          case'a'|'A':
//case A: change servo duty changing ratio when + or
- were pressed
            flagR = 1;                  //set flagR to 1
            while(flagR == 1){          //Servo ON
             SCI1_printf("Angle change ratio: %d (1:
Angle+, 2: Angle-, 0: Quit, Current angle:%d)\n",
APWM1, angle);
             do{        //infinite loop until '0' is input
             duty = getCharSCI1();
                        //check input for escape loop
             }
             while(duty == ('1'|'2'|'0'));
              switch(duty){
                case'1':
//case 1: when '1' was pressed plus servo certain duty
cycle
                  Servo_PWM = Servo_PWM - APWM;
                            //PWM servo duty cycle -
                  if(Servo_PWM <= 1280){    //fail safe
                    Servo_PWM = 1280;
                              //duty cycle max value
                  }
                  angle = (2400 - Servo_PWM) / 28;
                          //obtain output current angle
                  cur_pos(0,1);     //move cursor potion
                  lcdprintf("Guider enabled");
                                    //print on LCD
                 break;

                 case'2':
//case 2: when '2' was pressed subtract servo certain
duty cycle
                  Servo_PWM = Servo_PWM + APWM;
                            //PWM servo duty cycle +
                  if(Servo_PWM >= 2400){    //fail safe
                    Servo_PWM = 2400;
                              //duty cycle min value
                  }
```

```
            angle = (2400 - Servo_PWM) / 28;
                        //obtain output current angle
            cur_pos(0,1);    //move cursor potion
            lcdprintf("Guider enabled");
                                    //print on LCD
           break;

           case'0':  //case 0: back to mode 2 menu
            flagR = 0;
           break;

           default:
           break;
          }
         }
        break;

        case'd'|'D':   //case D: change servo duty cycle
         dutyS = getIntSCI1("Enter Actuator angle (0
- 40 degree): ");                    //input guider angle
         if(dutyS >= 0 && dutyS <=
40){                                    //limit the range
          Servo_PWM = 2400 - (28 * dutyS);
                            //set DC PWM duty cycle
          data = Servo_con();//obtain SG ADC value
          SCI1_printf("Guider angle is :%d\n",
dutyS);                                 //display on PC
          cur_pos(0,1);         //move cursor position
          lcdprintf("Guider enabled");//print on LCD
         } else{
          SCI1_printf("%d: Actuator duty cycle
invalid\n", dutyS);          //set servo duty to default
         }
        break;

        case's'|'S':                  //case S: Servo OFF
         Servo_PWM = 2400;
                          //set PWM servo duty cycle
         angle = 0;
         SCI1_printf("Guider disabled angle: %d\n",
angle);                                 //display on PC
         cur_pos(0,1);         //move cursor position
         lcdprintf("Guider disabled");//print on LCD
        break;

        case'z'|'Z':  //case Z: display SG ADC values
         wait = ADsample();
         flagA = 1;                     //set flagA to 1
         SCI1_printf("AD/C value SG set 1 SG set
2\n");                                  //display on PC
         while(flagA == 1){
                  //infinite loop until '0' is pressed
          stop = getCharSCI1M();      //check input
          SGval();     //display SG measured values
          long_wait(wait);
          if(stop == '0'){
                    //quit loop when '0' was input
           flagA = 0;                   //set flagA to 0
          }
         }
        break;

        case'c'|'C':
    //case C: change servo duty cycle changing ratio
         APWM = AcDuty();
                //rewrite servo duty changing ratio
        break;

        case'v'|'V':
          //case C: change SG ADC sampling time
         sampleT = ADsample();
                          //rewrite sampling time
        break;

        case'r'|'R':          //record SG ADC values
         ITU3_count = 0;      //ITU3 count refresh
         get_ready();
         SCI1_printf("Sampling time:%d, Guider
Angle:%d\n", sampleT, angle);
         flagA = 1;                     //set flagA to 1
         while(flagA == 1){
                  //infinite loop until '0' is input
          stop = getCharSCI1M();   //check input
          if(ITU3_count >= sampleT){;
```

```
                    //ADC with desired interval
            SGval();                        //ADC
           }
           ITU3_count = 0;    //ITU3 count refresh
           if(stop == '0'){
                  //quit loop when '0' was pressed
            flagA = 0;                  //set flagA to 0
           }
          }
         break;

         case'q'|'Q':                //back to main menu
          return;
        }
   }
}
//Manual Mode (END)

//*****************************************
//                Rewinding Tape Mode
//*****************************************
void Rmode(void){
                        //Rewinding Mode (STAT)
   int dutyM = 0, duty, flagM = 0, DPWM = 100;
//local variables
   char op;

   while(1){
      cur_pos(0,0);
      lcdprintf("RMode enabled");
      SCI1_printf("******************Rewinding
Mode Menu******************\n");
      SCI1_printf("A: motor ON, '1':duty+, '2':duty-,
'0':Quit\n");
      SCI1_printf("D: motor ON, enter duty cycle\n");
      SCI1_printf("Z: motor OFF\n");
      SCI1_printf("R: Rewind Tape(duty:5200)\n");
      SCI1_printf("C: Change Motor duty\n");
      SCI1_printf("Q: Return Main Menu\n");

SCI1_printf("**********************************
**********************\n");
      do{
       op = getCharSCI1();              //get operation
      }
      while(op ==
('a'|'A'|'d'|'D'|'z'|'Z'|'r'|'R'|'c'|'C'|'q'|'Q'));
      switch(op){
       case'a'|'A':                  //case A: motor ON
        flagM = 1;                       //set flagM to 1
        while(flagM == 1){
                        //infinite loop until '0' is input
          SCI1_printf("Set Motor Duty Cycle (stop
4689, default +-100): '1': Duty +, '2': Duty -, '0': Quit,
Duty:%d\n", DC_PWM);//display
          do{           //infinite loop until '0' is input
          duty = getCharSCI1();
                         //check input for escape loop
          }
          while(duty == ('1'|'2'|'0'));
           switch(duty){
            case'1':
//case 1: DC motor duty cycle is pulsed when '1' was
pressed
             DC_PWM = DC_PWM + DPWM;
                          //PWM motor duty cycle +
             if(DC_PWM >= 6250){       //fail safe
              DC_PWM = 6250;
                          //duty cycle max value
             }
             cur_pos(0,1);   //move cursor position
             lcdprintf("Motor enabled");
                                  //print on LCD
            break;

            case'2':
//case 2: DC motor duty cycle is subtracted when '2'
was pressed
             DC_PWM = DC_PWM - DPWM;
                        //PWM motor duty cycle -
             if(DC_PWM <= 3125){     //fail safe
              DC_PWM = 3125;
                          //duty cycle min value
             }
```

```
            cur_pos(0,1); //move cursor position
            lcdprintf("Motor enabled");
                                    //print on LCD
          break;

          case'0':          //back to mode 0 menu
            flagM = 0;              //set flagM to 0
          break;

          default:
          break;
         }
       }
      break;

      case'd'|'D':              //case D: DC motor ON
        dutyM = getIntSCI1("Enter motor duty cycle
(3125 - 6250): ");              //obtain DC duty cycle
        if(dutyM >= 3125 && dutyM <=
6250){     //limit dutyM range
         DC_PWM = dutyM;
                              //set DC PWM duty cycle
         SCI1_printf("Motor duty cycle %d\n",
DC_PWM);                                //display
         cur_pos(0,1);      //move cursor position
         lcdprintf("Motor enabled");
                                    //print on LCD
        } else{
         SCI1_printf("%d: Motor duty cycle
invalid\n", dutyM);                     //use default
        }
      break;

      case'z'|'Z':          //case Z: DC motor OFF
        dutyM = DC_PWM = 4689;
                //set DC PWM duty cycle to stop
        SCI1_printf("Motor duty cycle %d, motor
stopped\n", DC_PWM);                    //display
        cur_pos(0,1);         //move cursor position
        lcdprintf("Motor disabled");//print on LCD
      break;

      case'r'|'R':              //case R: rewind tape
        dutyM = DC_PWM = 5200;
              //set DC PWM duty cycle to 5000
        SCI1_printf("Motor duty cycle %d\n",
DC_PWM);//display
        cur_pos(0,1);         //move cursor position
        lcdprintf("Motor enabled"); //print on LCD
      break;

      case'c'|'C':
     //case C: change DC duty cycle changing ratio
        DPWM = AcDuty();
      //rewrite DC motor duty cycle changing ratio
      break;

      case'q'|'Q':              //back to main menu
      return;
     }
   }
}
//Tape Rewind Mode (END)

//*****************************************
//                  Main
//*****************************************
int main (void)
{
  unsigned int menu;                //local variable
  float a=4,b;

   b=sqrt(a);

DI;                                 //disable interrupts
  initLCD();                        //initialize LCD
  cls_lcd();                            //clear LCD
  initSCI1(38400,0);                //set SCI1 flags
to ON
  initADC();                        //initialize ADC

  SCI1_printf("Ready!! \n");
```

```
   DC_PWM = 4689;                    //DC PWM
duty cycle
   Servo_PWM = 2400;                 //PWM
servo duty cycle at the zero degree
   ITU3_val = 250;                   //set default
ITU3_val (10us)
   PWM_valD = 62500;                 //set default
DC motor duty cycle
   PWM_valS = 62500;                 //set default
servo duty cycle

   initITU3(1,1);                    //enable ITU3

EI;                                  //enable interrupts
   statITU3();                       //start ITU2
   initPWM1(PWM_valS, Servo_PWM);
//PWM servo, period = 20msec
   initPWM2(PWM_valD, DC_PWM);
//DC motor, off
   while (1){                        //Loop (STAT)
    cls_lcd();                       //display following
sentences
     lcdprintf("Choose Mode");       //print on LCD
     SCI1_printf("**************************Main
Menu*********************\n");
     SCI1_printf("1: Automatic Mode\n");
     SCI1_printf("2: Manual Mode\n");
     SCI1_printf("0: Rewind Tape Mode\n");

SCI1_printf("**********************************
**********************\n");
     do {                            //infinite loop
      menu=getCharSCI1();
     }
     while(menu == ('1'|'2'|'0'));   //switch cases
      switch(menu){
       case'1':                      //case 1: auto mode
        Amode();                     //call auto mode
function
       break;

       case'2':                      //case 2: manual
mode
        Mmode();                     //call manual
mode function
       break;

       case'0':                //case 3: tape rewinding mode
        Rmode();                     //call rewind mode
       break;

       default:                //otherwise back to main menu
       break;
      }
   }                                 //Loop (END)
   return 0;
}

//End of Program
```

Appendix D

Measured travelling tape tensions using the tension sensor were recorded through Data Acquisition (DAQ) PC in txt format and analyzed using MATLAB 2009a environment with offline. MATLAB codes were used for analysis and full functions of travelling tape tension transitions during the tape transportation process are shown and illustrated in following sections.

D.1 Matlab Codes

Two sets of MATLAB codes that were used for analysis measured travelling tape tension are shown below. The first set of codes filters measurements of SG set 1 and SG set 2 (tension sensors) separately in order to condition the signal with 0.5Hz low pass filter. After completion of filtering, signals are converted to tension in Newton, and then calculate total travelling tape tension in Newton based on both sets of signal. Finally plotting three tensions SG set 1 (T1), SG set 2 (T2), and total tension (T) with the trajectory of rotary guider and power spectrum of both SG set 1(T1) and 2 (T2). The second set of MATLAB codes plot the angle profile of rotary guider for particular target tension based on the calibrated results in chapter 3.

Tension, Rotary Guider Trajectory, and Power Spectrum Plot

```
figure(1)
cutoff = 0.5;  //low pass filter cut off frequency
period = 100; //nominal tape length
gain1 = 0.0738; //SG set 1 conversion gain
gain2 = 0.0708; //SG set 2 conversion gain
m = 0; //SG set 1 digital value of “zero point”
m1 = 0; //SG set 2 digital value of “zero point”

time = 0:period/length(x(:,1)):period-
(period/length(x(:,1))); //sampling time

//Low pass filter
s = tf('s');
T = 1/(2*pi*cutoff);
H = 1/(1+T*s);
freq = length(x(:,1))/period;
sampletime = cutoff/(freq/2);
Hd = c2d(H, sampletime);
[b, a] = tfdata(Hd, 'v');
//Low pass filter END

y = filtfilt(b, a, x(:,1)); //calculate filtered value for
SG set 1

tension = ((((y-m)*(5/1024)) )/gain1); //convert from
measured digital value to tension (N) for SG set 1

y1 = filtfilt(b, a, x(:,2)); //calculate filtered value for
SG set 2

tension1 = ((((y1-m1)*(5/1024)) )/gain2); //convert
from measured digital value to tension (N) for SG set
2

tensionT = sqrt((tension.^2)+(tension1.^2));
//calculate total Tape Tension T

//plot tension; SG set 1 T1 & 2 T2 and total tension T
subplot(411);
```

```
plot(time,tension,'b', time, tension1,'black', time, tensionT,'r', 'linewidth',2);
axis([0 period 0 1]);
xlabel('Tape Length (%)');
ylabel('Tension (N)');
//plot tension; SG set 1 T1 & 2 T2 and total tension T END

//plot angle trajectory of rotary guider
angle = abs(x(:,4)-2400)/28;
subplot(412);
plot(time, angle, 'black', 'linewidth',2);
axis([0 period 0 40]);
xlabel('Tape Length (%)');
ylabel('Rotation Angle (Degree)');
//plot angle trajectory of rotary guider END

//plot power spectrum of SG set 1 T1
sampleRate = length(x(:,1))/period;
fftRRO     = fft(x(:,1), length(x(:,1)));
magSpec    = abs(fftRRO)*2/length(fftRRO);
DataMag    = magSpec(1:fix(length(x(:,1))/2));
DataFreq   = (sampleRate*(0:length(x(:,1))/2-1)/length(x(:,1)))';
subplot(413);
plot(DataFreq, DataMag, 'black');
k = max(DataFreq);
axis([1 k 0 2]);
xlabel('Frequency (Hz)');
ylabel('Magnitue (power)');
//plot power spectrum of SG set 1 T1 END

//plot power spectrum of SG set 1 T2
sampleRate1 = length(x(:,2))/period;
fftRRO1     = fft(x(:,1), length(x(:,1)));
magSpec1    = abs(fftRRO1)*2/length(fftRRO1);
DataMag1    = magSpec1(1:fix(length(x(:,1))/2));
DataFreq1   = (sampleRate1*(0:length(x(:,1))/2-1)/length(x(:,1)))';
subplot(414);
plot(DataFreq1, DataMag1, 'black');
k1 = max(DataFreq1);
axis([1 k1 0 2]);
xlabel('Frequency (Hz)');
ylabel('Magnitue (power)');
//plot power spectrum of SG set 1 T2
```

Angle Profile of Rotary Guider for Particular Target Tension

```
//Mathematical model of calibrated tension curve for tape travelling speed 4m/s
a4 = -5.6e-007; //3rd order coefficient
b4 = 1.3e-004; //2nd order coefficient
c4 = -6.6e-003; //1st order coefficient
d4 = 0.18; //intercept
g4 = 0.0060; //tension increment (per 1 degree of rotary guider rotation)

//Mathematical model of calibrated tension curve for tape travelling speed 7m/s
a7 = 5.0e-007; //3rd order coefficient
b7 = -6.0e-005; //2nd order coefficient
c7 = 2.0e-003; //1st order coefficient
d7 = 0.49; //intercept
g7 = 0.0061; //tension increment (per 1 degree of rotary guider rotation)

T4 = 0.28 //target tension for 4m/s (0.28N ~ 0.32N)
T7 = 0.60; //target tension for 7m/s (0.60N ~ 0.70N)

L = 0:1:100; //nominal tape tension (100 points)

seta4 = (T4 - (a4*L.^3) - (b4*L.^2) - (c4*L) - d4) / g4; //find angle of rotary guider to maintain the tension as targeted for (4m/s)
seta7 = (T7 - (a7*L.^3) - (b7*L.^2) - (c7*L) - d7) / g7; //find angle of rotary guider to maintain the tension as targeted for (4m/s)
```

```
//Plotting angle profile of rotary guider to maintain
the tension as targeted for (4m/s)
figure(1)
plot(L, seta4, 'black','linewidth',2);
axis([0 100 0 40]);
```

```
//Plotting angle profile of rotary guider to maintain
the tension as targeted for (7m/s)
figure(2)
plot(L, seta7, 'black','linewidth',2);
axis([0 100 0 40]);
```

D.2 MATLAB Figures

Following graphs illustrate full measured tension transitions during the tape transportation process in chapter 3 and 4 in SG set 1(T1), SG set 2(T2), and total tension (T). Trajectories of rotary guider for dynamic tape path alternation are also illustrated.

D-1 Fixed Tape Path (4m/s)

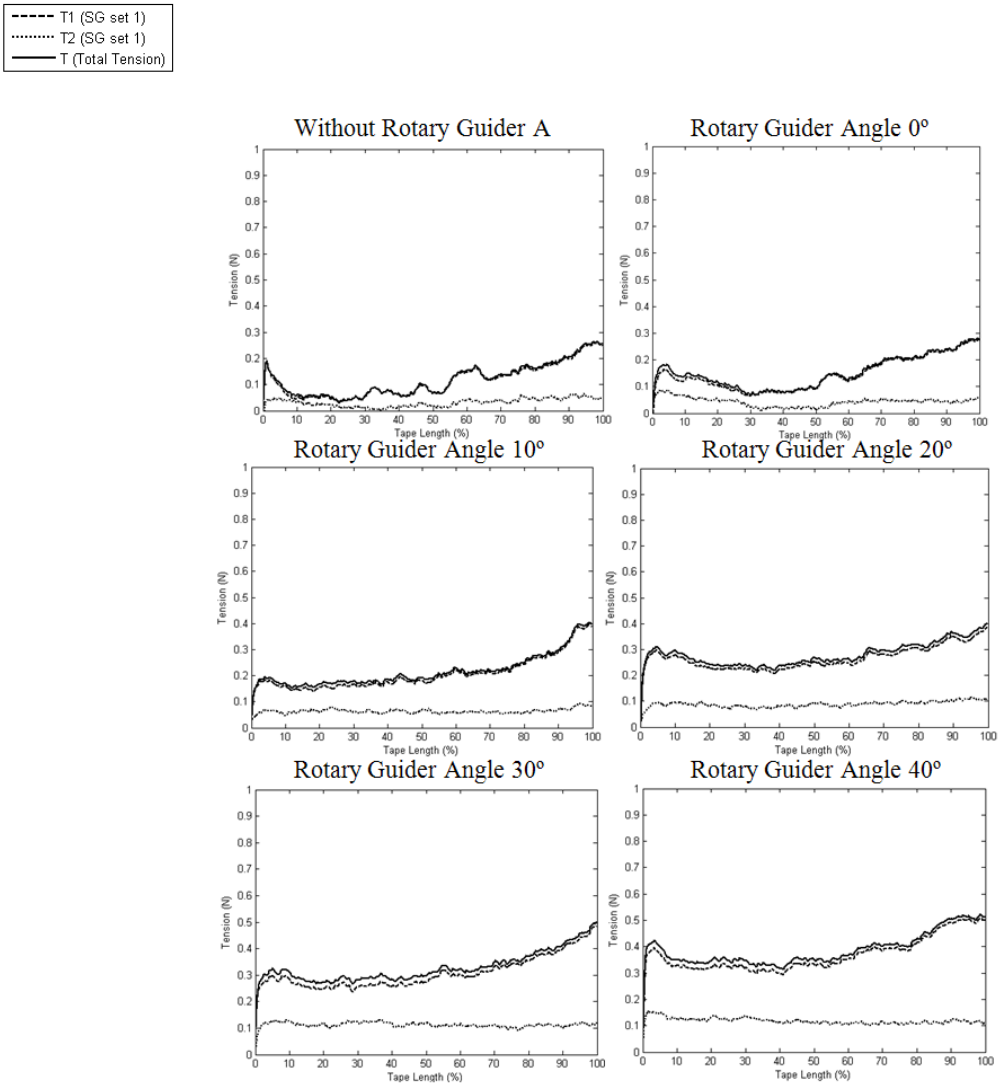

D-2 Fixed Tape Path (7m/s)

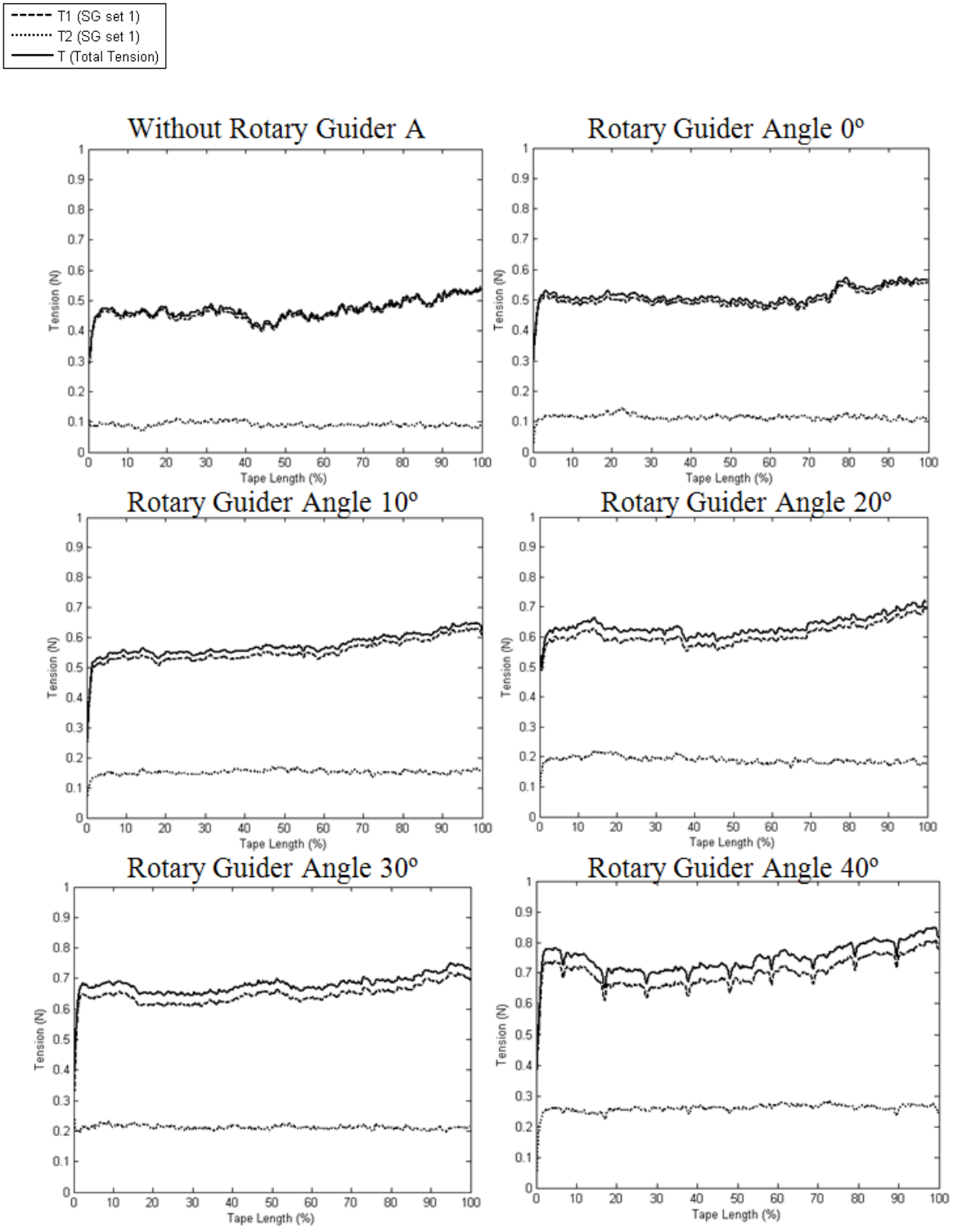

D-3 Dynamic Tape Path Alternation - Open Loop Controller (4m/s)

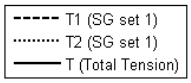

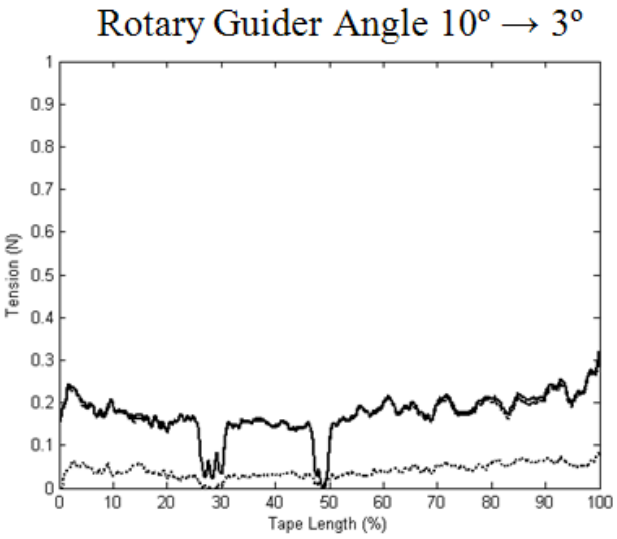

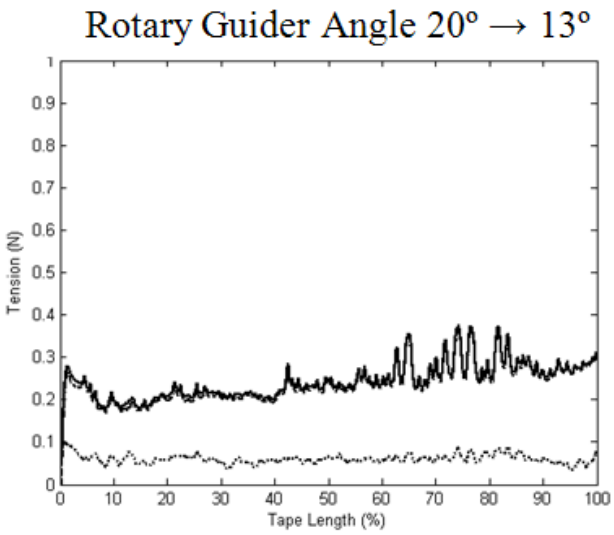

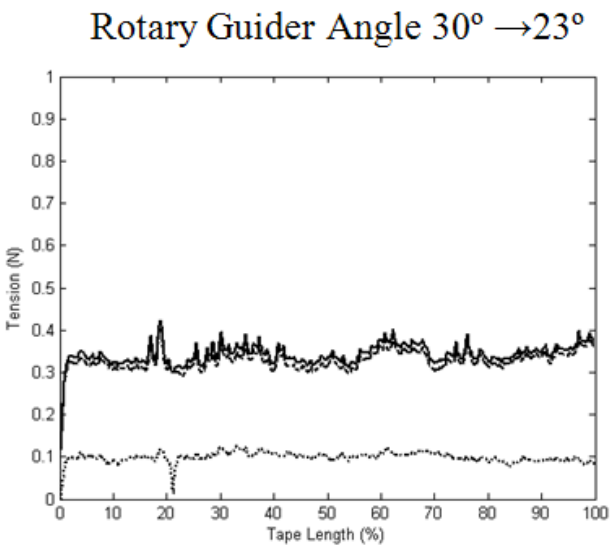

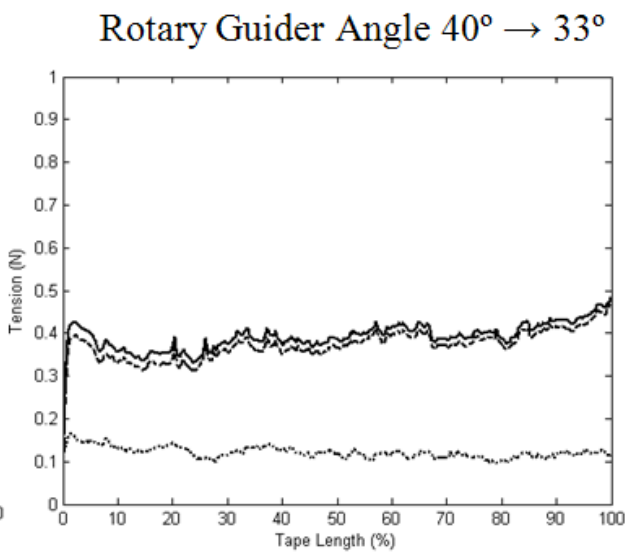

D-4 Dynamic Tape Path Alternation - Open Loop Controller (7m/s)

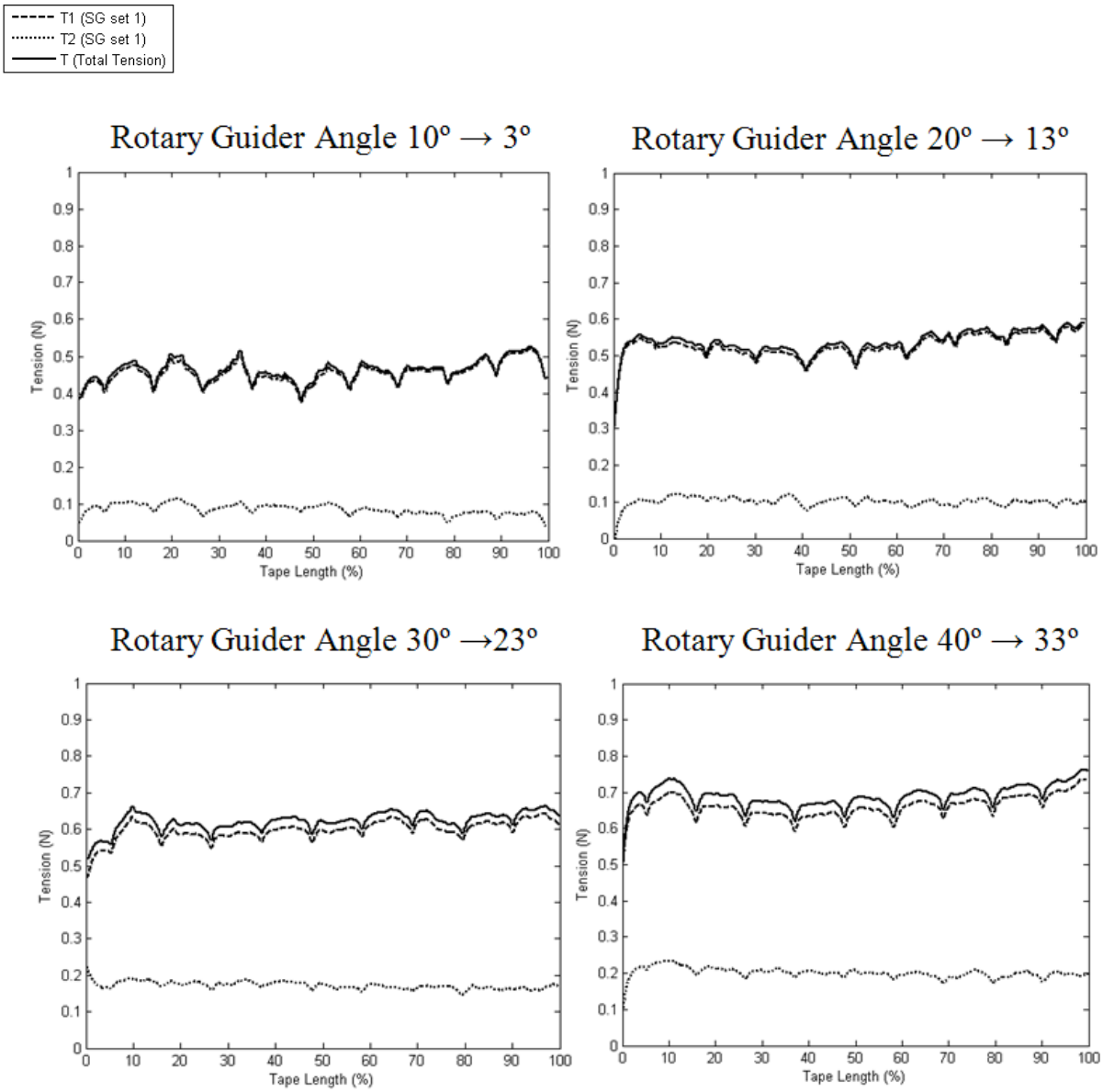

D-5 Dynamic Tape Path Alternation – Closed Loop Control with Proportional Controller (4m/s)

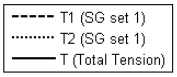

Target Tension 0.28N

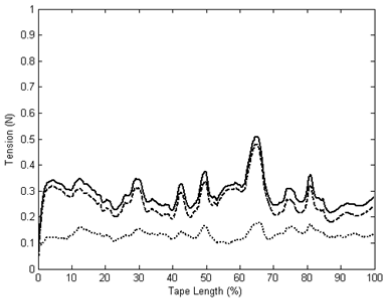

Target Tension 0.30N

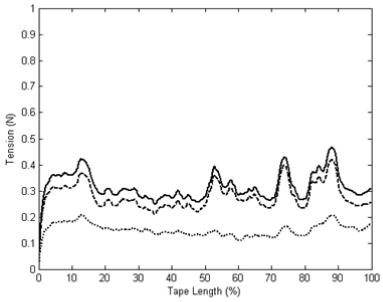

Rotary Guider Angle Trajectory: 0.28N

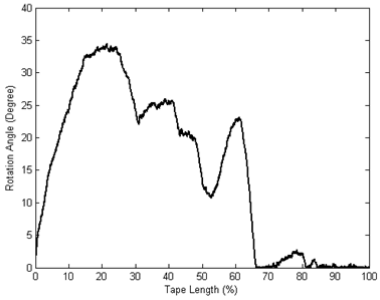

Rotary Guider Angle Trajectory: 0.30N

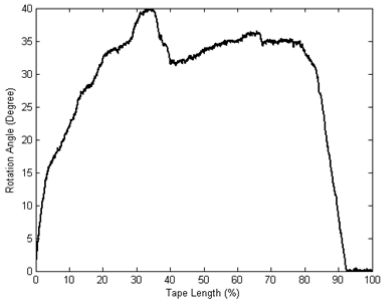

Target Tension 0.32N

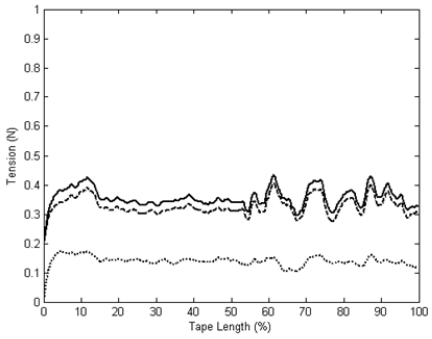

Rotary Guider Angle Trajectory: 0.32N

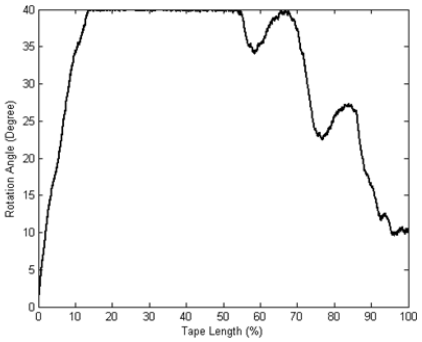

D-6 Dynamic Tape Path Alternation – Closed Loop Control with Proportional Controller (7m/s)

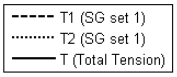

Target Tension 0.60N

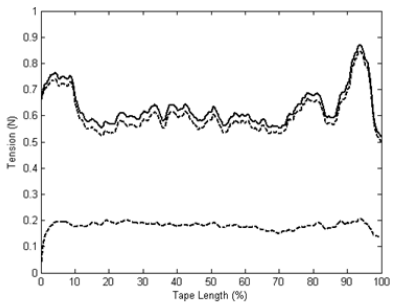

Target Tension 0.65N

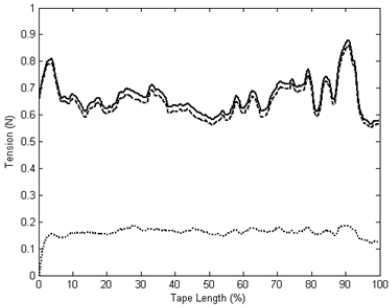

Rotary Guider Angle Trajectory: 0.60N

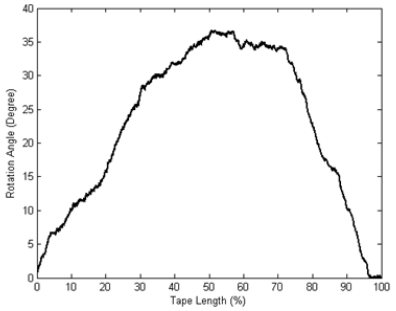

Rotary Guider Angle Trajectory: 0.65N

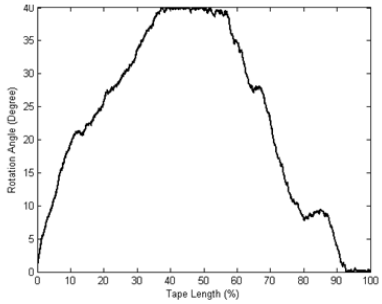

Target Tension 0.70N

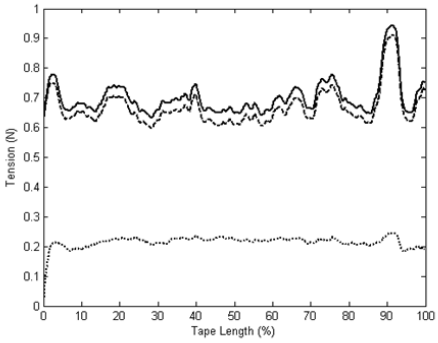

Rotary Guider Angle Trajectory: 0.70N